NEA/NSC/DOC(2002)12

NEA NUCLEAR SCIENCE COMMITTEE
NEA COMMITTEE ON SAFETY OF NUCLEAR INSTALLATIONS

PRESSURISED WATER REACTOR MAIN STEAM LINE BREAK (MSLB) BENCHMARK

Volume III: Results of Phase 2 on
3-D Core Boundary Conditions Model

by

N. Todorova, B. Taylor and K. Ivanov
Nuclear engineering Program
The Pennsylvania State University
University Park, PA 16802, USA

US Nuclear Regulatory Commission
OECD Nuclear Energy Agency

ORGANISATION FOR ECONOMIC CO-OPERATION AND DEVELOPMENT

Pursuant to Article 1 of the Convention signed in Paris on 14th December 1960, and which came into force on 30th September 1961, the Organisation for Economic Co-operation and Development (OECD) shall promote policies designed:

- to achieve the highest sustainable economic growth and employment and a rising standard of living in Member countries, while maintaining financial stability, and thus to contribute to the development of the world economy;
- to contribute to sound economic expansion in Member as well as non-member countries in the process of economic development; and
- to contribute to the expansion of world trade on a multilateral, non-discriminatory basis in accordance with international obligations.

The original Member countries of the OECD are Austria, Belgium, Canada, Denmark, France, Germany, Greece, Iceland, Ireland, Italy, Luxembourg, the Netherlands, Norway, Portugal, Spain, Sweden, Switzerland, Turkey, the United Kingdom and the United States. The following countries became Members subsequently through accession at the dates indicated hereafter: Japan (28th April 1964), Finland (28th January 1969), Australia (7th June 1971), New Zealand (29th May 1973), Mexico (18th May 1994), the Czech Republic (21st December 1995), Hungary (7th May 1996), Poland (22nd November 1996), Korea (12th December 1996) and the Slovak Republic (14 December 2000). The Commission of the European Communities takes part in the work of the OECD (Article 13 of the OECD Convention).

NUCLEAR ENERGY AGENCY

The OECD Nuclear Energy Agency (NEA) was established on 1st February 1958 under the name of the OEEC European Nuclear Energy Agency. It received its present designation on 20th April 1972, when Japan became its first non-European full Member. NEA membership today consists of 28 OECD Member countries: Australia, Austria, Belgium, Canada, Czech Republic, Denmark, Finland, France, Germany, Greece, Hungary, Iceland, Ireland, Italy, Japan, Luxembourg, Mexico, the Netherlands, Norway, Portugal, Republic of Korea, Slovak Republic, Spain, Sweden, Switzerland, Turkey, the United Kingdom and the United States. The Commission of the European Communities also takes part in the work of the Agency.

The mission of the NEA is:

- to assist its Member countries in maintaining and further developing, through international co-operation, the scientific, technological and legal bases required for a safe, environmentally friendly and economical use of nuclear energy for peaceful purposes, as well as
- to provide authoritative assessments and to forge common understandings on key issues, as input to government decisions on nuclear energy policy and to broader OECD policy analyses in areas such as energy and sustainable development.

Specific areas of competence of the NEA include safety and regulation of nuclear activities, radioactive waste management, radiological protection, nuclear science, economic and technical analyses of the nuclear fuel cycle, nuclear law and liability, and public information. The NEA Data Bank provides nuclear data and computer program services for participating countries.

In these and related tasks, the NEA works in close collaboration with the International Atomic Energy Agency in Vienna, with which it has a Co-operation Agreement, as well as with other international organisations in the nuclear field.

FOREWORD

Since the beginning of the pressurised water reactor (PWR) benchmark activities at the OECD/NEA, four benchmark workshops have taken place. The first was held in Washington DC, USA (April 1997), the second in Madrid, Spain (June 1998), the third in Garching near Munich, Germany (March 1999), and the fourth in Paris, France (January 2000). It was agreed that in performing this series of exercises participants would be working at the edge of present developments in coupling neutronics and thermal-hydraulics, and that this benchmark would lead to a common background understanding of the key issues. It was also agreed that the PWR MSLB Benchmark would be published in four volumes.

Volume 1 of the *PWR MSLB Benchmark: Final Specifications*, was issued in April 1999 [NEA/NSC/DOC(99)8]. A small team at the Pennsylvania State University (PSU) was responsible for authoring the final specification, co-ordinating the benchmark activities, answering the questions, analysing the solutions submitted by benchmark participants, and providing reports summarising the results for each phase. In performing these tasks the PSU team collaborated with Adi Irani and Nick Trikouros of GPU Nuclear Inc.

Volume 2 of the *PWR MSLB Benchmark: Results of Phase 1 on Point Kinetics*, was issued in December 2000 [NEA/NSC/DOC(2000)21]. It summarised the results for Phase 1 of the benchmark and identified the key parameters and important issues concerning thermal-hydraulic system modelling of the MSLB transient with specified point kinetics parameters. Phase 1 helped the participants initialise and test their system code models for further use in Phase 3 on coupled three-dimensional (3-D) kinetics/system thermal-hydraulics simulations.

Volume 3 summarises the results of Phase 2 on coupled 3-D kinetics core thermal-hydraulics boundary conditions modelling. The report is supplemented with brief descriptions of the coupled codes used (for modelling core neutronics and thermal-hydraulics) as provided by the participants (Appendix A). Descriptions (including graphs where useful) of the models used are also enclosed (Appendix B). The latter are presented as answers to the Questionnaire for the Second Exercise so that the compliance with specification can be verified. The list of deviations from the specification, if any, is provided and any specific assumptions are stated. Based on the information provided, the benchmark co-ordinators and the report reviewers decided whether the solution that was submitted matches with sufficient precision the core model provided. Solutions that deviated in the modelling in ways not compatible with specification were not included in the statistical evaluation procedure.

Appendices A and B are included in both the hard copy of the report and the electronic copy on CD-ROM. Appendices C and D are only provided in the CD-ROM version. Appendix C contains the mean solutions for each type of data and the parameters generated using the statistical methodology developed by PSU. These solutions are used as reference results for code-to-code comparisons with the participants' results. The participants' deviations and figures of merit for each parameter are presented in Appendix D. It was because Appendices C and D contain a large amount of data (approximately 1 000 pages) that it was decided at the 4th PWR MSLB Benchmark Workshop that they would be published in electronic format only. The electronic version can be obtained free on request from neapub@nea.fr.

Acknowledgements

This report is dedicated to the students of Penn State University, the next generation of nuclear engineers, who are the reason why we are here.

The authors would like to thank Dr. H. Finnemann from Siemens – former member of NSC/NEA, Dr. S. Langenbuch from the Gessellschaft fur Reaktorsicherheit (GRS), Prof. J. Aragones from Universidad Politecnica Madrid (UPM) – member of NSC/NEA, and Prof. F. D'Auria of University of Pisa (UP) – member of CSNI/NEA, whose support and encouragement in establishing and carrying out this benchmark were invaluable.

This report is the sum of many efforts, the participants, the funding agencies and their staff – the US Nuclear Regulatory Commission and the Organization of Economic Co-operation and Development. Special appreciation goes to the report reviewers: Prof. J. Aragones from UPM, Dr. S. Langenbuch from GRS, and R. Boeer from Framatome ANP GmbH. Their comments and suggestions were very valuable and improved significantly the quality of this report. We would like to thank them for the effort and time involved.

Particulars noteworthy were the efforts of Farouk Eltawila assisted by David Ebert, both of the US Nuclear Regulatory Commission. With their help, funding was secured, enabling this project to proceed. We also thank them for their excellent technical advice and assistance.

The authors wish to express their sincere appreciation for the outstanding support offered by Dr. Enrico Sartori, who not only provided efficient administration, organisation and valuable technical recommendations, but most importantly provided friendly counsel and advice.

Finally, we are grateful to Hélène Déry for having devoted her competence and skills to the preparation of this report for publication.

List of Abbreviations

1-D	One-Dimensional
2-D	Two-Dimensional
3-D	Three-Dimensional
ANL	Argonne National Laboratory
APSR	Axial Power Shape Rods
ARI	All Rods In
ARO	All Rods Out
BC	Boundary Conditions
BE	British Energy
BOC	Beginning of Cycle
BP	Burnable Poison
CA	Control Assembly
CEA	Commissariat à l'Énergie Atomique
CSA	Computer System Analysis
EDF	Électricité de France
EFPD	Effective Full Power Days
EOC	End of Cycle
EOT	End of Transient
EPRI	Electric Power Research Institute
FA	Fuel Assembly
FZK	Forschungs Zentrum Karlsruhe
FZR	Forschungs Zentrum Rossendorf
GPU	General Power Utility
GRS	Gesellschaft für Anlagen- und Reaktorsicherheit mbH
HFP	Hot Full Power
HZP	Hot Zero Power
KAERI	Korean Atomic Energy Research Institute
LWR	Light Water Reactor
MSLB	Main Steam Line Break
NEA	Nuclear Energy Agency
NEM	Nodal Expansion Method
NP	Normalized Power
NPP	Nuclear Power Plant
NRC	Nuclear Regulatory Commission
OECD	Organisation for Economic Co-operation and Development
PSU	Pennsylvania State University
PWR	Pressurized Water Reactor
SRW	Stuck Rod Worth
T-H	Thermal-Hydraulic
TMI-1	Three Mile Island – Unit 1
TR	Tripped Rod
TRW	Tripped Rod Worth
UP/UZ	University of Piza/University of Zagreb
UPM	Universidad Politecnica de Madrid
UPV	Universidad Politecnica de Valencia
VTT	Technical Research Center of Finland

TABLE OF CONTENTS

List of tables

List of Figures

Chapter 1

INTRODUCTION

Incorporation of full three-dimensional (3-D) models of the reactor core into system transient codes allows for a "best-estimate" calculation of interactions between the core behaviour and plant dynamics. Recent progress in the computer technology has made development of coupled system thermal-hydraulic (T-H) and neutron kinetics code systems feasible. Considerable efforts have been made in various countries and organisations in this direction. To verify the capability of the coupled codes to analyse complex transients with coupled core-plant interactions and to fully test thermal-hydraulic coupling, appropriate Light Water Reactor (LWR) transient benchmarks need to be developed on a higher "best-estimate" level. The previous sets of transient benchmark problems addressed separately system transients (designed mainly for thermal-hydraulic (T-H) system codes with point kinetics models) and core transients (designed for T-H core boundary conditions models coupled with a three-dimensional neutron kinetics models). The Nuclear Energy Agency (NEA) of the Organisation for Economic Co-operation and Development (OECD) has recently completed under the US Nuclear Regulatory Commission (NRC) sponsorship a PWR Main Steam Line Break (MSLB) Benchmark against coupled T-H and neutron kinetics codes. Small benchmark team from the Pennsylvania State University (PSU) has been responsible for developing the benchmark specification, assisting the participants and co-ordinating the benchmark activities.

The PWR MSLB Benchmark problem uses a three-dimensional neutronics core model to verify further the capability of coupled codes to analyse complex transients with coupled core-plant interactions and to test fully the thermal-hydraulic coupling. It is based on real plant design and operational data for Three Mile Island – Unit 1 Nuclear Power Plant (TMI-1 NPP). The purpose for this benchmark is three-fold: to verify the capability of system codes to analyse complex transients with coupled core-plant interactions; to test fully the 3-D neutronics/thermal-hydraulic coupling; and to evaluate discrepancies between the predictions of coupled codes in best-estimate transient simulations.

The purposes of this benchmark are met through the application of three exercises (phases), which are described in Volume 1 of the PWR MSLB Benchmark: Final Specifications [1]. Volume 2 summarised the results of Phase 1 of point kinetics [2]. The purpose of the first exercise was to test the thermal-hydraulic system response, based on the point kinetics plant simulations, which modelled the entire primary system. The participants were provided with compatible point kinetics model inputs that preserve axial and radial power distribution, and scram reactivity obtained using a 3-D core neutronics model and a complete system description. This report (Volume 3) summarises the results of Phase 2. The purpose of this phase is to test the neutronics response to imposed thermal-hydraulic boundary conditions. The participants are provided with transient boundary conditions (radial distribution of mass flow rates at the core inlet, and core-averaged pressure versus time at both the core inlet and outlet) and a complete core description.

As mentioned above this report presents the final results for the second exercise of the PWR MSLB Benchmark problem, the coupled 3-D neutronics/core thermal-hydraulics evaluation of core

response. This report is representative of twenty-two results received from sixteen participants representing twenty-five organisations from ten countries. A list of participants who have submitted information to the PSU benchmark team for the second exercise, along with the code used to perform the analysis, is found in Table 1.1. A more detailed description of each code is presented in Appendix A, while the modelling assumptions, made by each participant, are given in Appendix B. Notice that some participants have submitted results from different versions of the same code and/or using different models, or couplings of different codes. Chapter 2 contains a description of the second benchmark exercise including core and neutronics data; a definition of the core T-H boundary conditions model; details about neutronic/thermal-hydraulic coupling; and a summary of the states and transient scenarios, calculated in this exercise. Chapter 3 discusses the statistical methodology, employed in this benchmark to generate mean solutions. These mean solutions are presented in Appendix C and are used as reference solutions. Chapter 4 provides comparative analysis of the final results for the second exercise. The comparisons of results for each participant are provided in Appendix D. Chapter 5 provides a brief summary of the conclusions drawn from this exercise.

Table 1.1. List of participants in the first phase of the PWR MSLB Benchmark

Participant Number	Company Name	Country	Code
1	ANL	USA	SAS-DIF3DK
2	BE/Tractebel (1)	UK/Belgium	PANTHER (Standard)
3	BE/Tractebel (2)	UK/Belgium	PANTHER (Reference)
4	CEA (1)	France	CRONOS2-FLICA4
5	CEA (2)	France	CRONOS2-FLICA4/1D
6	CSA/GPUN/EPRI	USA	RETRAN-3D MOD2.0
7	EDF (1)	France	THYC-COCCINRLLE
8	EDF (2)	France	THYC3D-COCCINRLLE
9	Framatome ANP/FZK (1)	Germany	RELAP5/PANBOX-E
10	Framatome ANP/FZK (2)	Germany	RELAP5/PANBOX-I
11	FZR	Germany	DYN3D/R
12	GRS	Germany	QUABOX-CUBBOX
13	Iberdrola	Spain	RETRAN-3D MOD2
14	KAERI (1)	Korea	MARS/MASTER
15	KAERI (2)	Korea	MASTER
16	PSU	USA	TRAC-PF1/NEM
17	Purdue/NRC (1)	USA	TRAC-M/PARCS
18	Purdue/NRC (2)	USA	RELAP/PARCS
19	UP/UZ	Italy/Croatia	RELAP5/PARCS
20	UPM	Spain	SIMTRAN
21	UPV	Spain	TRAC-PF1/NEM
22	VTT	Finland	TRAB-3D

Chapter 2

DESCRIPTION OF SECOND BENCHMARK EXERCISE

The second exercise (phase) of the OECD/NRC PWR MSLB Benchmark is defined as an evaluation of core neutronics response to imposed thermal-hydraulic conditions. The participants are provided with complete core description and cross-section library as well as initial and transient boundary conditions (BC).

The reference design for the PWR is derived from the reactor geometry and operational data of the TMI-1 NPP. The full thermal-hydraulics (T-H) system model is converted to a core boundary model by defining aforementioned inlet conditions at the vessel bottom and the outlet condition at the vessel top. The set of data given in the following paragraphs, and in the pertinent tables and figures, completely defines the second PWR MSLB benchmark exercise.

2.1 Description of MSLB scenario

The transient being analysed is a MSLB in a PWR, which may occur as a consequence of the rupture of one steam line upstream of the cross-connect. Significant space-time effects in the core caused by asymmetric cooling and an assumed stuck-out control rod after the reactor trip characterises this event. One of the major concerns for the MSLB accident is the return-to-power and criticality. Because of this, the MSLB scenario was based on assumptions that conservatively maximise the consequences for a return-to-power. Two versions of this scenario were specified. The first version is the original scenario, which is employed in the current licensing practice. For this scenario point kinetics models usually predict return-to-power, while 3-D models do not despite conservative assumptions. The second scenario was specified upon request of participants in order to test better the predictions of coupled 3-D kinetics/thermal-hydraulic codes. In this scenario, 3-D models are expected to predict return-to-power also. Both versions have the same initial steady-state conditions and follow the same sequence of events. The difference is in the value of the tripped rod worth. In 3-D kinetics simulations the point kinetics tripped rod worth values are matched by two different rodded cross-section libraries, to be used in each scenario version – **nemtabr.norp** and **nemtabr.rp**. For the second exercise the original linear interpolation routine (which does not allow extrapolation) – **lint4d.2ndExercise**[1] is used.

2.2 Core neutronics model and cross-section library

The radial geometry of the reactor core is shown in Figure 2.1. Radially, the core is divided into cells 21.811 cm (0.7156 ft) wide, each corresponding to one fuel assembly (FA), plus a radial reflector (shaded area) of the same width. There are in total 241 assemblies, 177 FA and 64 reflector assemblies. Axially, the reactor core is divided into 24 layers with a height (starting from the bottom)

1. These data sets and others required for modeling the benchmark are available on CD-ROM.

of: 14.88 cm (0.4882 ft); 4.71 cm (0.1545 ft); 10.17 cm (0.3514 ft); 8x14.88 cm; 2x29.76 cm (0.9764 ft); 8x14.88 cm; 12.266 cm (0.4024 ft); 2.614 cm (0.0858 ft); 14.88 cm, adding up to a total active core height of 357.12 cm (11.717 ft). Both the upper and lower axial reflector have a thickness of 21.811 cm (0.7156 ft). The axial nodalisation scheme accounts for material changes in the fuel design and for the exposure and moderator temperature (spectral history) variations.

The mesh used for the calculation is up to the participant, and should be chosen according to the numerical capabilities of the code. Output should, however, give volume-averaged results on the specified mesh in the format described in Chapter 6 of Final Specifications [1].

Fuel assemblies with different ^{235}U enrichments and different numbers of burnable absorber rods are present in the core. The axial and radial distributions of the enrichment and absorbers can be found in Tables 2.4 and 2.5; the geometric data for the FA is given in Table 2.1. The available gap width is 0.00955 cm. For the neutronics problem, each of the FA's is considered to be homogeneous.

The radial arrangement of the control assemblies (CA) is shown in Figure 2.2. Sixty-one of these CAs, grouped into 7 groups, consist of full-length control rods. These rods contain a strong neutron absorber over a length that spans most of the active core region. Further the position of a control rod insertion in cm is given from the bottom of lower reflector. The total CA length, which coincides, with the absorber length, is 342.7055 cm (11.244 ft). No tip of control rods is defined. The position of the lower CA absorber edge from the bottom of the lower reflector is 36.2255 cm (1.189 ft) for a completely inserted CA, and 378.931 cm (12.4323 ft) for a completely withdrawn CA. Measured in units of steps, complete insertion and withdrawal of a CA correspond to 0 and 971 steps, respectively. Each step is 0.3531 cm (0.139 inch). If one multiplies 971x0.3531 and summates with 36.2255 the result is 379.0856 cm. The top edge of the core region is 378.931 cm *i.e.* there is a difference of 0.1546 cm, which is not modelled in this benchmark. Here the definition completely withdrawn means withdrawn from the active core *i.e.* out of the core. The real completely withdrawn position in terms of steps is 1 000 steps *i.e.* at 36.2255+353.1=389.3255 cm from the bottom of lower reflector which is in the region of upper reflector and is not modelled in this benchmark. In addition, eight of the CA (group 8) consists of part-length control rods (axial power shaping rods or APSR) whose presence is already accounted for in the cross-section tables.

Two neutron energy and six delayed neutron groups are modelled. The energy release per fission for the two prompt neutron groups is 0.3213×10^{-10} and 0.3206×10^{-10} W-s/fission, and it is considered to be independent of time and space. Table 2.2 shows the decay constants and fractions of delayed neutrons. No delayed energy release is considered.

It is recommended that the ANS-79 decay heat standard be used as a decay heat standard model. In total 71 decay-heat groups are used: 69 groups are used for the 3 isotopes ^{235}U, ^{239}Pu and ^{238}U with the decay-heat constants defined in the 1 979 ANS standard; plus the heavy-element decay heat groups for ^{239}U and ^{239}Np with constants given in Table 2.3. It is recommended that the participants also use the assumption of an infinite operation at power 2 772 MWt. For participants who are not capable of using the ANS-79 decay heat standard, a file of the decay heat evolution throughout the transient for both scenario versions has been provided. These predictions are obtained using the PSU coupled code TRAC-PF1/NEM [3] in order to avoid the uncertainties coming from using different decay-heat models. The effective decay heat energy fraction of the total thermal power (the relative contribution in the steady state) is equal to 0.07143.

Thirty assembly types are contained within the core geometry. There are 438 unrodded and 195 rodded compositions. The corresponding sets of cross sections are provided. Each composition is defined by material properties (due to changes in the fuel design) and burnup. The burnup dependence

is a 3-component vector of variables: exposure (GWd/t), spectral history (T_{mod}) and burnable poison (BP) history. The definition of assembly types is shown in Table 2.4. The radial distribution of these assembly types within the reactor geometry is shown in Figure 2.3. The 2-D assembly type map is shown in one-eight core symmetry sector together with the assembly exposure values at the end of cycle (EOC). The axial locations of compositions for each assembly are shown in Table 2.5.

A complete set of diffusion coefficients and macroscopic cross sections for scattering, absorption, and fission as a function of the moderator density and fuel temperature is defined for each composition. The assembly discontinuity factors (ADFs) are taken into consideration implicitly by incorporating them into the cross-sections in order to minimise the size of the cross-section tables. The group inverse neutron velocities are also provided for each composition. Dependence of the cross-sections on the above variables is specified through a two-dimensional table look-up. Each composition is assigned to a cross-section set containing separate tables for the diffusion coefficients and cross-sections, with each point in the table representing a possible core state. The expected range of the transient is covered by the selection of an adequate range for the independent variables shown in the Table 2.6. A linear interpolation scheme is used to obtain the appropriate total cross-sections from the tabulated ones based on the reactor conditions being modelled. The original interpolation procedure provided by PSU does not perform a linear extrapolation outside of the density boundaries, which can lead to an underestimation of the moderator density feedback. Since for the second exercise, the system T-H parameters are provided by the PSU best estimate TRAC-PF1/NEM calculations as boundary conditions, the effect of exceeding moderator density range is not so significant and can be neglected for the purposes of the second exercise. It was decided at the Fourth Benchmark Workshop that the participants will use the original interpolation procedure for the second exercise [4]. However, for the exercise 3 the original interpolation procedure was modified to perform linear extrapolation of out-of-bounds values. Table 2.7 shows the definition of a cross-section table associated with thermal-hydraulic conditions. Table 2.8 shows the macroscopic cross-section table structure for one cross-section set. All cross-section sets are assembled into a cross-section library. The cross-sections are provided in separate libraries for rodded **(nemtabr)** (numerical nodes with a CA) and unrodded compositions **(nemtab)**. The format of each library is as follows:

- The first line of data is used to show the number of data points used for the independent thermal-hydraulic parameters, *i.e.* fuel temperature, moderator density, boron concentration, and moderator temperature.

- Each cross-section set is in the order shown in Table 2.8. Each table is in the format described in Table 2.7. More detailed information on this format is presented in Appendix B of the Final Specifications [1]. First, the values of the independent thermal-hydraulic parameters (fuel temperature and moderator density) that are used to specify that particular set of cross-sections will be listed, followed by the values of the cross-sections.[2] Finally, the group inverse neutron velocities complete the data for a given cross-section set.

- The dependence on fuel temperature in the reflector cross-section tables is also modelled. This is because the reflector cross-sections are generated by performing 1-D transport calculations, including the next fuel region. In order to simplify the reflector feedback modelling the following assumptions are made for this benchmark: an average fuel temperature value equal to 600 K is used for the radial reflector cross-section modelling in

2. Please note that the provided absorption cross-sections already take the Xenon thermal cross-sections into account; however, at the participants' request, the Xenon cross-sections are listed in the cross-section sets.

both the initial steady-state and transient simulations, and an average coolant density for radial reflector equal to the inlet coolant density. For the axial reflector regions the following assumptions are made: for the bottom – the fuel temperature is equal to the inlet coolant temperature (per T-H channel or cell) and the coolant density is equal to the inlet coolant density (again per channel); for the top – the fuel temperature is equal to the outlet coolant temperature (per channel) and the coolant density is equal to the outlet coolant density (per channel).

- There is a second rodded library, generated for a hypothetical return to power scenario with 3-D kinetic models. It is named **nemtabr.rp**. The magnitude of the return to power is small; however, this is the maximum one can obtain by modifying the rodded thermal absorption cross-section for control rod groups 1 to 6. This additional non-realistic scenario (even with accounting for all the conservative assumptions used in the licensing practice) is defined upon the request of participants for more comprehensive testing of coupled 3-D kinetics/thermal-hydraulics models.

2.3 Definition of the core thermal hydraulics boundary conditions model

The full TMI-1 (T-H) Model can be converted to a core T-H boundary conditions model by defining an inlet condition at the vessel bottom and an outlet condition at the vessel top. The vessel in this case represents an isolated core with boundary conditions at its bottom and top. The boundary conditions are provided to the participants and these are taken from the TRAC-PF1/NEM best-estimate core-plant system code calculations. Radial distributions are provided for 18 T-H cells (from 1 to 18) as shown in Figure 2.4. These 18 T-H cells are coupled to the neutronic core model in the radial plane as shown in Figure 2.6. This mapping scheme follows the spatial mesh overlays developed for the TMI-1 TRAC-PF1/NEM model.

The TMI-1 TRAC-PF1 model is a 3-D vessel model in a cylindrical geometry. A majority of the existing coupled codes model the core thermal-hydraulically using parallel channel models, which leads to difficulties in the interpolation of the mass flow BC. In order to avoid this source of modelling uncertainty, BC have been generated where mass flows are corrected for direct use as input data in the multi-channel core models. A geometrical interpolation method is used to process the TRAC-PF1/NEM BC in order to obtain inlet condition for each assembly. The detailed mapping scheme (Figure 2.7) shows how the provided 18 BC values are distributed per assembly. For the central row of assemblies, it is recommended that the average values of the upper and lower halves are used.

There are several files of data that are used for definition of the core T-H boundary conditions model (exercise 2). This data is taken from the best-estimate core plant system code calculations performed with the PSU version of TRAC-PF1/NEM:

1. File TEMP.BC

   The transient inlet radial distribution of liquid temperatures from 0 s to 100 s during the transient. The values are extracted from the TRAC vessel axial layer #3 (Figure 2.5) which is mapped to the bottom reflector of the core neutronics model. For each time interval the first number is the time, followed by 18 numbers corresponding to the liquid temperatures in (^{o}K) in the 18 azimuthal sectors that make up the core region.

2. File MASS_FLOWS.BC

   The same as above for the inlet radial distribution of axial mass flows (kg/s).

3. File Press_Inlet.BC

   The same as above for the inlet radial distribution of pressure (Pa).

4. File Press_Outlet.BC

   The same as above for the outlet radial distribution of pressure (Pa). The values in the file Press_Outlet.BC are extracted from the TRAC vessel axial layer #10, which is mapped to the top reflector.

The average pressure drop between TRAC axial layers 3 and 10 (*i.e.* in fact across the core) at time = 0 s is about 0.136 MPa. In the TRAC nodalisation (Figure 2.5) the lower plenum is represented with the first, second, and third layers. The upper plenum is represented with eleventh and twelfth layers. The average pressure drop between plenums at t=0 sec is 0.199 MPa.

At the request of some participants; a new file, Cold_Temp.BC, is provided. The file contains cold leg temperatures for the two loops (the 1st column is for Loop A – broken loop – and the 2nd for Loop B – intact loop) as a function of time.

2.4 Neutronic/thermal-hydraulic coupling

The feedback or coupling between neutronics and thermal-hydraulics can be characterised by choosing user-supplied mapping schemes (spatial mesh overlays) in the radial and axial core planes.

Some of the inlet perturbations (inlet disturbances of both temperature and flow rate) are specified as a fraction of the position across the core inlet. This requires either 3-D modelling of the vessel or some type of a multi-channel model.

For the purposes of this benchmark (Exercises 2 and 3), it is recommended that an assembly flow area of 40.061 in^2 (0.0262 m^2) be used in the core T-H multi-channel models.

2.5 Initial steady state conditions

The reactor is assumed to be at the end of cycle (EOC), 650 EFPD (24.58 GWD/MT average core exposure), with a boron concentration of 5 ppm, and equilibrium Xe and Sm concentration (Table 2.9). Control rod groups from 1 to 6 are completely withdrawn (wd). Group 7 is 90% wd, or 900 steps (354.0155 cm) from the bottom of lower reflector except the rod at position N12, which is stuck throughout the transient and is out of the core. The position of group 7 in terms of insertion from the top of core region is 26.9155 cm. The position of group 8 is modelled implicitly through the cross-sections and the participants do not have to account for it in their control rod models.

Five steady states at EOC are defined for initialisation of the 3-D core neutronics models for the second and third exercises. The initial steady state for the MSLB simulation, as described above, is to be calculated at both hot zero power (HZP) conditions (used to evaluate the scram worth and stuck rod worth) and HFP conditions (used as initial steady state for the transient simulation). The steady states

at HZP for both versions of the MSLB scenario are defined as follows: all the control rods (groups 1 through 7) are completely inserted except the stuck rod at position N12, which is completely wd. In state 0, all groups are completely wd. The HZP conditions are defined as follows: the power level is 2772 kWt; the fuel and moderator temperatures are 532°F (551 K); and the moderator density is 766 kg/m^3. The scram and stuck rod worths for both scenarios are evaluated by using calculated eigenvalues for states 1 and 3 for the first scenario and for states 1 and 4 for the second scenario. The scram worth is defined as:

$$\frac{dk}{k}\% = \frac{k_m - k_n}{k_m k_n} \times 100$$

where m=3, 4 and n=1.

The above-discussed five steady states are described in Table 2.10 and are used for detailed comparisons of results. For the purposes of the second exercise, one additional steady state (2a) is defined in order to address better the T-H modelling effects when making code-to-code comparisons: this additional state is the same as the second steady-state (HFP) but with uniform BC.

The calculated effective multiplication factor, k_{eff}, for the second steady state is used to divide the number of neutrons produced per fission, in order to obtain a critical initial steady state for the transient calculations. This adjustment procedure should be applied to the provided cross-section tables.

2.6 Transient calculations

For the second exercise, reactor scram is modelled to occur at 6.65 seconds into the transient. Subsequent to the reactor trip signal, the most reactive control rod (the position of the rod is N12) is assumed stuck in its fully withdrawn position. The control rod movement during the scram in the second and third exercises is modelled with a speed of 155.773 cm/sec.

Table 2.1. FA geometry data

Parameter	Value
Pellet diameter	9.391 mm/0.3697 in
Clad diameter (outside)	10.928 mm/0.43 in
Clad wall thickness	0.673 mm/0.0265 in
Fuel rod pitch	14.427 mm/0.568 in
Guide tube diameter (outside)	13.462 mm/0.53 in
Guide tube diameter (inside)	12.650 mm/0.498 in
Geometry	15×15
Number of fuel pins	208
Number of guide tubes	16
Number of in-core instrument positions per fit	1

Table 2.2. Decay constants and fractions of delayed neutrons

Group	Decay constant (s^{-1})	Relative fraction of delayed neutrons in %
1	0.012818	0.0153
2	0.031430	0.1086
3	0.125062	0.0965
4	0.329776	0.2019
5	1.414748	0.0791
6	3.822362	0.0197

Total fraction of delayed neutrons: 0.5211%.

Table 2.3. Heavy-element decay heat constants

Group No. (isotope)	Decay constant (s^{-1})	Available energy from a single atom (MeV)
70 (^{239}U)	4.91×10^{-4}	0.474
71 (^{239}Np)	3.41×10^{-6}	0.419

Table 2.4. Definition of assembly types

Assembly	Characteristics		
1	4.00 w/o	No BP	No Gd pins
2	4.95 w/o	3.5% BP	4 Gd pins
3	5.00 w/o	3.5% BP pulled	4 Gd pins
4	4.95 w/o	3.5% BP	4 Gd pins
5	4.40 w/o	No BP	No Gd pins
6	5.00 w/o	3.5% BP	4 Gd pins
7	4.85 w/o	No BP	4 Gd pins
8	4.85 w/o	No BP	4 Gd pins
9	4.95 w/o	3.5% BP pulled	4 Gd pins
10	4.95 w/o	3.5% BP	4 Gd pins
11	4.85 w/o	3.5% BP pulled	4 Gd pins
12	4.95 w/o	3.5% BP	4 Gd pins
13	5.00 w/o	3.5% BP pulled	4 Gd pins
14	5.00 w/o	No BP	8 Gd pins
15	4.95 w/o	No BP	8 Gd pins
16	4.95 w/o	3.5% BP pulled	4 Gd pins
17	4.95 w/o	3.5% BP	4 Gd pins
18	4.95 w/o	3.5% BP pulled	4 Gd pins
19	5.00 w/o	3.5% BP	4 Gd pins
20	4.40 w/o	No BP	No Gd pins
21	4.85 w/o	3.5% BP pulled	4 Gd pins
22	4.40 w/o	No BP	No Gd pins
23	4.95 w/o	3.5% BP	No Gd pins
24	4.95 w/o	3.5% BP pulled	4 Gd pins
25	5.00 w/o	No BP	8 Gd pins
26	5.00 w/o	No BP	4 Gd pins
27	5.00 w/o	No BP	No Gd pins
28	4.95 w/o	3.5% pulled	4 Gd pins
29	5.00 w/o	No BP	4 Gd pins
30	–	Radial reflector	–

Table 2.5. Composition numbers in axial layers for each assembly type

Bottom

	1	2	3	4	5	6	7	8	9	10	11	12	13	14	15	16	17	18	19	20	21	22	23	24	25	26	27	28	29	30
1	24	24	24	24	24	24	24	24	24	24	24	24	24	24	24	24	24	24	24	24	24	24	24	24	24	24	24	24	24	24
2	1	16	34	49	64	79	94	109	124	139	154	169	184	199	214	229	244	259	274	289	304	319	334	349	364	379	394	409	424	25
3	2	17	35	50	65	80	95	110	125	140	155	170	185	200	215	230	245	260	275	290	305	320	335	350	365	380	395	410	425	25
4	3	18	36	51	66	81	96	111	126	141	156	171	186	201	216	231	246	261	276	291	306	321	336	351	366	381	396	411	426	25
5	4	19	37	52	67	82	97	112	127	142	157	172	187	202	217	232	247	262	277	292	307	322	337	352	367	382	397	412	427	25
6	5	20	38	53	68	83	98	113	128	143	158	173	188	203	218	233	248	263	278	293	308	323	338	353	368	383	398	413	428	25
7	6	21	39	54	69	84	99	114	129	144	159	174	189	204	219	234	249	264	279	294	309	324	339	354	369	384	399	414	429	25
8	7	22	40	55	70	85	100	115	130	145	160	175	190	205	220	235	250	265	280	295	310	325	340	355	370	385	400	415	430	25
9	7	22	40	55	70	85	100	115	130	145	160	175	190	205	220	235	250	265	280	295	310	325	340	355	370	385	400	415	430	25
10	7	22	40	55	70	85	100	115	130	145	160	175	190	205	220	235	250	265	280	295	310	325	340	355	370	385	400	415	430	25
11	7	22	40	55	70	85	100	115	130	145	160	175	190	205	220	235	250	265	280	295	310	325	340	355	370	385	400	415	430	25
12	8	23	41	56	71	86	101	116	131	146	161	176	191	206	221	236	251	266	281	296	311	326	341	356	371	386	401	416	431	25
13	8	23	41	56	71	86	101	116	131	146	161	176	191	206	221	236	251	266	281	296	311	326	341	356	371	386	401	416	431	25
14	8	23	41	56	71	86	101	116	131	146	161	176	191	206	221	236	251	266	281	296	311	326	341	356	371	386	401	416	431	25
15	8	23	41	56	71	86	101	116	131	146	161	176	191	206	221	236	251	266	281	296	311	326	341	356	371	386	401	416	431	25
16	9	27	42	57	72	87	102	117	132	147	162	177	192	207	222	237	252	267	282	297	312	327	342	357	372	387	402	417	432	25
17	9	27	42	57	72	87	102	117	132	147	162	177	192	207	222	237	252	267	282	297	312	327	342	357	372	387	402	417	432	25
18	9	27	42	57	72	87	102	117	132	147	162	177	192	207	222	237	252	267	282	297	312	327	342	357	372	387	402	417	432	25
19	9	27	42	57	72	87	102	117	132	147	162	177	192	207	222	237	252	267	282	297	312	327	342	357	372	387	402	417	432	25
20	10	28	43	58	73	88	103	118	133	148	163	178	193	208	223	238	253	268	283	298	313	328	343	358	373	388	403	418	433	25
21	11	29	44	59	74	89	104	119	134	149	164	179	194	209	224	239	254	269	284	299	314	329	344	359	374	389	404	419	434	25
22	12	30	45	60	75	90	105	120	135	150	165	180	195	210	225	240	255	270	285	300	315	330	345	360	375	390	405	420	435	25
23	13	31	46	61	76	91	106	121	136	151	166	181	196	211	226	241	256	271	286	301	316	331	346	361	376	391	406	421	436	25
24	14	32	47	62	77	92	107	122	137	152	167	182	197	212	227	242	257	272	287	302	317	332	347	362	377	392	407	422	437	25
25	15	33	48	63	78	93	108	123	138	153	168	183	198	213	228	243	258	273	288	303	318	333	348	363	378	393	408	423	438	25
26	26	26	26	26	26	26	26	26	26	26	26	26	26	26	26	26	26	26	26	26	26	26	26	26	26	26	26	26	26	26

Top

Table 2.6. Range of variables

T Fuel (°K)	Void	T Mod (°K)	Pressure (psia/MPa)	Rho M. (kg/m^3/lb/ft^3)	Boron (ppm)
500.00	0.00	605.22	2200.0/15.17	641.40/8.2385	5.00
760.22	0.00	605.22	2200.0/15.17	641.40/8.2385	5.00
867.27	0.00	605.22	2200.0/15.17	641.40/8.2385	5.00
921.88	0.00	605.22	2200.0/15.17	641.40/8.2385	5.00
1500.00	0.00	605.22	2200.0/15.17	641.40/8.2385	5.00
500.00	0.00	579.35	2200.0/15.17	711.43/9.1379	5.00
760.22	0.00	579.35	2200.0/15.17	711.43/9.1379	5.00
867.27	0.00	579.35	2200.0/15.17	711.43/9.1379	5.00
921.88	0.00	579.35	2200.0/15.17	711.43/9.1379	5.00
1500.00	0.00	579.35	2200.0/15.17	711.43/9.1379	5.00
500.00	0.00	551.00	2200.0/15.17	769.47/9.8834	5.00
760.22	0.00	551.00	2200.0/15.17	769.47/9.8834	5.00
867.27	0.00	551.00	2200.0/15.17	769.47/9.8834	5.00
921.88	0.00	551.00	2200.0/15.17	769.47/9.8834	5.00
1500.00	0.00	551.00	2200.0/15.17	769.47/9.8834	5.00
500.00	0.00	545.00	1300.00/8.963	772.44/9.9216	5.00
760.22	0.00	545.00	1300.00/8.963	772.44/9.9216	5.00
867.27	0.00	545.00	1300.00/8.963	772.44/9.9216	5.00
921.88	0.00	545.00	1300.00/8.963	772.44/9.9216	5.00
1500.00	0.00	545.00	1300.00/8.963	772.44/9.9216	5.00
500.00	0.00	538.71	1000.00/6.895	781.31/10.035	5.00
760.22	0.00	538.71	1000.00/6.895	781.31/10.035	5.00
867.27	0.00	538.71	1000.00/6.895	781.31/10.035	5.00
921.88	0.00	538.71	1000.00/6.895	781.31/10.035	5.00
1500.00	0.00	538.71	1000.00/6.895	781.31/10.035	5.00
500.00	0.00	520.00	800.00/5.516	810.10/10.405	5.00
760.22	0.00	520.00	800.00/5.516	810.10/10.405	5.00
867.27	0.00	520.00	800.00/5.516	810.10/10.405	5.00
921.88	0.00	520.00	800.00/5.516	810.10/10.405	5.00
1500.00	0.00	520.00	800.00/5.516	810.10/10.405	5.00

Table 2.7. Key to macroscopic cross-section tables

T_{f1}	T_{f2}	T_{f3}	T_{f4}	T_{f5}
ρ_{m1}	ρ_{m2}	ρ_{m3}	ρ_{m4}	ρ_{m5}
ρ_{m6}	Σ_1	Σ_2	...	
		...	Σ_{29}	Σ_{30}

Where:

– T_f is the Doppler (fuel) temperature (°K)

– ρ_m is the moderator density (kg/m^3)

Macroscopic cross-sections are in units of cm^{-1}

Table 2.8. Macroscopic cross-section tables structure

NEM – cross-section table input.

T fuel	Rho mod.	Boron ppm.	T mod.
5	6	0	0

Cross section set #

#

Group No. 1

- Diffusion coefficient table.
- Absorption cross section table.
- Fission cross section table.
- Nu-fission cross section table.
- Scattering from group 1 to 2 cross section table.

Group No. 2

- Diffusion coefficient table.
- Absorption cross section table.
- Fission cross section table.
- Nu-fission cross section table.
- Xenon absorption cross section table.

Inv. neutron velocities.

Table 2.9. Initial conditions for TMI-1 at 2 772 MWt

Parameter	Value
Core power	2 772.00 MWt
RCS cold leg temperature	555°F/563.76°K
RCS hot leg temperature	605°F/591.43°K
Lower plenum pressure	2 228.5 psia/15.36 MPa
Outlet plenum pressure	2 199.7 psia/15.17 MPa
RCS pressure	2 170.00 psia/14.96 MPa
Total RCS flow rate	38 806.2 lb/sec/17 602.2 kg/sec
Core flow rate	35 389.5 lb/sec/16 052.4 kg/sec
Bypass flow rate	3 416.7 lb/sec/1 549.8 kg/sec
Pressuriser level	220 inches/558.8 cm
Feedwater/steam flow per OTSG	1 679 lb/sec/761.59 kg/sec
OTSG outlet pressure	930.00 psia/6.41 MPa
OTSG outlet temperature	571°F/572.63°K
OTSG superheat	35°F/19.67°K
Initial SG inventory	57 320 lbm/26 000 kg.
Feedwater temperature	460°F/510.93°K

Table 2.10. Definition of steady-states

Number	T-H conditions	Control rod positions	Scenario version
0	HZP	Groups 1-7 ARO*	
1	HZP	Groups 1-6 ARO Group 7 is 90% wd N12 is 100% wd	
2	HFP	Groups 1-6 ARO Group 7 is 90% wd N12 is 100% wd	
3	HZP	Group 1-7 ARI N12 is 100% wd	1
4	HZP	Group 1-7 ARI N12 is 100% wd	2

* ARO – all rods out; ARI – all rods inserted.

Figure 2.1. Cross-section of the reactor core

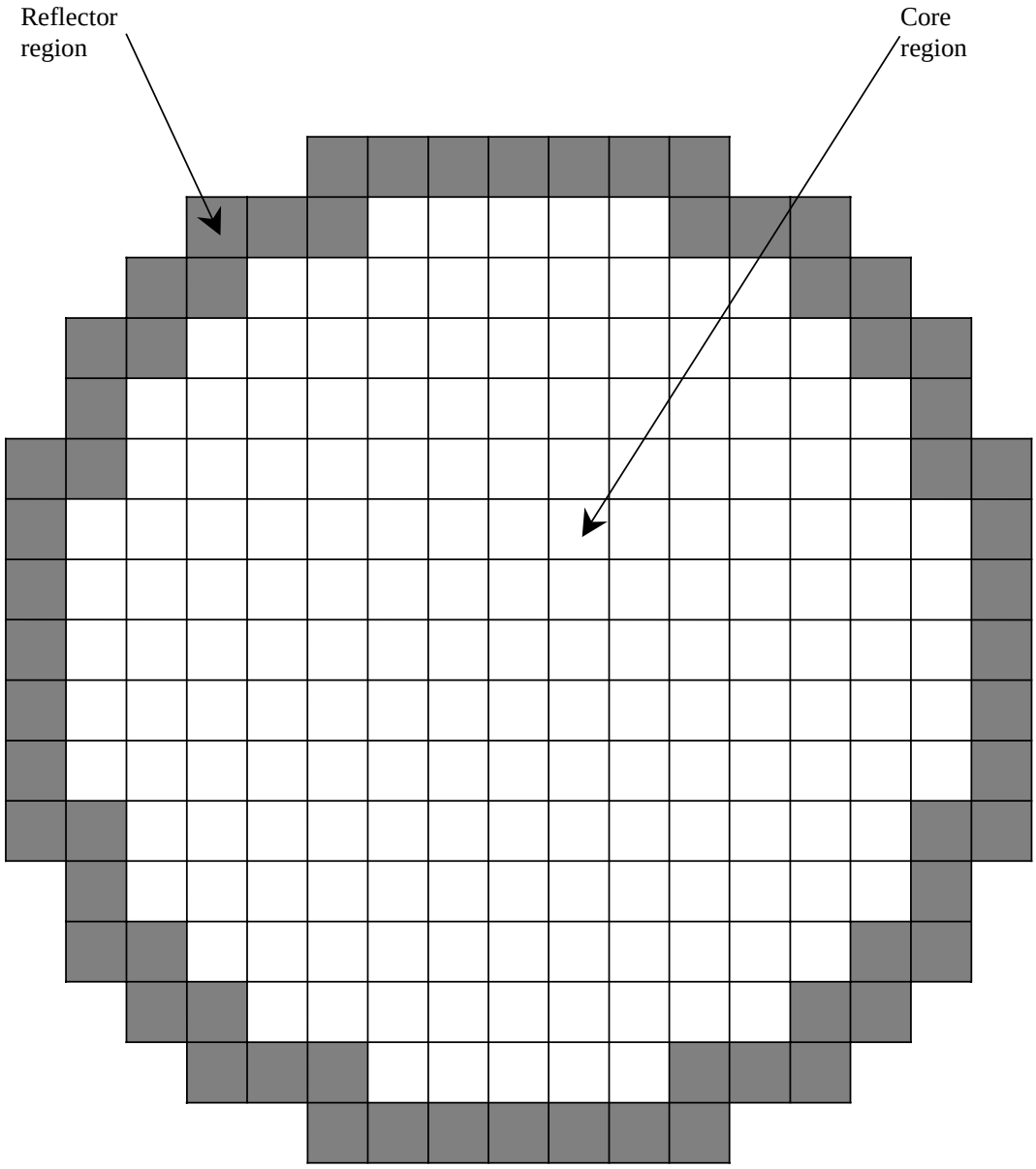

Figure 2.2. Arrangement of control rods

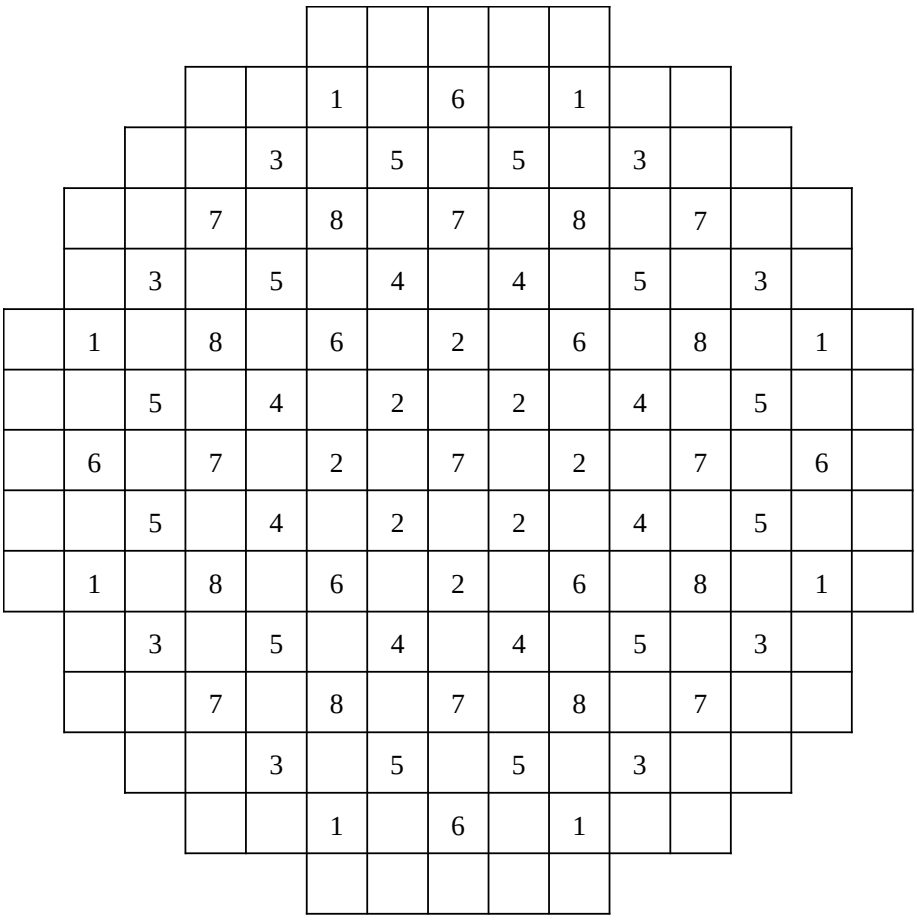

Bank	No. Rods	Purpose
1	8	Safety
2	8	Safety
3	8	Safety
4	8	Safety
5	12	Regulating
6	8	Regulating
7	9	Regulating
8	8	APSR

Figure 2.3. Two-dimensional assembly type map

	8	9	10	11	12	13	14	15
H	1 52.863	2 30.192	3 56.246	4 30.852	5 49.532	6 28.115	7 53.861	8 55.787
K		9 57.945	10 30.798	11 55.427	12 29.834	13 53.954	14 25.555	15 49.166
L			16 57.569	17 30.218	18 54.398	19 27.862	20 23.297	21 47.300
M				22 49.712	23 28.848	24 52.846	25 40.937	
N					26 48.746	27 23.857	28 41.453	
O						29 37.343	A B	
P								
R								

A. Type of fuel assembly.
B. Assembly average burn-up in GWD/T.

Figure 2.4. TRAC-PF1 vessel radial and azimuthal nodalization

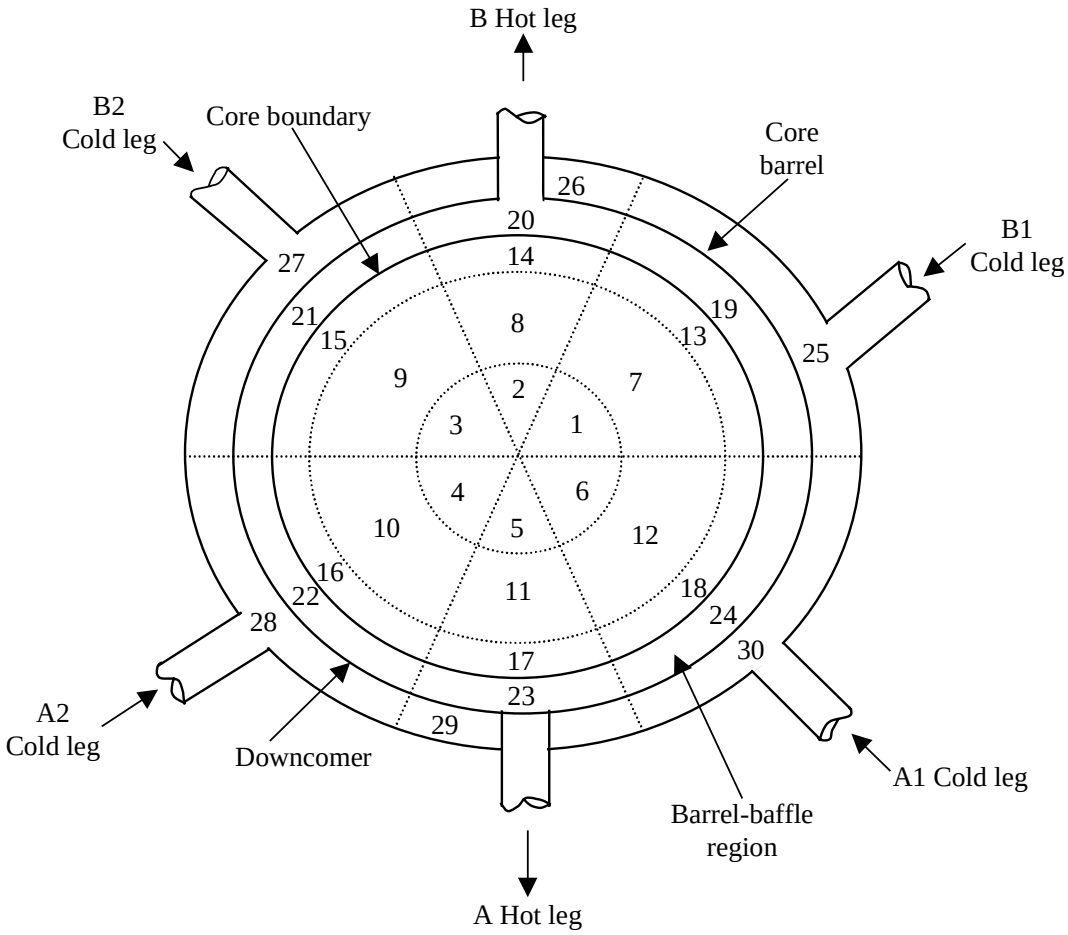

Figure 2.5. TRAC-PF1 vessel axial nodalization

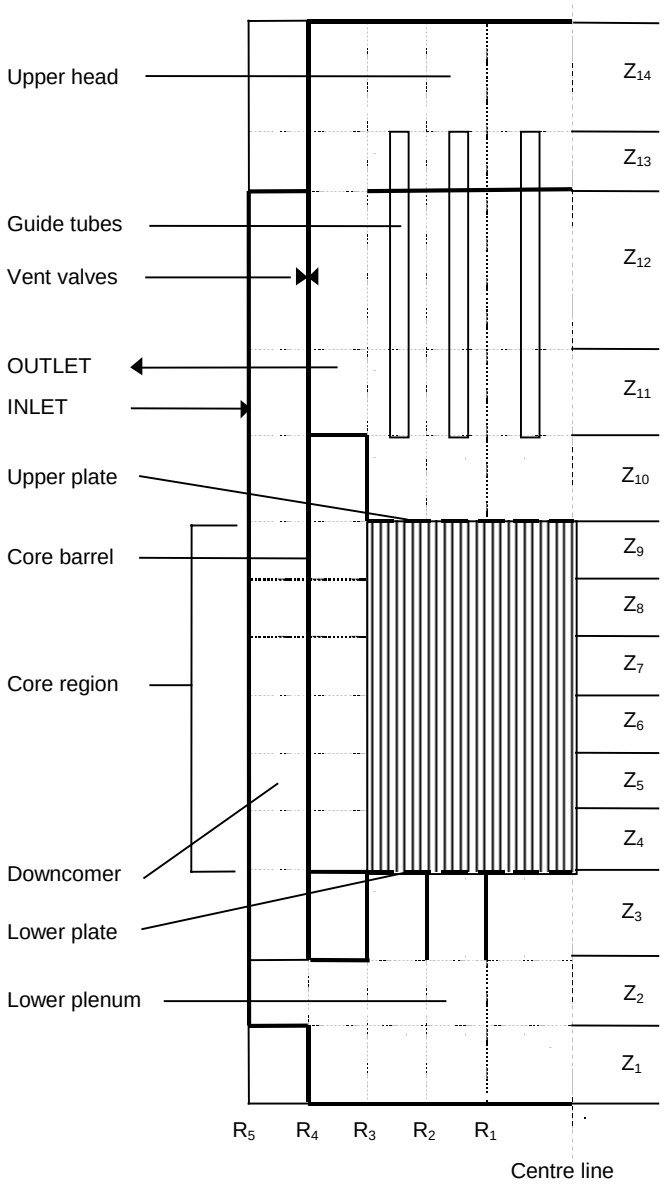

Figure 2.6. TRAC-PF1/NEM radial mapping scheme between core neutronics model and heat structure component

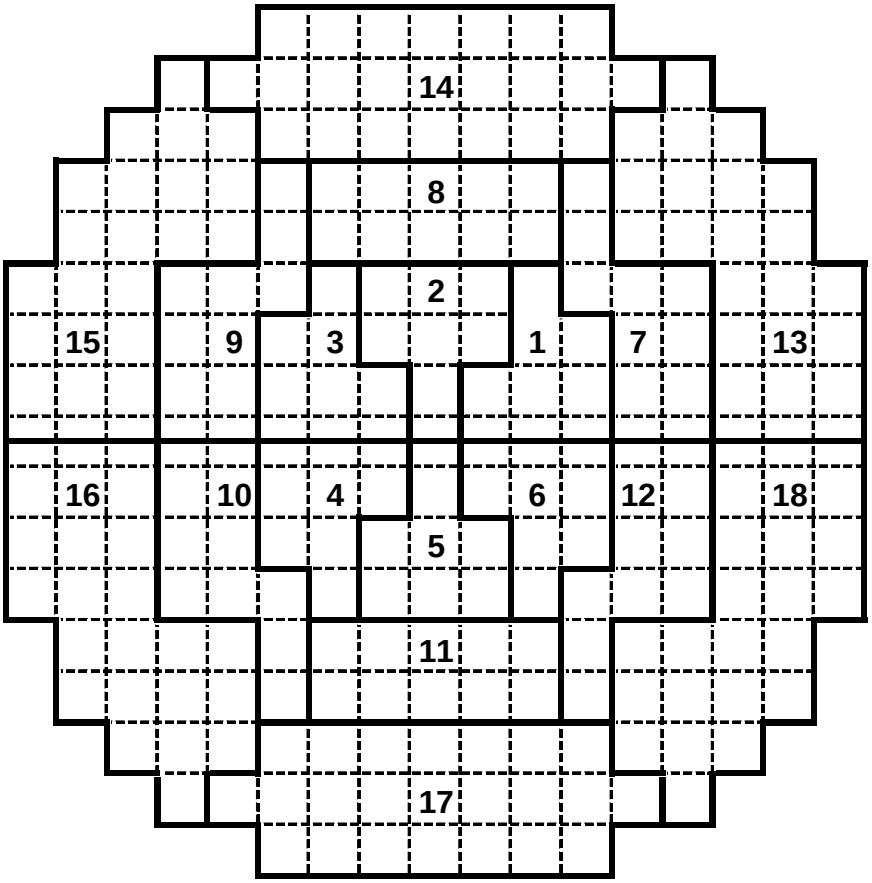

Figure 2.7. Transient core boundary conditions mapping scheme for the second exercise

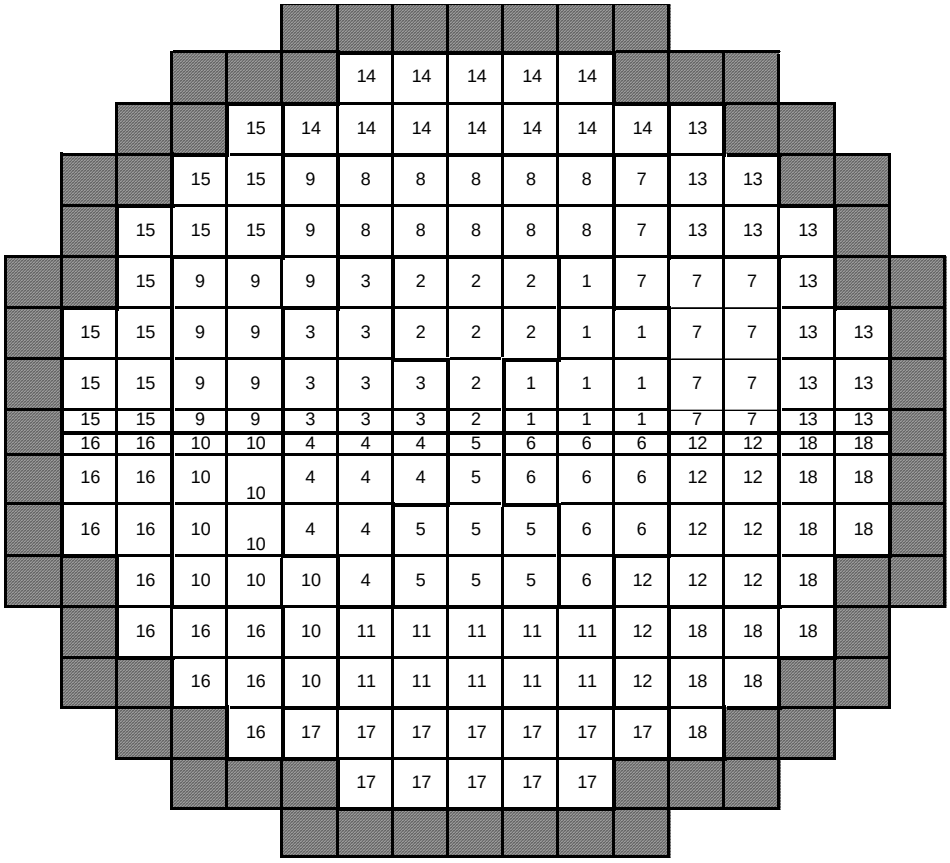

Chapter 3

STATISTICAL METHODOLOGY

Due to the lack of experimental data for the current phase of the benchmark problem, the reference solution for each requested parameter is based upon the statistical mean value of all submitted results. The comparisons to follow in this and later chapters are thus properly called code-to-code comparisons, rather than code-to-data comparisons. While perhaps not ideal, this method provides the strongest basis from which to complete a statistical analysis and comparison of the results for this exercise. In Section 3.1, the standard methods used to generate the reference solution will be presented. Special methods used for the analysis of normalised parameters will be presented in Section 3.2, and some remaining issues will be discussed in Section 3.3. Finally, in Section 3.4, a list of the parameters for which reference values have been calculated will be provided.

3.1 Standard techniques for comparison of results

In exercise 2 of this benchmark problem, several types of data must be analysed and the results of all participants compared. These data types are:

1. Time history data.
2. 2-D radial distributions.
3. 1-D axial distributions.
4. Integral parameter values.

It is necessary to develop a suite of statistical methods for each of these data types, to be applied whenever a comparison is desired. What follows is a description of each of these methods.

3.1.1 Time history data

In this exercise, various parameters such as power, temperature, and coolant density are plotted as a function of time. Points of interest are isolated and submitted to a basic statistical analysis as described below.

Step 1: *Isolate points of interest.* Such points include the highest return-to-power, the time of highest power before and after trip, and values at the end-of-transient for all parameters. These points are identified for all time history sets, and the values of all participants are collected. For Exercise 2, these points are listed in Table 3.1.

Table 3.1. Points of interest for exercise two time histories

Time History	Point of interest	Scenario
Total power	Highest power before trip	2
Total power	Highest power after trip	2
Total power	Power at EOT	1, 2
Total power	Time of highest return to power	2
Fission power	Highest power before trip	2
Fission power	Highest power after trip	2
Fission power	Power at EOT	1, 2
Coolant density	Density at EOT	1, 2
Doppler temperature	Temperature at EOT	1, 2
Maximum nodal Doppler temperature	Temperature at EOT	1, 2

Step 2: *Calculate mean value and standard deviation.* These two standard statistical values are calculated according to the formulae:

$$\bar{x} = \frac{\sum_{i}^{N} x_i}{N} \tag{3.1}$$

$$\sigma = \pm\sqrt{\frac{\sum_{i}^{N} (x_i - \bar{x})^2}{N-1}} \tag{3.2}$$

Mean values and standard deviations are calculated at each of the points defined in Step 1, to be used in the remaining steps.

Step 3: *Determine and report the deviation and figure of merit for each participant's value.* The deviation, e, which is merely the difference between the participant's value and the mean as determined in Step 2, is calculated according to:

$$e_i = (x_i - \bar{x}) \tag{3.3}$$

After calculating the deviation, the figure of merit, Φ, can be determined according to the formula:

$$\Phi_i = \frac{e_i}{\sigma} \tag{3.4}$$

This figure of merit provides a means for comparison that is perhaps easier to interpret than the raw deviations, relating the participant's deviation to the overall standard deviation. After calculating the deviations and figures of merit, comparison values are tabulated.

3.1.2 2-D radial distributions

Exercise 2 contains many steady state and transient snapshots of the radial distribution through the core for certain parameters. Due to the two-dimensional nature of such data, it is difficult to plot the results as with time history data and 1-D distributions. However, the same statistical methods can be used to generate mean values, standard deviations and participant deviations, and figures of merit.

Step 1: *Calculate mean and standard deviation for each 2-D cell.* These reference values are calculated according to equations (3.1) and (3.2). Such an analysis results in a 2-D map for both mean values and standard deviations, rather than a single value for each parameter. Comparisons can thus be made for each cell, rather than only specific cells of interest.

Step 2: *Tabulate deviations and figures of merit.* For each participant, a map will be generated that shows deviations from the mean at each radial position. A second map will report the figures of merit.

3.1.3 1-D axial distributions

Exercise 2 also contains many steady state and transient snapshots of the axial distribution of certain parameters through the core. These parameters will usually be a function of height, and can thus be displayed as an x-y plot. Similar methods of statistical analysis will be applied as with the previous two data types.

Step 1: *Calculate mean and standard deviation for each 1-D cell.* This analysis is similar to that for the 2-D distributions, and 1-D maps will be generated for the mean values and standard deviations in each axial layer.

Step 2: *Determine deviations and figures of merit.* For each participant, a single table will be prepared that shows deviations from the mean and figures of merit at each axial position.

3.1.4 Integral parameters

These parameters include such values as multiplication factor, power peaking factors, and control rod worths. In this case, there is no need to condition the data by isolating points of interest. Likewise, there are no curves to analyse. Thus, the mean value and standard deviation should be sufficient to facilitate a comparison of the results.

Step 1: *Calculate mean and standard deviation.* Reference values are calculated according to equations (3.1) and (3.2).

Step 2: *Determine deviations and figures of merit.* These values are calculated according equations (3.3) and (3.4).

3.2 Statistical analysis of normalised parameters

In exercise 2, three parameters are provided as normalised relative distributions: 2-D core-averaged radial power, 1-D core-averaged axial power, and 1-D axial power at the position of the stuck rod. These parameters must be given special attention during the statistical analysis because under certain circumstances the normalisation will become skewed. Treating each of these parameters separately, the procedure for generating a comprehensive analysis that preserves the normalisation will be discussed.

3.2.1 2-D core-averaged radial power distribution

This parameter is collected for all of the steady state cases and transient snapshots. The goal of the statistical analysis is to derive an average normalised power for each assembly,

$$\overline{NP_i} = \frac{\overline{p_i}}{\overline{p_{FA}}} \tag{3.5}$$

where, for N participants, $\overline{p_i}$, the average power density in radial assembly location i, is

$$\overline{p_i} = \frac{1}{N}\sum_{j=1}^{N} p_{ij} \tag{3.6}$$

and $\overline{p_{FA}}$, the averaged assembly power density, is

$$\overline{p_{FA}} = \frac{1}{N}\sum_{j=1}^{N} p_{FA,j} \tag{3.7}$$

Thus,

$$\overline{NP_i} = \frac{\sum_{j=1}^{N} p_{ij}}{\sum_{j=1}^{N} p_{FA,j}} \tag{3.8}$$

In the initial steady state cases the total core power is specified as Q=2772 MW for the hot-full-power (HFP) cases, and Q=2772 kW (0.1% of full power) for the hot-zero-power cases (HZP), so that the average power per fuel assembly is the same for all participants and:

$$\overline{NP_i} = \frac{1}{N}\frac{\sum_{j=1}^{N} p_{ij}}{p_{FA,c}} = \frac{1}{N}\sum_{j=1}^{N}\frac{p_{ij}}{p_{FA,c}} = \frac{1}{N}\sum_{j=1}^{N} NP_{ij} \qquad (3.9)$$

where given the total number of fuel assemblies, M is 177,

$$p_{FA,c} = \frac{Q}{M} \qquad (3.10)$$

Thus, for the steady state cases the standard techniques described above can be applied directly to the normalised values provided by each participant. For the transient snapshots, however, where total power level and power per assembly vary among the participants, the following corrected procedure must be applied.

Step 1: *Convert normalised values into absolute values.* Absolute values are achieved by multiplying the normalised value in each 2-D cell for each participant by the average power per assembly for the same participant, where the latter value is just the total core power for that participant divided by 177 fuel assemblies.

Step 2: *Calculate participant-averaged average power per assembly.* All participant values for total core power are averaged by the standard averaging technique to get the average core power. This value is divided by the number of fuel assemblies, 177, to get the average power per assembly, averaged over all participants. The same result can be obtained by averaging directly, with equation (3.1), all participants' values for average power per assembly.

Step 3: *Generate mean solution using absolute values.* The map of absolute mean values is generated by the standard averaging procedure.

Step 4: *Re-normalise mean solution.* Normalisation is attained by dividing each cell of the absolute map by the average power per assembly calculated in Step 2.

Unfortunately, the standard deviation and figure-of-merit can not be included in a normalised form, since the meaning of these statistical functions would be lost. Therefore, three maps must be provided instead of the usual two. Mean values and standard deviations are provided using absolute powers, and are accompanied by maps of the normalised mean values. Participant deviations and figures of merit are calculated relative to the absolute mean solution.

3.2.2 1-D core-averaged axial power distribution

This parameter is also collected for every steady state case and transient snapshot, and the final specifications require that all participants divide the core into 24 equal axial nodes. Where this is the case, the statistical analysis will be similar to that for the radial power distribution. The normalised mean axial power for a given axial node is given by

$$\overline{NP_{z,i}} = \frac{\overline{p_{z,i}}}{\overline{p_z}} \tag{3.11}$$

where $\overline{p_{z,i}}$, the average power density axial layer i, is given by

$$\overline{p_{z,i}} = \frac{1}{N}\sum_{j=1}^{N} p_{z,ij} \tag{3.12}$$

and $\overline{p_z}$, the core-averaged axial power density, is

$$\overline{p_z} = \frac{1}{N}\sum_{j=1}^{N} p_{z,j} = \frac{1}{N}\sum_{j=1}^{N} \frac{p_{FA,j}}{24} \tag{3.13}$$

Thus,

$$\overline{NP_{z,i}} = \frac{\sum_{j=1}^{N} p_{z,ij}}{\sum_{j=1}^{N} \frac{p_{FA,j}}{24}} \tag{3.14}$$

For the steady state cases, where the total power level, Q, and the average power per assembly are constant for all participants,

$$\overline{NP_{z,i}} = \frac{1}{N}\frac{1}{24}\sum_{j=1}^{N} \frac{p_{z,ij}}{p_{FA,j}} = \frac{1}{N}\sum_{j=1}^{N} NP_{z,ij} \tag{3.15}$$

As a result, the standard techniques for 1-D distribution can be applied for the steady state cases; however, for the transient snapshots, where the average power per assembly will vary among the participants, the following procedure must be utilised.

Step 1: *Convert normalised values into absolute values.* Absolute values are achieved by multiplying the normalised value in each axial node for each participant by the average power per node in the average assembly for the same participant, where the latter value is just the total core power for that participant divided by 177 fuel assemblies and 24 axial nodes.

Step 2: *Calculate participant-averaged average power per axial node.* All participant values for total core power are averaged by the standard averaging technique to get the average core power. This value is divided by the number of fuel assemblies, 177, to get the average power per assembly, which is finally divided by 24 to get the average power per axial node, averaged over all participants. The same result can be obtained by averaging directly all participants' values for average power per axial node, using equation (3.1).

Step 3: *Generate mean solution using absolute values.* The table of absolute mean values is generated by the standard averaging procedure.

Step 4: *Re-normalise mean solution.* Normalisation is attained by dividing each cell of the absolute map by the average power per node calculated in Step 2.

Once again, the standard deviation and figure-of-merit can not be included in a normalised form and two axial tables will be provided. Absolute mean values and standard deviations are provided along with re-normalised mean values in one table. Participant deviations and figures of merit, calculated relative to the absolute values are presented in a second table. It should be noted that this procedure could be applied only where the participants have used 24 equal axial layers. Results from participants who do not adhere to this specification must first have their data converted to 24 equal nodes via a cell-volume weighting procedure.

3.2.3 1-D axial power distribution in the stuck rod

This parameter is collected for the HFP steady state cases and all transient snapshots, and is treated in a similar manner as for the core-averaged axial power. Again, the specifications request that the stuck rod assembly be divided into 24 equal nodes. In the case of the steady state at HFP, where the distributions are based on the known whole-core volume normalisation, the standard techniques can be applied. For the transient snapshots, the power in the stuck rod varies among the participants and the average normalised power per node is given by

$$\overline{NP_{z,i}} = \frac{\sum_{j=1}^{N} p_{z,ij}}{\sum_{j=1}^{N} \frac{p_{N12,j}}{24}} \qquad (3.16)$$

where the total power in the stuck rod assembly at position N12 can be extracted from each participant's 2-D core-averaged radial power distribution. The following method must be applied in every transient case.

Step 1: *Convert normalised values into absolute values.* The absolute values are found by multiplying the normalised value in each axial node for each participant by the average power per 3-D node in the core for the same participant, where the latter value is the total core power divided 177 assemblies and 24 axial nodes.

Step 2: *Calculate participant-averaged average power per axial node.* All participant values for total core power are averaged by the standard averaging technique to get the average core power. This value is divided by the number of cells in the core – 177 assemblies times 24 axial layers – to get the average power per 3-D node, averaged over all participants.

Step 3: *Generate mean solution using absolute values.* The map of absolute mean values is generated by the standard averaging procedure.

Step 4: *Re-normalise mean solution.* Normalisation is attained by dividing each cell of the absolute map by the average power per node calculated in Step 2.

As with the previous two parameters, the results are reported in the form of mean values and standard deviations of the absolute values along with a re-normalised mean solution. Participant deviations and figures of merit are again calculated relative to the absolute mean solution

3.2.4 Multiple code dependencies

It has been noted that some of the sets of results that have been submitted for this exercise are not fully independent of each other. That is, certain participants have submitted multiple sets from codes that differ from each other to varying degrees. In some cases, the differences are significant, and involve quite different kinetics models. In other cases, the differences are subtler, involving different nodalisation schemes. In the case of codes with only subtle differences, it may not be appropriate to treat the results as fully separate, and therefore subject to independent treatment in the averaging techniques described above.

To account for this circumstance, a two step averaging process has been developed whereby sets of results that are determined to be "dependent" on each other are first averaged together, and the subsequent mean participant values are then included in the final averaging process. However, after examining the descriptions of each code that has been used in developing the submitted results, it was determined that such a two-step averaging process is not necessary in the present case, and so has not been applied.

3.2.5 Reference results

Analysis is performed for six steady state cases, four transient snapshots, and five time histories. Steady state cases 0, 1, 3, and 4 are performed at HZP, while steady state cases 2 and 2a are performed at HFP. Transient snapshots are taken at the highest power before scram (state 5), highest power after scram for scenario 2 (state 6), EOT for scenario 1 (state 7), and EOT for scenario 2 (state 8).

The reference solutions for all parameters are provided in Appendix C, with the steady state values presented first, followed by transient snapshot parameters, and ending with the time history solutions. The parameters that are analysed, in the order in which they are found in the Appendix C, are listed below:

- For the initial HZP states (0, 1, 3 and 4), the following parameters are analysed: k_{eff}; 2-D normalised power (NP) distribution; core-averaged axial power distribution; the power peaking factors F_{xy}, F_z and axial offset.

- For the initial HFP steady-states (2 and 2a), the same information as for the HZP states plus: 2-D maps for inlet coolant temperature, inlet flow rate and outlet coolant temperature; axial distributions for the stuck rod (position N12) – relative power (normalised to the core power level), coolant density, mass flow rate and Doppler temperature.

- Scram and stuck rod worths for both scenarios.

- Snapshots at time of maximum power before reactor trip, at time of maximum power after reactor trip, and at 100 seconds of the transient – the same data as for the HFP steady states except the total and fission power levels are analysed instead of k_{eff}.

- Time histories (core volume averaged without the reflector region): total power, fission power, coolant density, and Doppler temperature. In addition, the maximum nodal Doppler temperature vs. time is compared also.

As it can be seen above the local parameter distributions are monitored at the position of the stuck rod. Since the local parameter predictions are sensitive to the spatial coupling schemes it was decided at the Third Benchmark Workshop [5] that in the final report these results are compared in two groups: one cluster for very detailed spatial mesh overlays (one neutronics node per thermal-hydraulic cell/channel) – this is called 177 channel cluster, and one separate cluster for coarse mesh overlays – it is called 18 channel cluster. Subsequently separate mean solutions and standard deviations are produced for these two clusters.

The participant deviations and figures of merit are presented in Appendix D, and are listed in the same order as the reference solutions. In each case, where separate tables are necessary for each participant, these are listed in alphabetical order. A full list of the tables and figures presented in the Appendices C and D can be found in the table of contents.

Chapter 4

RESULTS AND DISCUSSION

The tables and figures in this chapter provide a comparison of the participants' results with the reference solution for the parameters that have the greatest effect on the initial steady state and the two versions of the transient scenario. In each case, the tables show values of standard deviation and figure of merit (as defined in Chapter 3) for each participant's result for a given parameter. Selected figures, included in this Chapter, show the scatter of data about the reference (mean) solution. The analysis of results is grouped in three sections. In Section 4.1 steady state results at initial conditions are discussed. The analysis of results for the transient snapshots is presented in Section 4.2. For these two groups of results the discussion is further subdivided in three subsections: singular (integral) parameter values, 1-D axial distributions, and 2-D radial distributions. The transient time history data is discussed in Section 4.3. The complete detailed comparison of the participants' results is provided in Appendix D (D1 – integral parameters, D2 – 1-D axial distributions, D3 – 2-D radial distributions, and D4 – core-averaged time evolutions).

4.1 Steady state results

4.1.1 Integral parameters

Six states at EOC were defined for initialisation of coupled 3-D coupled core models for the second exercise. Steady state cases 0, 1, 3, and 4 are performed at HZP, while steady state cases 2 and 2a are performed at HFP. The four of them, which are calculated at HZP conditions, are modelled with fixed thermal-hydraulic feedback *i.e.* they can be considered as "clean" neutronics problems. Keeping in mind that that the participants are provided with the cross-section libraries and the linear interpolation routine, one can conclude that the discrepancies for these state should result from different methods for solving the steady-state diffusion problem, and the neutronics nodalisation schemes especially in radial plane (1 node per assembly – 1 npa – vs. 4 npa schemes). This conclusion is supported by the fact that larger deviations are observed in more heterogeneous core configurations namely rodded states 3 and 4 at HZP conditions. For example the reference set of the BE/Tractebel results (Appendix B) as well as the both EDF sets of results (Appendix B) are obtained with 4 npa radial scheme while the rest of participants have used 1 npa scheme. The HFP states 2 and 2a are modelled with full thermal-hydraulic feedback, which represented more difficult modelling challenge to participants. The differences in core thermal-hydraulic models used by participants as 1-D parallel channels vs. 3-D models; and coarse-mesh (18 channels/cells in radial plane) vs. detailed (177 channels/cells); and heat-structure nodding and mapping schemes and etc. caused larger discrepancies as compared to the HZP comparisons.

The following integral parameters were compared: multiplication factor (k_{eff}), radial and axial power peaking factors (Fxy and Fz), and axial offset (all of these parameters are unit less), and the tripped rod worth (TRW) and stuck rod worth (SRW) (both in dk/k). These comparisons are

summarised in Tables 4.1-4.10. In each case the participants are in a reasonable agreement. The results of Iberdrola show the largest deviations for k_{eff} and in some cases for Fxy. The reason can be found in the fact that RETRAN-3D/MOD002 only works with a limited number of compositions (298) (Appendix B). Due to the number of compositions given in the specifications are 438, a procedure of reduction has been made to obtain the desired number. The final number of compositions used is 264 (261 compositions + 3 reflector comp.), which affects the accuracy of the obtained results.

Table 4.1. Participant deviations for steady state k_{eff}

Participants	**0**	**1**	**2**	**2a**	**3**	**4**
Mean	**1.0337**	**1.0318**	**1.0039**	**1.0023**	**0.9854**	**1.0002**
ANL	0.0012	0.0011	0.0011	0.0028	0.0014	0.0014
BE/Tractebel 1	0.0018	0.0018	0.0000	0.0017	0.0021	0.0020
BE/Tractebel 2	0.0017	0.0016	0.0010	0.0014	0.0016	0.0017
CEA 1	0.0016	0.0016	0.0005	0.0023	0.0015	0.0016
CEA 2	–	–	0.0004	–	–	–
CSA/GPUN	0.0019	0.0019	0.0028	–	0.0023	0.0022
EDF	0.0015	0.0016	-0.0008	0.0019	0.0022	0.0020
Framatome ANP/FZK 1	0.0017	0.0016	0.0010	–	0.0015	0.0016
Framatome ANP/FZK 2	–	–	0.0018	–	–	–
FZR	0.0017	0.0015	0.0009	0.0022	0.0014	0.0016
GRS	0.0010	0.0008	-0.0006	–	0.0002	0.0005
Iberdrola	-0.0298	-0.0280	-0.0199	-0.0183	-0.0323	-0.0322
KAERI 1	0.0018	0.0017	0.0032	–	0.0021	0.0020
KAERI 2	0.0018	0.0017	0.0012	0.0025	0.0021	0.0020
PSU	0.0017	0.0015	0.0030	–	0.0023	0.0024
Purdue/NRC 1	0.0018	0.0017	0.0022	–	0.0021	0.0020
Purdue/NRC 2	0.0018	0.0017	0.0023	–	0.0021	0.0020
UP/UZ	0.0004	0.0003	0.0005	–	-0.0002	0.0001
UPM	0.0021	0.0020	0.0018	0.0023	0.0030	0.0026
UPV	0.0018	0.0016	-0.0025	–	0.0020	0.0020
VTT	0.0024	0.0022	0.0001	0.0013	0.0029	0.0027

Table 4.2. Participant figures of merit for steady state k_{eff}

Participants	0	1	2	2a	3	4
Standard Devaition	**0.0072**	**0.0068**	**0.0048**	**0.0064**	**0.0079**	**0.0078**
ANL	0.1649	0.1620	0.2372	0.4323	0.1730	0.1800
BE/Tractebel 1	0.2534	0.2622	-0.0022	0.2566	0.2621	0.2579
BE/Tractebel 2	0.2354	0.2416	0.2183	0.2115	0.2074	0.2170
CEA 1	0.2258	0.2298	0.1028	0.3577	0.1916	0.2055
CEA 2	–	–	0.0860	–	–	–
CSA/GPUN	0.2673	0.2754	0.5839	–	0.2940	0.2771
EDF	0.0015	0.0016	-0.0008	0.0019	0.0022	0.0020
Framatome ANP/FZK 1	0.0017	0.0016	0.0010	–	0.0015	0.0016
Framatome ANP/FZK 2	–	–	0.0018	–	–	–
FZR	0.2327	0.2218	0.1801	0.3361	0.1843	0.1981
GRS	0.1331	0.1237	-0.1304	–	0.0227	0.0676
Iberdrola	-4.1221	-4.1215	-4.1826	-2.8383	-4.1091	-4.1163
KAERI 1	0.2534	0.2519	0.6700	–	0.2621	0.2553
KAERI 2	0.2534	0.2519	0.2456	0.3856	0.2621	0.2553
PSU	0.2313	0.2268	0.6259	–	0.2913	0.3039
Purdue/NRC 1	0.2538	0.2525	0.4679	–	0.2623	0.2571
Purdue/NRC 2	0.2534	0.2519	0.4872	–	0.2621	0.2566
UP/UZ	0.0515	0.0383	0.1070	–	-0.0295	0.0075
UPM	0.2839	0.2902	0.3717	0.3608	0.3793	0.3269
UPV	0.2451	0.2430	-0.5169	–	0.2527	0.2528
VTT	0.3364	0.3196	0.0167	0.2084	0.3704	0.3409

Table 4.3. Participant deviations for steady state Fxy

Participants	0	1	2	2a	3	4
Mean	**1.3609**	**1.4324**	**1.3536**	**1.3320**	**5.4579**	**3.6304**
ANL	0.0031	0.0036	-0.0153	0.0064	-0.0659	-0.0384
BE/Tractebel 1	0.0021	0.0016	-0.0266	-0.0050	-0.0089	-0.0124
BE/Tractebel 2	0.0021	-0.0004	-0.0146	-0.0040	-0.0269	-0.0084
CEA 1	-0.0009	-0.0034	-0.0276	0.0020	-0.0179	-0.0094
CEA 2	–	–	-0.0296	–	–	–
CSA/GPUN	0.0030	0.0211	-0.0139	–	0.0175	0.0049
EDF	0.0015	0.0016	-0.0008	0.0019	0.0022	0.0020
Framatome ANP/FZK 1	0.0017	0.0016	0.0010	–	0.0015	0.0016
Framatome ANP/FZK 2	–	–	0.0018	–	–	–
FZR	0.0014	0.0038	-0.0171	-0.0062	0.0263	-0.0012
GRS	-0.0089	-0.0084	-0.0264	–	0.1761	0.0566
Iberdrola	0.0034	-0.0423	0.0002	0.0121	-0.4358	-0.1787
KAERI 1	0.0019	0.0046	-0.0144	–	-0.0094	-0.0117
KAERI 2	0.0019	0.0046	-0.0157	-0.0047	-0.0094	-0.0117
PSU	0.0018	0.0031	0.0619	–	-0.1148	-0.0112
Purdue/NRC 1	0.0019	0.0045	0.2165	–	-0.0103	-0.0141
Purdue/NRC 2	0.0019	0.0045	–	–	-0.0103	-0.0141
UP/UZ	-0.0102	-0.0058	-0.0263	–	0.2120	0.0755
UPM	-0.0079	0.0106	-0.0216	-0.0090	0.4581	0.2186
UPV	-0.0114	-0.0118	0.0301	–	-0.1965	-0.0877
VTT	0.0154	0.0225	-0.0059	0.0057	-0.0570	0.0137

Table 4.4. Participant figures of merit for steady state Fxy

Participants	0	1	2	2a	3	4
Standard Deviation	**0.0061**	**0.0136**	**0.0555**	**0.0068**	**0.1735**	**0.0744**
ANL	0.5021	0.2623	-0.2752	0.9376	-0.3798	-0.5161
BE/Tractebel 1	0.3385	0.1155	-0.4788	-0.7404	-0.0513	-0.1666
BE/Tractebel 2	0.3385	-0.0313	-0.2626	-0.5932	-0.1551	-0.1128
CEA 1	-0.1524	-0.2515	-0.4968	0.2900	-0.1032	-0.1263
CEA 2	–	–	-0.5329	–	–	–
CSA/GPUN	0.4857	1.5468	-0.2500	–	0.1008	0.0659
EDF	0.0015	0.0016	-0.0008	0.0019	0.0022	0.0020
Framatome ANP/FZK 1	0.0017	0.0016	0.0010	–	0.0015	0.0016
Framatome ANP/FZK 2	–	–	0.0018	–	–	–
FZR	0.2239	0.2770	-0.3076	-0.9170	0.1515	-0.0161
GRS	-1.4615	-0.6185	-0.4752	–	1.0149	0.7609
Iberdrola	0.5512	-3.1067	0.0041	1.7767	-2.5116	-2.4020
KAERI 1	0.3057	0.3357	-0.2590	–	-0.0542	-0.1572
KAERI 2	0.3057	0.3357	-0.2824	-0.6962	-0.0542	-0.1572
PSU	0.2894	0.2256	1.1161	–	-0.6616	-0.1505
Purdue/NRC 1	0.3057	0.3284	3.9022	–	-0.0594	-0.1895
Purdue/NRC 2	0.3057	0.3284	–	–	-0.0594	-0.1895
UP/UZ	-1.6743	-0.4276	-0.4734	–	1.2218	1.0150
UPM	-1.2979	0.7761	-0.3887	-1.3292	2.6401	2.9385
UPV	-1.8706	-0.8680	0.5430	–	-1.1325	-1.1788
VTT	2.5148	1.6496	-0.1058	0.8346	-0.3285	0.1842

Table 4.5. Participant deviations for steady state Fz

Participants	0	1	2	2a	3	4
Mean	**2.6842**	**2.4522**	**1.0858**	**1.0828**	**2.7538**	**2.7384**
ANL	-0.0222	-0.0282	-0.0327	-0.0296	-0.0248	-0.0224
BE/Tractebel 1	-0.0112	-0.0072	0.0052	0.0082	-0.0118	-0.0094
BE/Tractebel 2	0.0358	0.0078	-0.0198	0.0152	0.0422	0.0426
CEA 1	-0.0082	0.0068	-0.0208	-0.0248	-0.0038	-0.0004
CEA 2	–	–	-0.0188	–	–	–
CSA/GPUN	0.0058	0.1189	0.0361	–	0.0443	0.0385
EDF	0.0015	0.0016	-0.0008	0.0019	0.0022	0.0020
Framatome ANP/FZK 1	0.0017	0.0016	0.0010	–	0.0015	0.0016
Framatome ANP/FZK 2	–	–	0.0018	–	–	–
FZR	0.0052	-0.0055	-0.0281	-0.0075	0.0051	0.0074
GRS	-0.0142	-0.0122	-0.0317	–	0.0062	0.0016
Iberdrola	–	–	-	–	–	–
KAERI 1	-0.0112	-0.0188	0.0193	–	-0.0120	-0.0100
KAERI 2	-0.0112	-0.0188	-0.0267	-0.0073	-0.0120	-0.0100
PSU	-0.0052	-0.0122	0.0212	–	-0.0498	-0.0484
Purdue/NRC 1	-0.0110	-0.0184	0.0214	–	-0.0128	-0.0101
Purdue/NRC 2	-0.0110	-0.0184	–	–	-0.0128	-0.0101
UP/UZ	0.0058	-0.0010	0.0057	–	0.0182	0.0153
UPM	0.0248	0.0308	-0.0328	0.0002	0.0622	0.0476
UPV	0.0016	-0.0104	0.0843	–	-0.0590	-0.0387
VTT	0.0473	0.0382	0.0041	0.0171	0.0705	0.0604

Table 4.6. Participant figures of merit for steady state Fz

Participants	0	1	2	2a	3	4
Standard Deviation	**0.0190**	**0.0360**	**0.0308**	**0.0193**	**0.0365**	**0.0319**
ANL	-1.1665	-0.7840	-1.0610	-1.5302	-0.6790	-0.7024
BE/Tractebel 1	-0.5872	-0.2008	0.1678	0.4261	-0.3226	-0.2948
BE/Tractebel 2	1.8877	0.2157	-0.6428	0.7884	1.1577	1.3353
CEA 1	-0.4293	0.1880	-0.6752	-1.2818	-0.1033	-0.0127
CEA 2	–	–	-0.6103	–	–	–
CSA/GPUN	0.3080	3.3009	1.1697	–	1.2152	1.2068
EDF	0.0015	0.0016	-0.0008	0.0019	0.0022	0.0020
Framatome ANP/FZK 1	0.0017	0.0016	0.0010	–	0.0015	0.0016
Framatome ANP/FZK 2	–	–	0.0018	–	–	–
FZR	0.2764	-0.1536	-0.9119	-0.3864	0.1407	0.2318
GRS	-0.7452	-0.3397	-1.0286	–	0.1708	0.0500
Iberdrola	–	–	–	–	–	–
KAERI 1	-0.5872	-0.5229	0.6250	–	-0.3281	-0.3136
KAERI 2	-0.5872	-0.5229	-0.8665	-0.3761	-0.3281	-0.3136
PSU	-0.2713	-0.3397	0.6866	–	-1.3643	-1.5174
Purdue/NRC 1	-0.5767	-0.5118	0.6931	–	-0.3500	-0.3168
Purdue/NRC 2	-0.5767	-0.5118	–	–	-0.3500	-0.3168
UP/UZ	0.3080	-0.0286	0.1840	–	0.4998	0.4795
UPM	1.3085	0.8544	-1.0643	0.0121	1.7059	1.4921
UPV	0.0831	-0.2877	2.7345	–	-1.6182	-1.2140
VTT	2.4933	1.0599	0.1322	0.8867	1.9335	1.8933

Table 4.7. Participant deviations for steady state axial offset

Participants	0	1	2	2a	3	4
Mean	**0.7796**	**0.7169**	**0.0370**	**-0.0308**	**0.7907**	**0.7908**
ANL	-0.0256	-0.0209	–	–	-0.0277	-0.0268
BE/Tractebel 1	-0.0231	-0.0162	-0.0709	-0.0031	-0.0245	-0.0238
BE/Tractebel 2	-0.0229	-0.0163	-0.0527	-0.0062	-0.0249	-0.0238
CEA 1	-0.0246	-0.0170	-0.0528	0.0193	-0.0248	-0.0235
CEA 2	–	–	-0.0542	–	–	–
CSA/GPUN	-0.0241	-0.0195	-0.0398	–	-0.0255	-0.0248
EDF	0.0015	0.0016	-0.0008	0.0019	0.0022	0.0020
Framatome ANP/FZK 1	0.0017	0.0016	0.0010	–	0.0015	0.0016
Framatome ANP/FZK 2	–	–	0.0018	–	–	–
FZR	-0.0193	-0.0151	-0.0487	0.0074	-0.0205	-0.0199
GRS	0.0274	0.0361	-0.0450	–	0.0263	0.0262
Iberdrola	–	–	–	–	–	–
KAERI 1	-0.0230	-0.0184	-0.0075	–	-0.0245	-0.0240
KAERI 2	-0.0230	-0.0184	-0.0502	0.0059	-0.0245	-0.0240
PSU	-0.0210	-0.0158	-0.0102	–	-0.0043	-0.0075
Purdue/NRC 1	-0.0231	-0.0186	-0.0078	–	-0.0246	-0.0240
Purdue/NRC 2	-0.0231	-0.0186	–	–	-0.0246	-0.0240
UP/UZ	-0.0193	-0.0134	-0.0131	–	-0.0176	-0.0182
UPM	-0.0148	-0.0064	-0.0441	0.0038	-0.0063	-0.0102
UPV	0.3323	0.2374	0.7165	–	0.3251	0.3270
VTT	-0.0100	-0.0044	-0.0669	-0.0101	-0.0055	-0.0081

Table 4.8. Participant figures of merit for steady state axial offset

Participants	0	1	2	2a	3	4
Standard Deviation	**0.0840**	**0.0610**	**0.1803**	**0.0115**	**0.0825**	**0.0829**
ANL	-0.3045	-0.3426	–	–	-0.3350	-0.3227
BE/Tractebel 1	-0.2748	-0.2655	-0.3931	-0.2663	-0.2962	-0.2865
BE/Tractebel 2	-0.2724	-0.2672	-0.2922	-0.5358	-0.3011	-0.2865
CEA 1	-0.2926	-0.2787	-0.2927	1.6814	-0.2999	-0.2829
CEA 2	–	–	-0.3005	–	–	–
CSA/GPUN	-0.2867	-0.3197	-0.2206	–	-0.3083	-0.2986
EDF	0.0015	0.0016	-0.0008	0.0019	0.0022	0.0020
Framatome ANP/FZK 1	0.0017	0.0016	0.0010	–	0.0015	0.0016
Framatome ANP/FZK 2	–	–	0.0018	–	–	–
FZR	-0.2295	-0.2475	-0.2700	0.6467	-0.2478	-0.2395
GRS	0.3265	0.5923	-0.2495	–	0.3192	0.3166
Iberdrola	–	–	–	–	–	–
KAERI 1	-0.2736	-0.3016	-0.0415	–	-0.2962	-0.2889
KAERI 2	-0.2736	-0.3016	-0.2783	0.5163	-0.2962	-0.2889
PSU	-0.2498	-0.2590	-0.0567	–	-0.0515	-0.0899
Purdue/NRC 1	-0.2748	-0.3049	-0.0432	–	-0.2974	-0.2889
Purdue/NRC 2	-0.2748	-0.3049	–	–	-0.2974	-0.2889
UP/UZ	-0.2293	-0.2199	-0.0725	–	-0.2127	-0.2193
UPM	-0.1759	-0.1048	-0.2445	0.3337	-0.0757	-0.1225
UPV	3.9563	3.8929	3.9735	–	3.9384	3.9448
VTT	-0.1188	-0.0720	-0.3709	-0.8750	-0.0660	-0.0972

Table 4.9. Participant deviations for steady state scram and stuck rod worths

Participants	TRW-V1	SRW-V1	TRW-V2	SRW-V2
Mean	**4.5352**	**0.7031**	**3.0411**	**0.4276**
ANL	-0.0042	-0.0401	-0.0171	-0.0476
BE/Tractebel 1	-0.0127	-0.0336	-0.0139	-0.0425
BE/Tractebel 2	0.0182	-0.0295	0.0049	-0.0413
CEA 1	0.0238	-0.0271	0.0059	-0.0406
CEA 2	–	–	–	–
CSA/GPUN	–	–	–	–
EDF	0.0015	0.0016	-0.0008	0.0019
Framatome ANP/FZK 1	0.0017	0.0016	0.0010	–
Framatome ANP/FZK 2	–	–	0.0018	–
FZR	0.0245	-0.0165	0.0071	-0.0355
GRS	0.0928	0.0229	0.0469	-0.0176
Iberdrola	0.0448	–	0.0029	–
KAERI 1	-0.0192	-0.0331	-0.0181	-0.0426
KAERI 2	-0.0192	-0.0331	-0.0181	-0.0426
PSU	-0.0585	–	-0.0722	–
Purdue/NRC 1	-0.0192	-0.0341	0.1639	-0.0426
Purdue/NRC 2	-0.0192	-0.0341	-0.0191	-0.0436
UP/UZ	0.0808	0.0259	0.0389	-0.0156
UPM	-0.0892	0.0549	-0.0501	-0.0026
UPV	-0.0172	0.2843	-0.0221	0.5746
VTT	-0.0578	-0.0409	-0.0459	-0.0477

Table 4.10. Participant figures of merit for steady state scram and stuck rod worths

Participants	TRW-V1	SRW-V1	TRW-V2	SRW-V2
Standard Deviation	**0.0466**	**0.0780**	**0.0493**	**0.1486**
ANL	-0.0908	-0.5139	-0.3476	-0.3205
BE/Tractebel 1	-0.2732	-0.4306	-0.2827	-0.2862
BE/Tractebel 2	0.3899	-0.3781	0.0987	-0.2781
CEA 1	0.5101	-0.3473	0.1190	-0.2734
CEA 2	–	–	–	–
CSA/GPUN	–	–	–	–
EDF	0.0015	0.0016	-0.0008	0.0019
Framatome ANP/FZK 1	0.0017	0.0016	0.0010	–
Framatome ANP/FZK 2	–	–	0.0018	–
FZR	0.5251	-0.2115	0.1434	-0.2391
GRS	1.9907	0.2935	0.9508	-0.1186
Iberdrola	0.9607	–	0.0582	–
KAERI 1	-0.4127	-0.4242	-0.3679	-0.2869
KAERI 2	-0.4127	-0.4242	-0.3679	-0.2869
PSU	-1.2560	–	-1.4654	–
Purdue/NRC 1	-0.4127	-0.4370	3.3244	-0.2869
Purdue/NRC 2	-0.4127	-0.4370	-0.3882	-0.2936
UP/UZ	1.7332	0.3320	0.7885	-0.1052
UPM	-1.9148	0.7037	-1.0171	-0.0177
UPV	-0.3680	3.6436	-0.4485	3.8671
VTT	-1.2410	-0.5242	-0.9318	-0.3212

4.1.2 1-D axial distributions

4.1.2.1 1-D core-averaged axial power distributions

The results for 1-D core-averaged axial power distributions are compared and analysed for the above-described six steady states. The comparisons of participants' predictions and mean distribution in a form of graphs are presented in Figures 4.1 through 4.6. In each case, the participants are in good agreement, and the results form a single cluster around the mean solution. The local deviations increase towards the top of the core for the HZP cases and towards the bottom and top of the core for the HFP cases. Unlike HZP states, in HFP states the spatial distribution of the thermal-hydraulic feedback plays an important role. Since the core inlet and outlet thermal-hydraulic boundary conditions are specified, the observed deviations in HFP cases are believed to be mostly due to different thermal-hydraulics models, nodding and mapping schemes. The participants with different degree of detail of spatial nodalisation utilise two different types of core thermal-hydraulics models. Majority of submitted results are based on parallel channels models (which is basically 1-D modelling) ranging between 18 and 192 channels in radial plane. The most detail models of this type are the models of BE/Tractebel (reference results – 241 T-H channels with 4 cells per channel in radial plane – Appendix B) and of EDF (192 T-H channels with 4 x 4 cells – Appendix B). Some of the participants used 3-D core thermal-hydraulics models also with different degree of spatial detail in radial plane – from 18 T-H cells (PSU and UPV) to 177 T-H cells (CEA – first reference set of results) and 192 T-H cells (the EDF second set of results). The used axial nodalization by the participants is also different ranging form 8 to 50 axial T-H nodes. Interestingly, for steady state 2 (the initial steady state for the transient), the different distributions have very similar shapes, which cross each other in

the central part of the core and are slightly shifted at the core ends (Figure 4.3). Comparing Figures 4.3 and 4.4 one can see that most of these deviations at the core ends are removed in steady state 2a (which is the same HFP state as state 2 but with uniform inlet mass flow distribution). This fact indicates that is very important how the participants distribute the provided inlet mass flow rate boundary conditions (BC). These BC are obtained from the best-estimate core-plant system calculations performed with the PSU version of TRAC-PF1/NEM. The radial distributions are provided for 18 T-H cells in radial plane following the nodalisation of the TMI-1 TRAC-PF1 model, which includes a 3-D vessel (including the core) model in cylindrical geometry. Difficulties have arisen in the interpretation of the mass flow BC, provided by the above-described TRAC-PF1 model, since the most of the participant's codes model the core thermal-hydraulically by parallel channels. In order to avoid this source of modelling uncertainties new BC have been generated, where mass flows are corrected for direct use as input data in the participants' codes. A geometrical interpolation method is used to process the TRAC-PF1/NEM BC in order to obtain inlet conditions per assembly. How further these assembly-wise inlet conditions are distributed per channel depends on the participants' thermal-hydraulic nodding and mapping schemes.

4.1.2.2 1-D axial distributions in the stuck rod

The local parameter distributions are monitored at the position of the stuck rod for the initial steady state. These results are compared in two groups: one cluster for very detailed spatial mesh overlays – this is called 177 channel cluster, and one separate cluster for coarse mesh overlays – it is called 18 channel cluster (Figures 4.7 and 4.8). These figures illustrate the effect of the T-H model on local power distributions, which is a result of the local distributions of the T-H feedback parameters – moderator (coolant density) and Doppler temperature (Figures 4.9-4.10).

Figure 4.1. Core-averaged axial power distribution, state 0

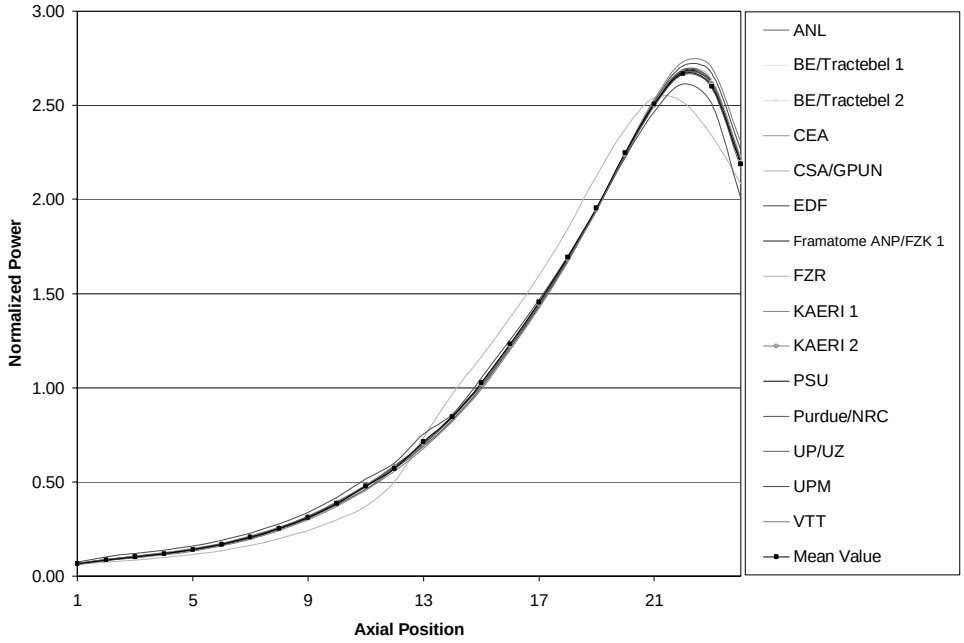

Figure 4.2. Core-averaged axial power distribution, state 1

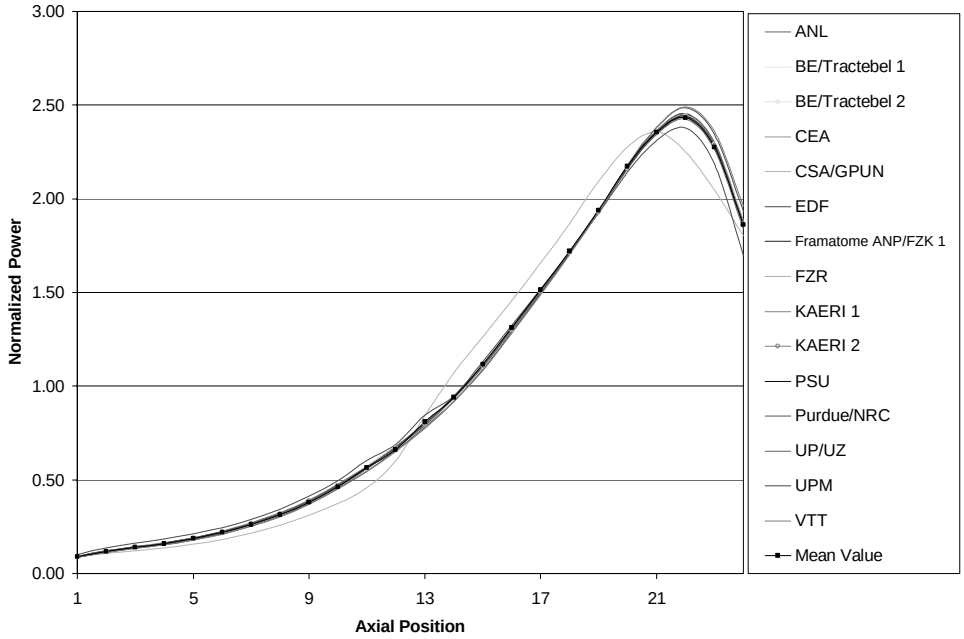

Figure 4.3. Core-averaged axial power distribution, state 2

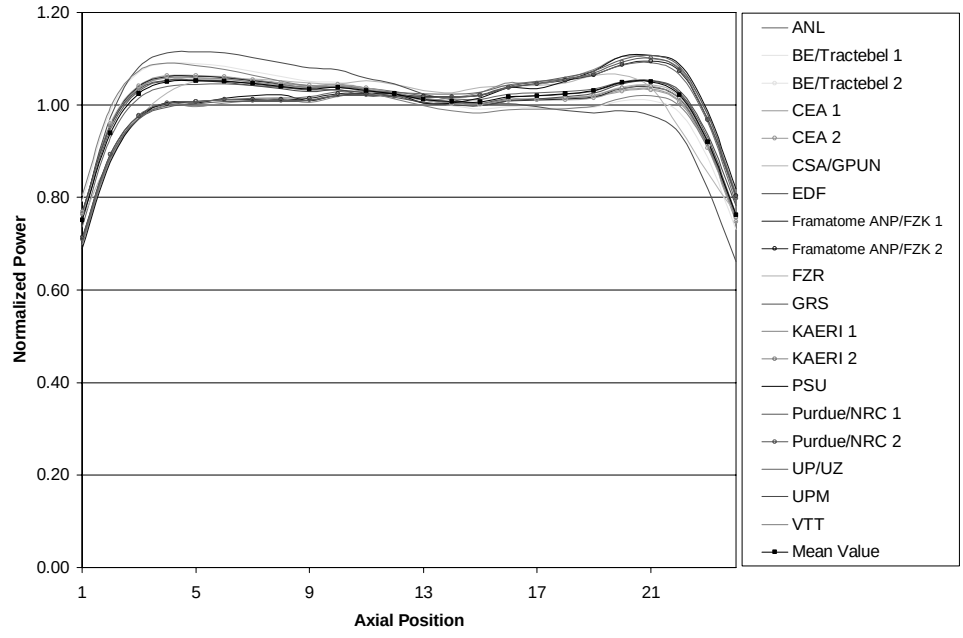

Figure 4.4. Core-averaged axial power distribution, state 2a

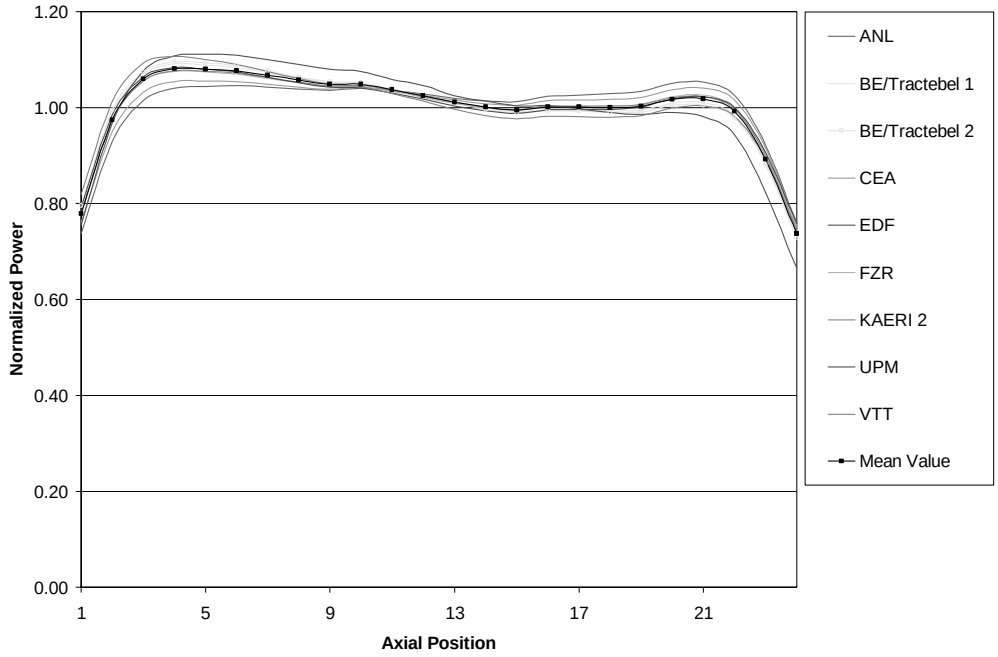

Figure 4.5. Core-averaged axial power distribution, state 3

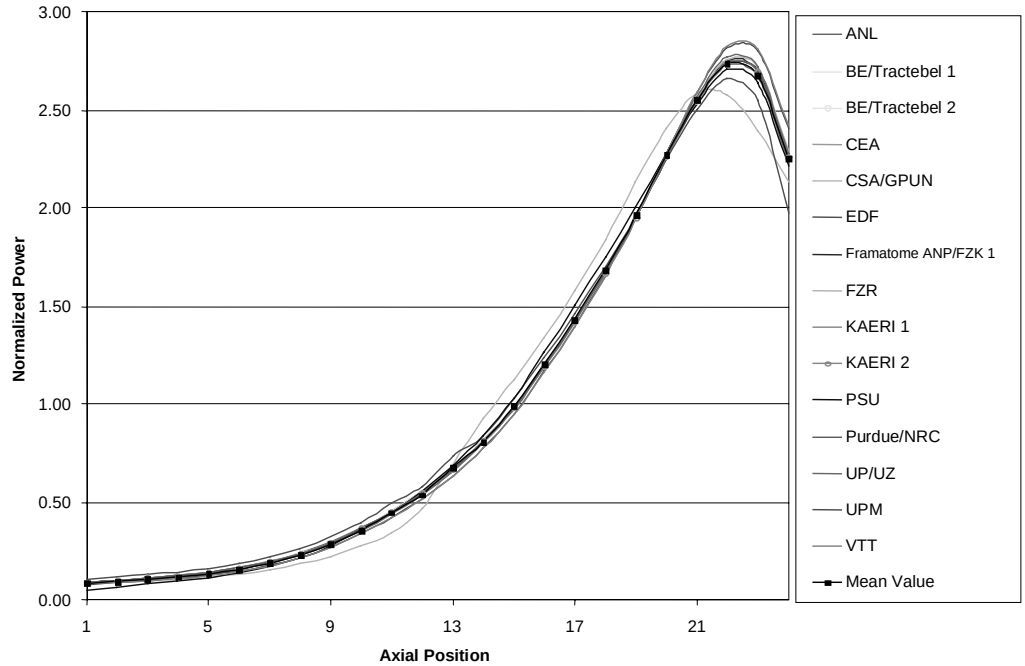

Figure 4.6. Core-averaged axial power distribution, state 4

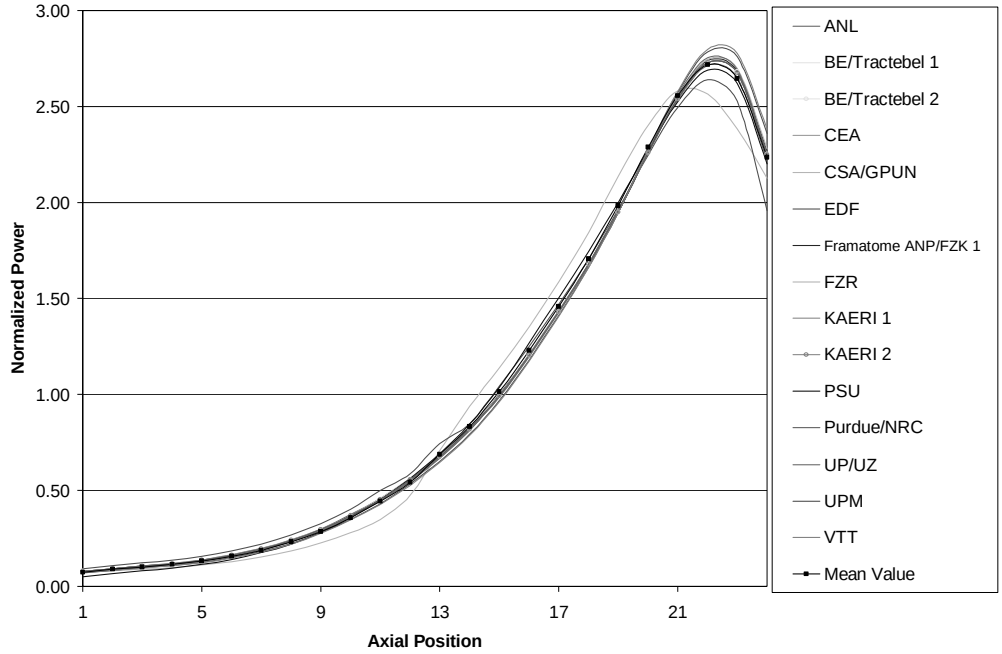

Figure 4.7. Normalised power distribution at the stuck rod (N12) – 18 channels, state 2

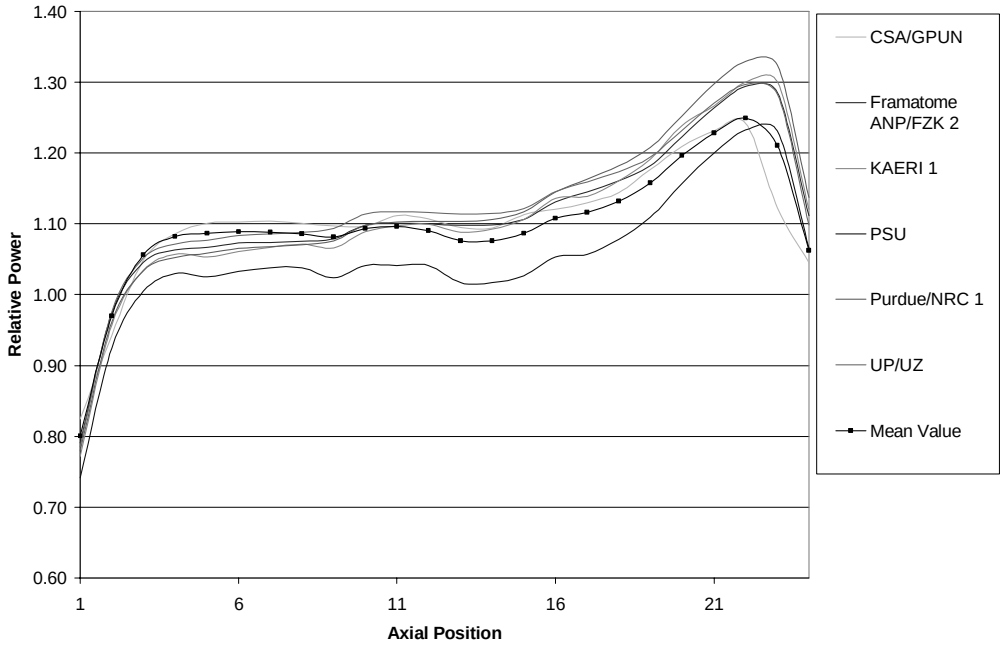

Figure 4.8. Normalised power distribution at the stuck rod (N12) – 177 channels, state 2

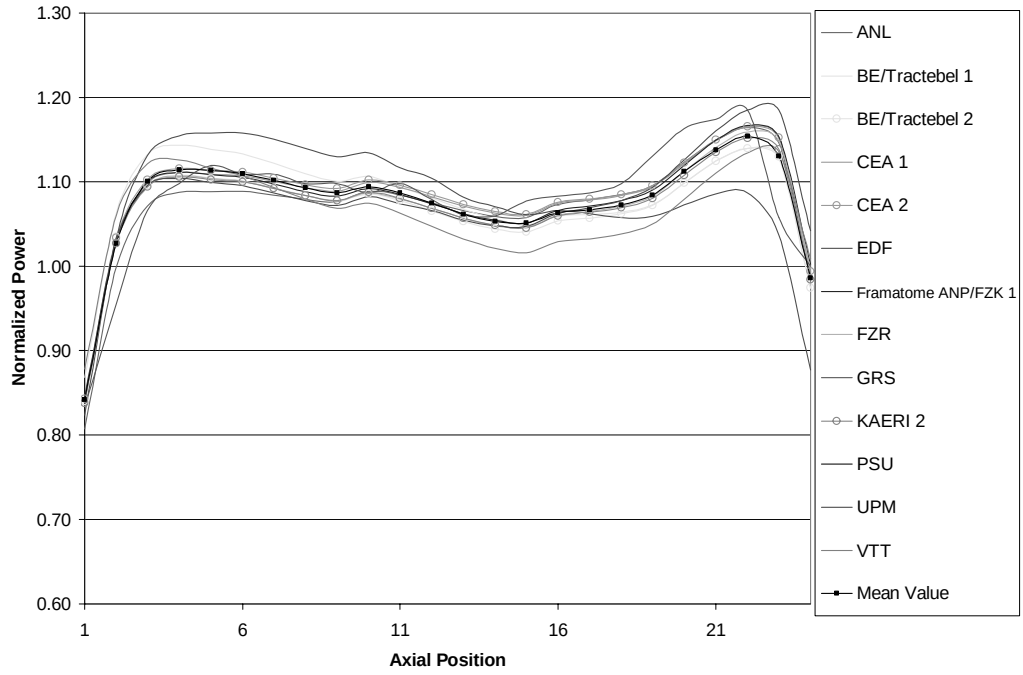

Figure 4.9. Coolant density at stuck rod (N12) – 177 channels, state 2

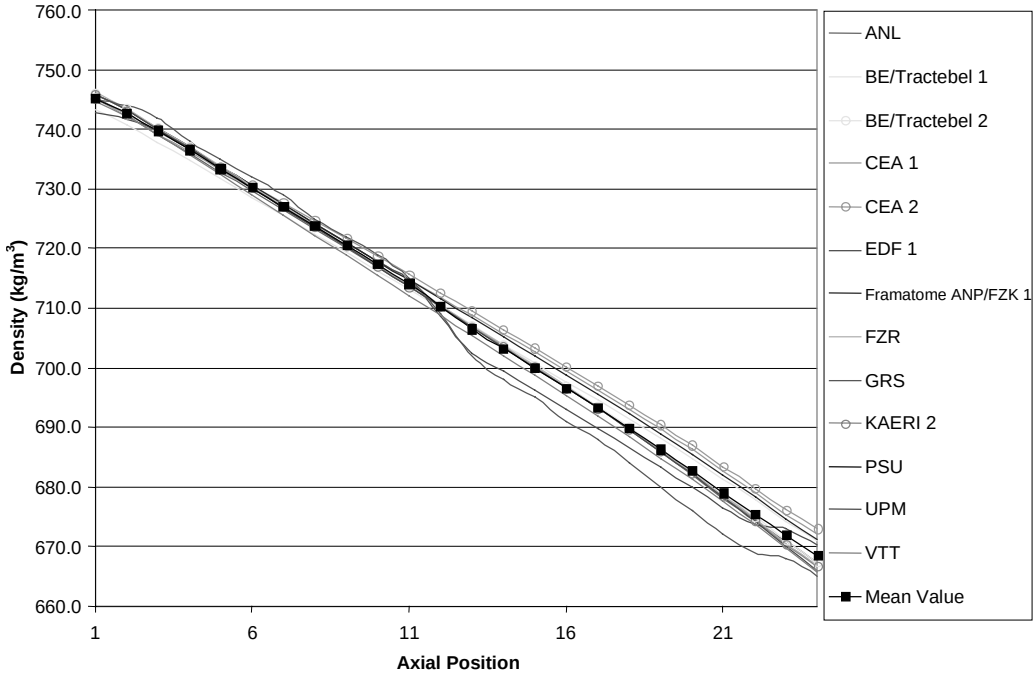

Figure 4.10. Doppler temperature at stuck rod (N12) – 177 channels, state 2

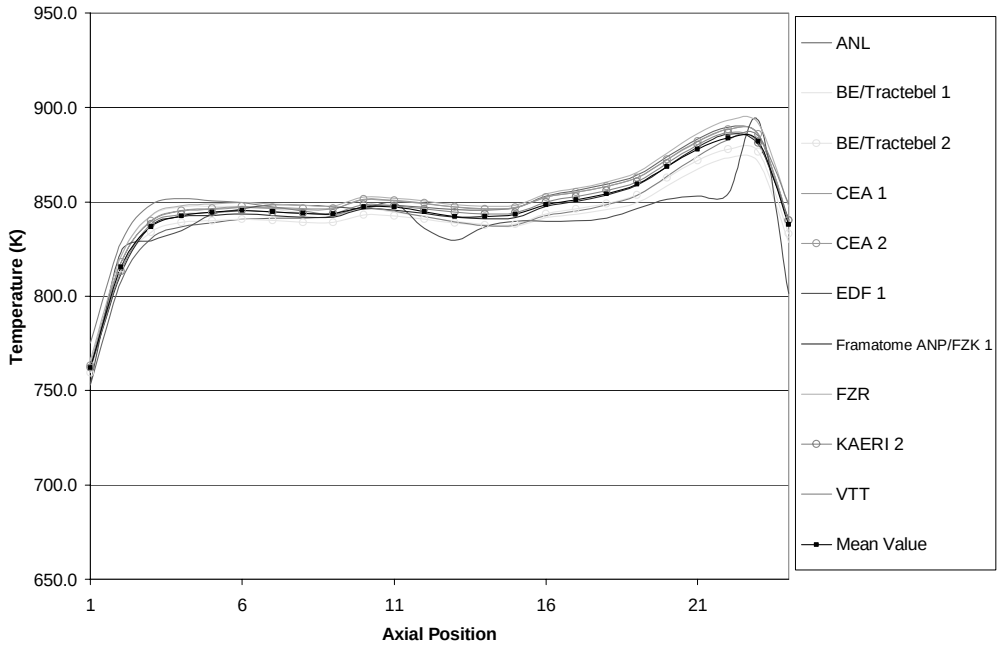

4.1.3 2-D radial distributions

4.1.3.1 2-D core-averaged radial power distributions

For the initial HZP states (0, 1, 3 and 4), the following parameter is analysed: 2-D normalised power (NP) distribution; for the initial HFP steady states (2 and 2a), the same information as for the HZP states plus: 2-D maps for inlet coolant temperature, inlet flow rate and outlet coolant temperature. The 2-D mean distributions are provided in Appendix C while the participants' deviations are calculated for each radial node and provided in the form of 2-D maps in Appendix D. The discrepancies among participants' results for HZP states are due to the differences of neutronics models since the thermal-hydraulics feedback is frozen in the HZP calculations. The differences in neutronics models are mostly coming from the radial nodalisation scheme (one node per assembly – 1 npa vs. 4 npa schemes) and the spatial discretisation method used. These methods are described in Appendix A for each participant. As expected the deviations are greater for the heterogeneous rodded cases – 3 and 4.

For HFP cases – states 2 and 2a – the thermal-hydraulic feedback is modelled and impacts the 2-D power distributions; however, the effect is not so strong as on the core-averaged axial power distributions. As it is the case with core-averaged axial power comparisons in case 2a the radial uniform inlet flow rate modelling smoothes the deviations in the participants' predictions of the 2-D coolant temperature distributions and as result in the 2-D radial power distributions.

4.2 Transient snapshots

Transient snapshots are taken at the highest power before scram (state 5), highest power after scram for scenario 2 (state 6), EOT for Scenario 1 (state 7), and EOT for scenario 2 (state 8). The data compared and analysed consists also as in the case of the steady state results of three types of data – integral parameters, 1-D axial distributions and 2-D radial distributions.

4.2.1 Integral parameters

The following integral parameters are compared and analysed for the transient snapshots – the total and fission power levels (in MW), the time of maximum return-to-power for second scenario (in seconds), radial and axial power peaking factors (Fxy and Fz), and axial offset (unit less). The mean solutions are provided in Appendix C. The participants' deviations are given in Appendix D and are summarised in Tables 4.11-4.22, given below. For each case the participants are in reasonable agreement. The most interesting snapshot is 6 – return-to-power for the second transient scenario. PSU, VTT, UPV and Iberdrola are predicting the highest power peaks after the scram, which is resulting also in higher power level at the end of the transient for the second scenario. The Iberdrola results actually are bounding the cluster of the participants' results (Figure 4.32). This power over-prediction during the transient can be attributed to several facts – first, the approximations introduced in the core neutronics model (explained above), and second – the used different than specified correlation for fuel properties vs. temperature and different relation for Doppler temperature. There is very good agreement between different codes predictions of the timing of the return-to-power except PSU. This is an interesting fact since the PSU has provided the time-dependent inlet and outlet boundary conditions using coupled 3-D kinetics system calculations. In the system calculations the timing of the peak is later as predicted by PSU using TRAC-PF1/NEM boundary conditions model, which can be explained with the consistent T-H modelling in both system and core boundary conditions simulations.

Table 4.11. Participant deviations for transient total core power

Participant	5	6	7	8
Mean	**3271.88**	**866.91**	**121.14**	**233.92**
ANL	–	–	–	–
BE/Tractebel 1	-13.85	-2.88	-0.36	-7.37
BE/Tractebel 2	-35.19	-20.29	–	-10.34
CEA 1	-24.44	13.31	-0.69	1.43
CEA 2	-18.29	-1.86	–	-2.52
CSA/GPUN	50.82	55.56	1.70	1.08
EDF 1	42.39	-1.78	-0.91	-9.10
EDF 2	52.66	19.28	-0.34	-3.51
Framatome ANP/FZK 1	19.76	-10.49	-0.60	-5.16
Framatome ANP/FZK 2	31.68	-8.29	-1.80	-12.50
FZR	-49.78	-20.41	-0.54	-7.02
GRS	40.02	-21.91	-7.04	-0.12
Iberdrola	–	175.1	–	270.30
KAERI 1	-30.78	-32.74	–	-37.07
KAERI 2	18.32	-1.71	–	-10.18
PSU	-48.88	70.09	6.36	44.08
Purdue/NRC 1	35.52	-29.83	0.23	-25.54
Purdue/NRC 1	16.22	-47.93	–	-23.02
UP/UZ	-1.00	-93.47	-7.91	-44.87
UPM	-33.30	-32.56	-0.89	-15.41
UPV	–	100.1	–	55.23
VTT	-51.88	67.89	-1.24	17.18

Table 4.12. Participant figures of merit for transient total core power

Participant	5	6	7	8
Standard Deviation	**36.50**	**54.13**	**6.43**	**49.09**
ANL	–	–	–	–
BE/Tractebel 1	-0.38	-0.05	-0.06	-0.15
BE/Tractebel 2	-0.96	-0.37	–	-0.21
CEA 1	-0.67	0.25	-0.11	0.03
CEA 2	-0.50	-0.03	–	-0.05
CSA/GPUN	1.39	1.03	0.26	0.02
EDF 1	1.16	-0.03	-0.14	-0.19
EDF 2	1.44	0.36	-0.05	-0.07
Framatome ANP/FZK 1	0.54	-0.19	-0.09	-0.11
Framatome ANP/FZK 2	0.87	-0.15	-0.28	-0.25
FZR	-1.36	-0.38	-0.08	-0.14
GRS	1.10	-0.40	-1.09	0.00
Iberdrola	–	3.23	–	5.5
KAERI 1	-0.84	-0.60	–	-0.76
KAERI 2	0.50	-0.03	–	-0.21
PSU	-1.34	1.29	1.17	0.90
Purdue/NRC 1	0.97	-0.55	0.04	-0.52
Purdue/NRC 1	0.44	-0.89	–	-0.47
UP/UZ	-0.03	-1.73	-1.23	-0.91
UPM	-0.91	-0.60	-0.14	-0.31
UPV	–	1.85	–	1.12
VTT	-1.42	1.25	-0.19	0.35

Table 4.13. Participant deviations for transient total fission power

Participant	5	6	7	8
Mean	**3093.75**	**729.52**	**21.50**	**113.98**
ANL	178.32	49.22	1.39	-7.10
BE/Tractebel 1	-35.72	3.68	1.16	6.02
BE/Tractebel 2	-56.85	-13.26	–	3.32
CEA 1	-41.79	13.00	-0.18	7.87
CEA 2	-35.64	-2.16	–	3.92
CSA/GPUN	31.85	60.04	0.54	11.66
EDF 1	26.98	-2.09	-0.40	-2.66
EDF 2	37.25	18.97	0.16	2.92
Framatome ANP/FZK 1	-2.11	-5.49	-0.21	-0.14
Framatome ANP/FZK 2	9.81	-3.29	-1.41	-7.43
FZR	-71.25	-15.42	-0.20	-2.08
GRS	37.65	-12.92	0.10	13.92
Iberdrola	–	–	–	–
KAERI 1	-2.55	-2.32	–	-14.32
KAERI 2	46.45	28.65	–	12.57
PSU	–	–	–	–
Purdue/NRC 1	18.35	-22.71	-0.74	-13.56
Purdue/NRC 1	-0.85	-40.44	–	-10.84
UP/UZ	-20.95	-82.32	-3.97	-27.70
UPM	-55.17	-27.56	-0.50	-10.46
UPV	–	–	–	–
VTT	-63.75	79.08	4.28	34.12

Table 4.14. Participant figures of merit for transient total fission power

Participant	5	6	7	8
Standard Deviation	**57.30**	**35.90**	**1.77**	**13.51**
ANL	3.11	1.37	0.79	-0.53
BE/Tractebel 1	-0.62	0.10	0.65	0.45
BE/Tractebel 2	-0.99	-0.37	–	0.25
CEA 1	-0.73	0.36	-0.10	0.58
CEA 2	-0.62	-0.06	–	0.29
CSA/GPUN	0.56	1.67	0.31	0.86
EDF 1	0.47	-0.06	-0.23	-0.20
EDF 2	0.65	0.53	0.09	0.22
Framatome ANP/FZK 1	-0.04	-0.15	-0.12	-0.01
Framatome ANP/FZK 2	0.17	-0.09	-0.80	-0.55
FZR	-1.24	-0.43	-0.12	-0.15
GRS	0.66	-0.36	0.05	1.03
Iberdrola	–	–	–	–
KAERI 1	-0.04	-0.06	–	-1.06
KAERI 2	0.81	0.80	–	0.93
PSU	–	–	–	–
Purdue/NRC 1	0.32	-0.63	-0.42	-1.00
Purdue/NRC 1	-0.01	-1.13	–	-0.80
UP/UZ	-0.37	-2.29	-2.24	-2.05
UPM	-0.96	-0.77	-0.28	-0.77
UPV	–	–	–	–
VTT	-1.11	2.20	2.42	2.53

Table 4.15. Participant deviations for time of maximum return to power

Participant	Snapshot 6
Mean	**58.38**
ANL	-1.63
BE/Tractebel 1	-0.38
BE/Tractebel 2	-0.38
CEA 1	-0.81
CEA 2	-0.78
CSA/GPUN	-0.38
EDF 1	-0.43
EDF 2	-0.43
Framatome ANP/FZK 1	-0.44
Framatome ANP/FZK 2	-0.58
FZR	-0.25
GRS	0.89
Iberdrola	1.62
KAERI 1	-0.28
KAERI 2	-0.48
PSU	7.38
Purdue/NRC 1	-0.18
Purdue/NRC 1	-0.38
UP/UZ	0.63
UPM	-0.45
UPV	-1.38
VTT	-0.68

Table 4.16. Participant figures of merit for time of maximum return to power

Participant	Snapshot 6
Standard Deviation	**1.81**
ANL	-0.90
BE/Tractebel 1	-0.21
BE/Tractebel 2	-0.21
CEA 1	-0.45
CEA 2	-0.43
CSA/GPUN	-0.21
EDF 1	-0.24
EDF 2	-0.24
Framatome ANP/FZK 1	-0.24
Framatome ANP/FZK 2	-0.32
FZR	-0.14
GRS	0.49
Iberdrola	0.90
KAERI 1	-0.15
KAERI 2	-0.26
PSU	4.08
Purdue/NRC 1	-0.10
Purdue/NRC 1	-0.21
UP/UZ	0.35
UPM	-0.25
UPV	-0.76
VTT	-0.37

Table 4.17. Participant deviations for transient Fxy

Participant	5	6	7	8
Mean	**1.5156**	**3.3284**	**2.1935**	**2.6330**
ANL	0.00	0.05	1.00	0.43
BE/Tractebel 1	-0.02	-0.17	-0.49	-0.19
BE/Tractebel 2	-0.03	-0.19	–	-0.20
CEA 1	-0.03	0.08	1.18	0.67
CEA 2	-0.02	0.09	–	0.66
CSA/GPUN	0.04	–	–	–
EDF 1	0.00	0.12	1.13	0.66
EDF 2	-0.01	0.10	1.17	0.65
Framatome ANP/FZK 1	-0.02	-0.21	-0.54	-0.33
Framatome ANP/FZK 2	-0.01	0.06	-0.55	-0.29
FZR	-0.03	-0.24	-0.54	-0.35
GRS	-0.02	-0.24	-0.52	-0.26
KAERI 1	-0.01	0.21	–	-0.23
KAERI 2	-0.01	-0.18	–	-0.20
PSU	-0.02	-0.08	1.90	0.38
Purdue/NRC 1	0.28	0.83	-1.39	-0.45
Purdue/NRC 1	-0.02	-0.05	–	-0.23
UP/UZ	-0.01	0.18	-0.60	-0.27
UPM	-0.02	-0.16	-0.55	-0.35
UPV	-0.01	–	-0.81	–
VTT	-0.02	-0.20	-0.38	-0.08

Table 4.18. Participant figures of merit for transient Fxy

Participant	5	6	7	8
Standard Deviation	**0.0652**	**0.2519**	**0.9793**	**0.4134**
ANL	-0.06	0.19	1.02	1.03
BE/Tractebel 1	-0.35	-0.66	-0.50	-0.46
BE/Tractebel 2	-0.44	-0.74	–	-0.49
CEA 1	-0.50	0.33	1.21	1.61
CEA 2	-0.36	0.34	–	1.60
CSA/GPUN	0.56	–	–	–
EDF 1	-0.04	0.49	1.15	1.58
EDF 2	-0.10	0.39	1.19	1.58
Framatome ANP/FZK 1	-0.25	-0.85	-0.55	-0.79
Framatome ANP/FZK 2	-0.14	0.23	-0.56	-0.70
FZR	-0.44	-0.95	-0.56	-0.85
GRS	-0.31	-0.96	-0.53	-0.63
KAERI 1	-0.10	0.84	–	-0.56
KAERI 2	-0.19	-0.73	–	-0.48
PSU	-0.24	-0.33	1.94	0.92
Purdue/NRC 1	4.26	3.30	-1.42	-1.09
Purdue/NRC 1	-0.27	-0.18	–	-0.56
UP/UZ	-0.16	0.70	-0.61	-0.65
UPM	-0.36	-0.64	-0.56	-0.85
UPV	-0.15	–	-0.83	–
VTT	-0.34	-0.78	-0.39	-0.19

Table 4.19. Participant deviations for transient Fz

Participant	5	6	7	8
Mean	**1.1108**	**2.0423**	**1.4407**	**1.8843**
ANL	-0.01	-0.09	0.33	0.32
BE/Tractebel 1	0.00	-0.04	-0.27	-0.13
BE/Tractebel 2	0.01	-0.03	–	-0.14
CEA 1	0.01	0.06	0.22	0.40
CEA 2	0.00	0.07	–	0.39
CSA/GPUN	0.04	–	–	–
EDF 1	0.04	0.00	0.25	0.31
EDF 2	0.04	-0.02	0.27	0.31
Framatome ANP/FZK 1	0.01	-0.05	-0.28	-0.22
Framatome ANP/FZK 2	-0.05	0.00	-0.24	-0.20
FZR	0.00	-0.05	-0.28	-0.22
GRS	-0.01	-0.03	-0.25	-0.12
KAERI 1	-0.05	0.09	–	-0.16
KAERI 2	0.00	-0.04	–	-0.13
PSU	-0.04	-0.01	0.77	0.39
Purdue/NRC 1	-0.05	0.07	-0.22	-0.16
Purdue/NRC 1	-0.05	0.05	–	-0.15
UP/UZ	-0.04	0.08	-0.26	-0.19
UPM	0.01	-0.02	-0.27	-0.24
UPV	0.12	–	0.46	–
VTT	0.02	-0.04	-0.23	-0.06

Table 4.20. Participant figures of merit for transient Fz

Participant	5	6	7	8
Standard Deviation	**0.0415**	**0.0530**	**0.3472**	**0.2512**
ANL	-0.28	-1.64	0.94	1.28
BE/Tractebel 1	-0.02	-0.76	-0.77	-0.53
BE/Tractebel 2	0.12	-0.61	–	-0.54
CEA 1	0.20	1.14	0.64	1.58
CEA 2	-0.02	1.31	–	1.57
CSA/GPUN	0.93	–	–	–
EDF 1	0.88	-0.06	0.72	1.22
EDF 2	1.06	-0.33	0.78	1.24
Framatome ANP/FZK 1	0.18	-0.96	-0.82	-0.87
Framatome ANP/FZK 2	-1.31	0.09	-0.69	-0.79
FZR	0.06	-1.03	-0.81	-0.87
GRS	-0.26	-0.55	-0.72	-0.49
KAERI 1	-1.13	1.68	–	-0.65
KAERI 2	0.02	-0.77	–	-0.52
PSU	-1.01	-0.21	2.22	1.56
Purdue/NRC 1	-1.11	1.28	-0.64	-0.64
Purdue/NRC 1	-1.27	0.90	–	-0.59
UP/UZ	-0.86	1.55	-0.74	-0.77
UPM	0.22	-0.35	-0.78	-0.94
UPV	3.00	–	1.32	–
VTT	0.59	-0.70	-0.66	-0.24

Table 4.21. Participant deviations for transient axial offset

Participant	5	6	7	8
Mean	**0.0139**	**0.4895**	**0.1886**	**0.3895**
ANL	–	–	–	–
BE/Tractebel 1	-0.06	-0.03	-0.13	-0.06
BE/Tractebel 2	-0.06	-0.03	–	-0.07
CEA 1	-0.06	0.02	0.07	0.18
CEA 2	-0.06	0.03	–	0.18
CSA/GPUN	-0.05	–	–	–
EDF 1	-0.08	0.01	0.09	0.16
EDF 2	-0.09	0.01	0.10	0.17
Framatome ANP/FZK 1	-0.06	-0.03	-0.14	-0.10
Framatome ANP/FZK 2	-0.02	-0.01	-0.11	-0.09
FZR	-0.06	-0.04	-0.14	-0.10
GRS	0.03	0.07	-0.04	0.04
KAERI 1	–	–	–	–
KAERI 2	–	–	–	–
PSU	–	0.01	–	–
Purdue/NRC 1	-0.01	0.01	-0.10	-0.07
Purdue/NRC 1	–	–	–	–
UP/UZ	0.00	0.02	-0.12	-0.09
UPM	-0.06	-0.03	-0.14	-0.11
UPV	0.74	–	0.80	–
VTT	-0.07	-0.03	-0.13	-0.04

Table 4.22. Participant figures of merit for transient axial offset

Participant	5	6	7	8
Standard Deviation	**0.2012**	**0.0312**	**0.2584**	**0.1197**
ANL	–	–	–	–
BE/Tractebel 1	-0.29	-0.85	-0.52	-0.52
BE/Tractebel 2	-0.31	-0.94	-	-0.56
CEA 1	-0.32	0.76	0.25	1.53
CEA 2	-0.29	0.88	–	1.53
CSA/GPUN	-0.27	–	–	–
EDF 1	-0.42	0.37	0.36	1.36
EDF 2	-0.45	0.21	0.40	1.38
Framatome ANP/FZK 1	-0.32	-1.10	-0.56	-0.86
Framatome ANP/FZK 2	-0.12	-0.25	-0.44	-0.75
FZR	-0.31	-1.16	-0.55	-0.85
GRS	0.16	2.36	-0.16	0.30
KAERI 1	–	–	–	–
KAERI 2	–	–	–	–
PSU	–	0.39	–	–
Purdue/NRC 1	-0.07	0.39	-0.40	-0.58
Purdue/NRC 1	–	–	–	–
UP/UZ	-0.01	0.78	-0.47	-0.71
UPM	-0.31	-0.80	-0.53	-0.96
UPV	3.70	–	3.10	–
VTT	-0.37	-1.05	-0.49	-0.31

4.2.2 1-D axial distributions

4.2.2.1 1-D core-averaged axial power distribution

During the comparison of the participants' results, more pronounced deviations in the relative core-averaged axial shapes were observed for the transient snapshots after reactor scram. Based on the results of sensitivity study, performed by PSU, it was suggested that this anomaly is connected with the spatial decay heat modelling. The time evolution of the core-averaged decay heat power is provided to the participants for both scenarios (no return-to-power and return-to-power). This average value at each time step should be re-distributed spatially according to the fission power spatial distribution, and the spatial decay distribution should follow the fission power distribution at the initial HFP nominal steady state conditions. Some participants instead distributed the decay heat by following the fission power distribution at each time step, which introduced the deviations. This can be seen especially for the EOT snapshots – states 7 and 8 – Figures 4.13 and 4.14. For example, the BE/Tractebel results are obtained by redistributing the decay heat following the fission power distribution at each time step, and these results fall in the cluster, which has higher normalised power at the core bottom and lower normalised power at the core top (Figures 4.13 and 4.14). In difference the CEA results, for example, are obtained by distributing the decay heat following the initial steady state fission power distribution, and subsequently fall in the other cluster. In addition some participants like KAERI and UP/UZ used independent decay heat data and models.

Figure 4.11. Core-averaged axial power shape, state 5

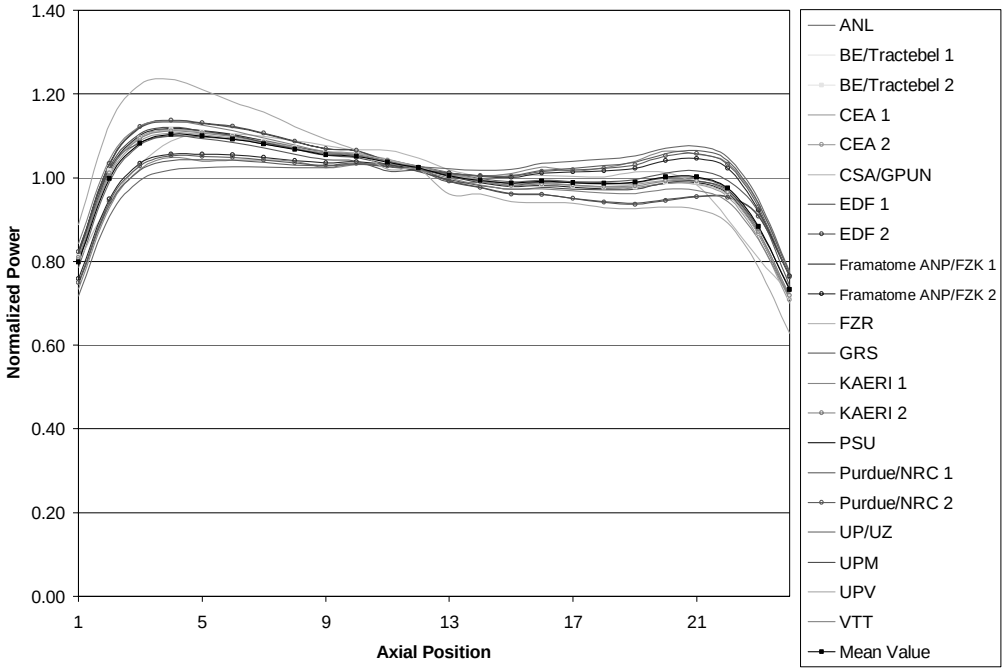

Figure 4.12. Core-averaged axial power shape, state 6

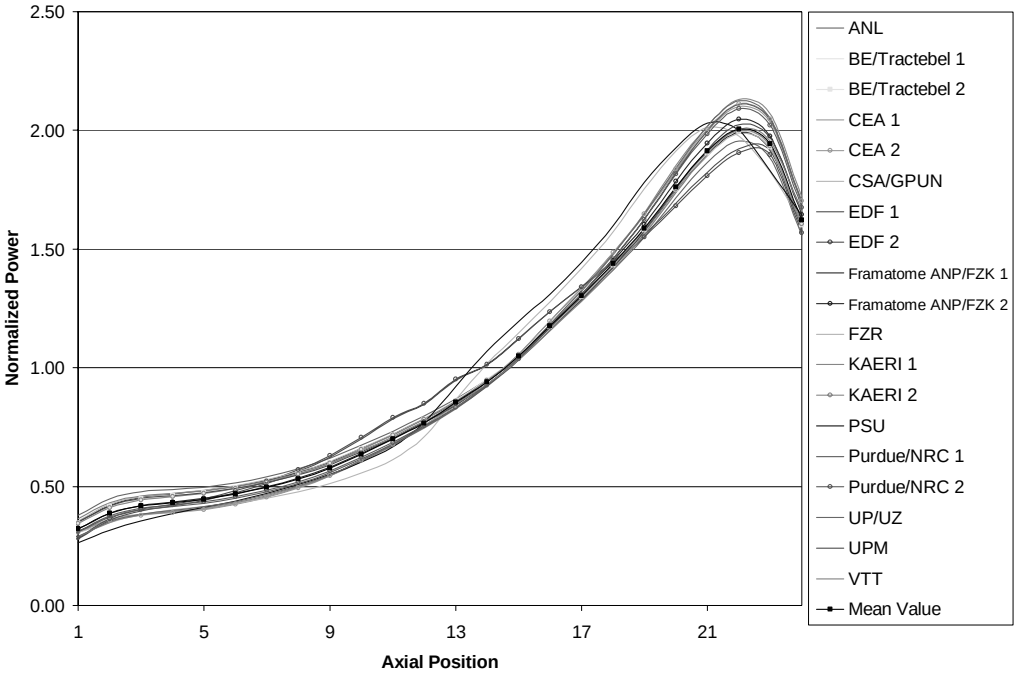

Figure 4.13. Core-averaged axial power shape, state 7

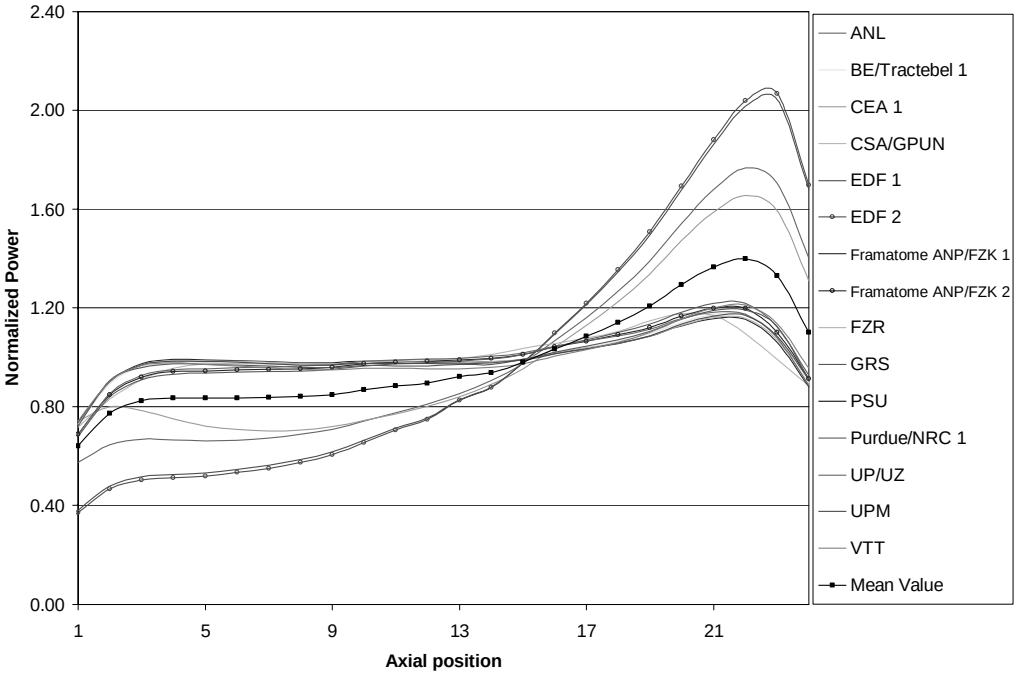

Figure 4.14. Core-averaged axial power shape, state 8

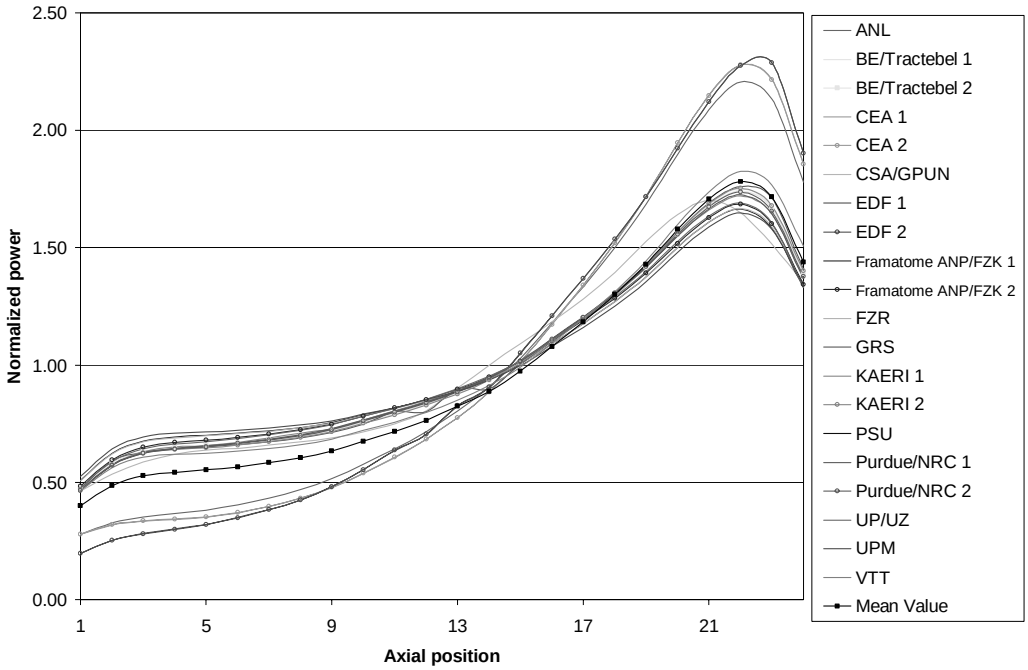

4.2.2.2 1-D axial distributions in the stuck rod position

The local parameter distributions are monitored at the position of the stuck rod. Since the local parameter predictions are sensitive to the spatial coupling schemes it was decided at the third benchmark workshop [5] that in the final report these results are compared in two groups: one cluster for very detailed spatial mesh overlays (one neutronics node per thermal-hydraulic cell/channel) – this is called 177 channel cluster, and one separate cluster for coarse mesh overlays – it is called 18 channel cluster. Subsequently separate mean solutions and standard deviations are produced for these two clusters.

During the preliminary stages of exercise 2 it was noticed that the core thermal-hydraulic model used by the participants could be an important source of deviations for local parameters, especially for the relative power distribution at the position of the stuck rod. While one node per assembly is the standard neutronics model utilised in radial plane by the participants the used core thermal-hydraulics models differ in the degree of spatial detail. Some participants have applied the 18-channel/cell models, while others have used a more refined model with approximately one channel/cell per fuel assembly, or 177 thermal-hydraulic channels/cells. Accordingly, for the statistical comparisons described in the next section, the results for all local parameters have been divided into two clusters, one for those codes using 18 channels and the other for those with the more refined model.

During the course of the MSLB transient, a power spike is seen at the position of the stuck rod. However, in the 18-channel model this assembly is averaged with several of the surrounding assemblies while mapping the neutronics model to the thermal-hydraulics model. This has the significant effect of underestimating the feedback in this part of the core. On the other hand, the

177-channel model is expected to more accurately predict the feedback (as a result of a better spatial feedback resolution), and therefore the relative power shape, near the stuck rod. Figures 4.15a, b – 4.18a, b show the axial power normalised power shapes averaged over all participants in each of the two clusters and confirm this expectation. The mean curves in these figures show that the averaged 18-channel results over-predict the power in the upper half of the core at the position of the stuck rod when compared to similar results from a 177-channel model. The standard deviations for the 18-channel model are also much larger as compared to those of the 177-channel model. For the representative of the snapshot of highest power after scram for the second transient scenario – RP (state 6) also the axial distributions of the feedback parameters in the stuck rod position are shown for both clusters to illustrate the effect of the spatial feedback distributions – Figures 16c-16f.

4.2.3 2-D radial distributions

4.2.3.1. 2-D core-averaged radial power distributions

For the transient snapshots states (5, 6, 7 and 8), the following 2-D nodal radial distributions are compared: normalised power (NP), inlet coolant temperature, and inlet flow rate and outlet coolant temperature. The means distributions are provided in Appendix C while the participants' deviations are calculated for each radial node and provided in a form of 2-D maps in Appendix D.

The observed discrepancies in the core-averaged radial distributions (especially for the return to power scenario) are mostly due to the detail of spatial coupling schemes: from very detailed spatial mesh overlays (one neutronics node per thermal-hydraulic cell/channel) to coarser mesh overlays. During the course of the MSLB transient, a power spike is seen at the position of the stuck rod. However, in the 18-channel model this assembly is averaged with several of the surrounding assemblies while mapping the neutronics model to the thermal-hydraulics model. This has the significant effect of underestimating the feedback in this part of the core. On the other hand, the 177-channel model is expected to more accurately predict the feedback (as a result of a better spatial feedback resolution), and therefore the relative power shape, near the stuck rod. This can be seen very clearly from the comparisons of participants' results for the snapshot (state 6) taken at time of highest return to power for transient scenario 2. In summary the maximum observed deviations in radial power distributions between the coarse-mesh 18 channel models and the fine-mesh 177-channel models are about 15% (for snapshot 6), where up to 5% are due to the different thermal-hydraulic nodalisation and mapping schemes and up to 10% are due to different heat structure nodalisation and mapping schemes.

Figure 4.15. Relative axial power shape in stuck rod position, state 5 – 18 channels

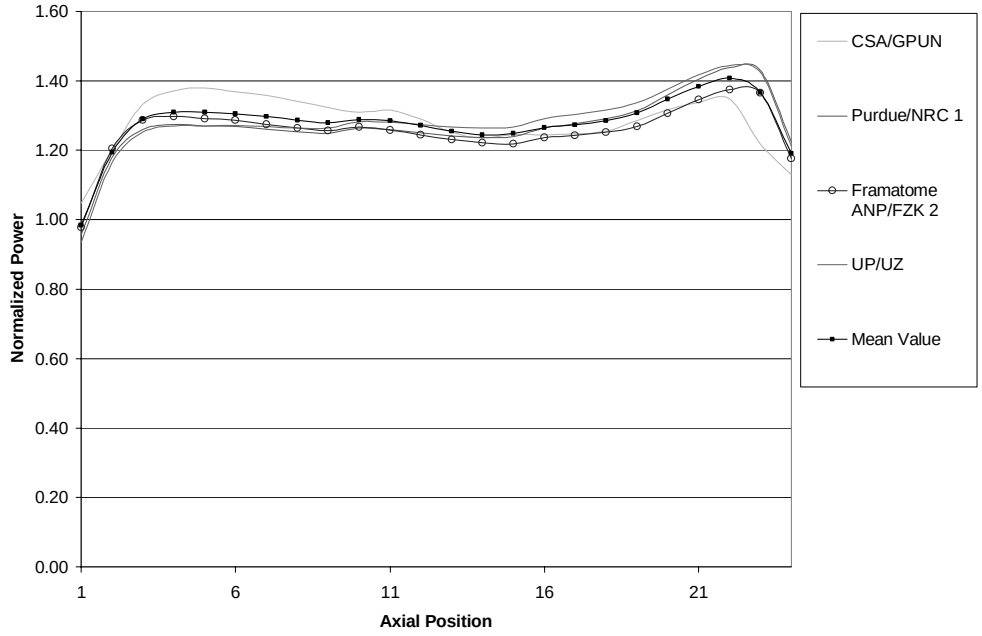

Figure 4.16. Relative axial power shape in stuck rod position, state 5 – 177 channels

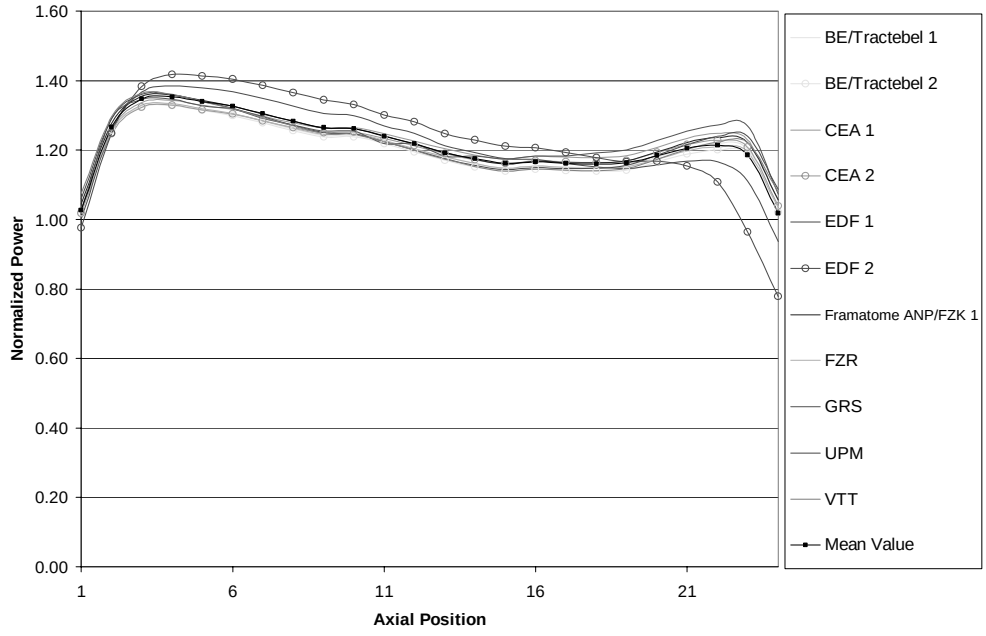

Figure 4.17. Relative axial power in stuck rod position, state 6 – 18 channels

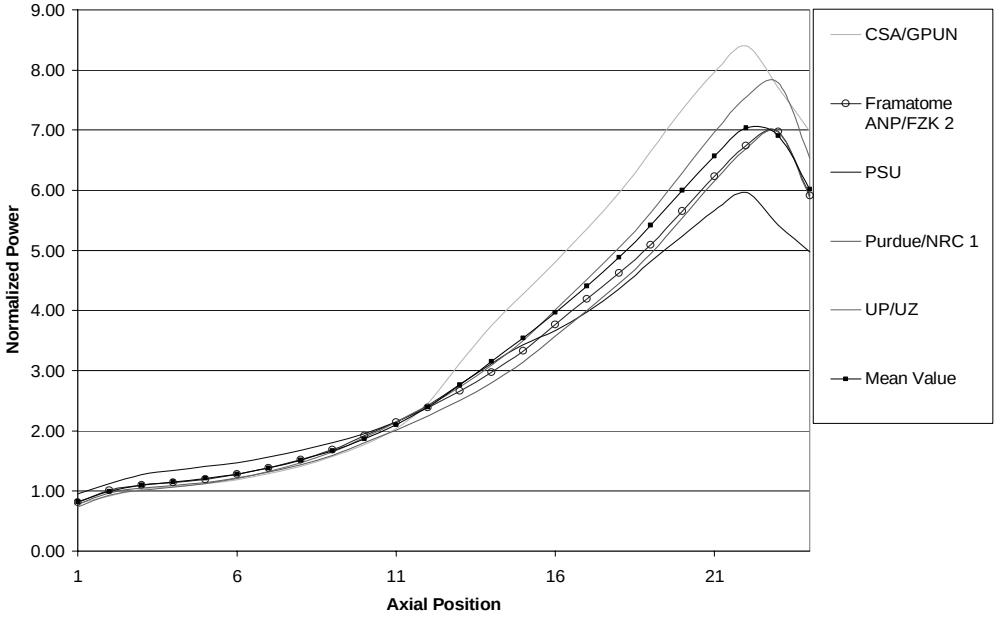

Figure 4.18. Relative axial power in stuck rod position, state 6 – 177 channels

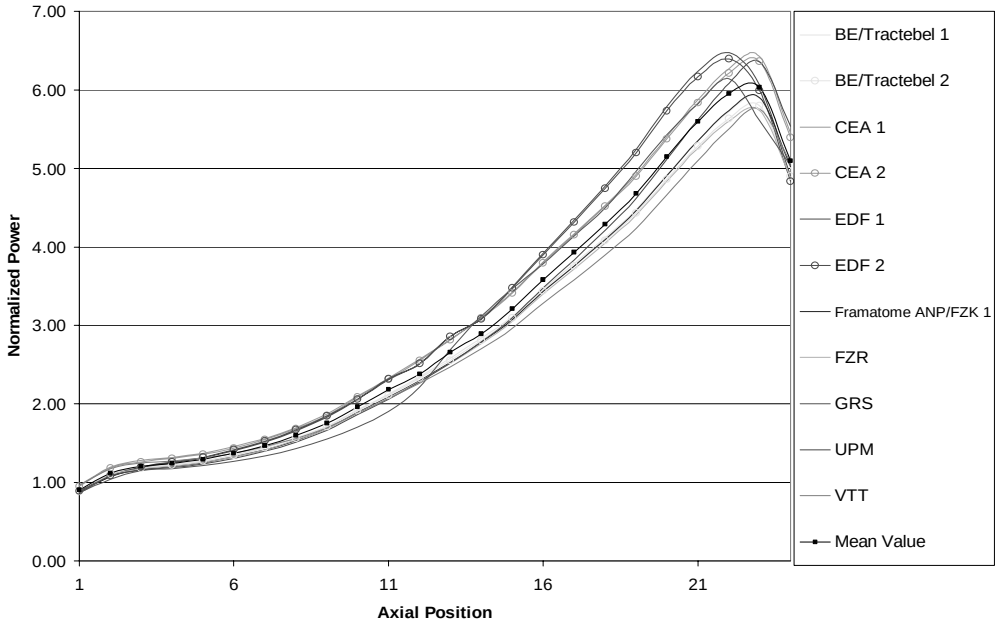

Figure 4.19. Axial Doppler temperature distribution in stuck rod position, state 6 – 18 channels

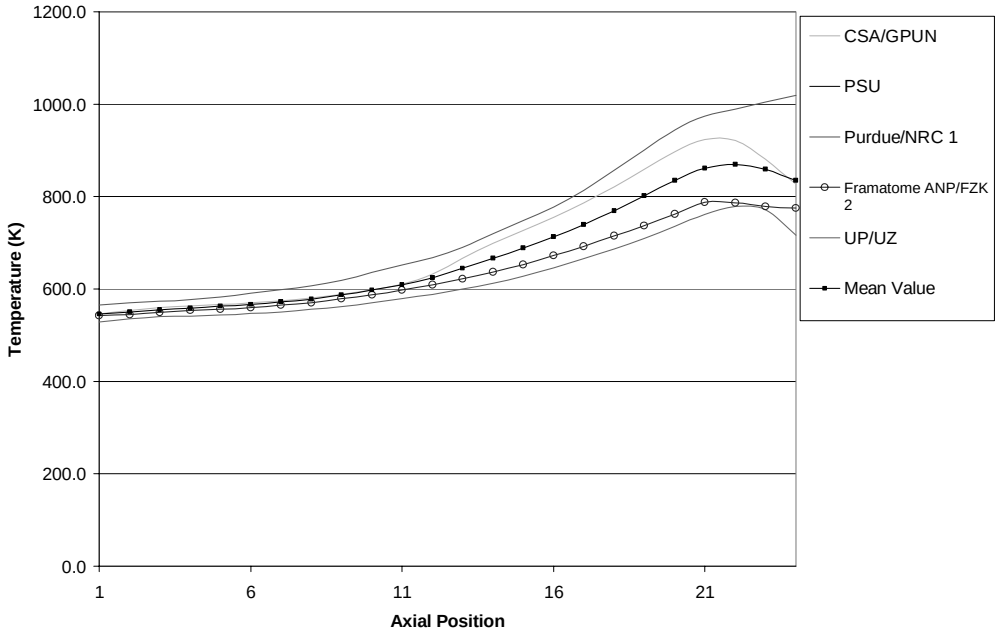

Figure 4.20. Axial Doppler temperature distribution in stuck rod position, state 6 – 177 channels

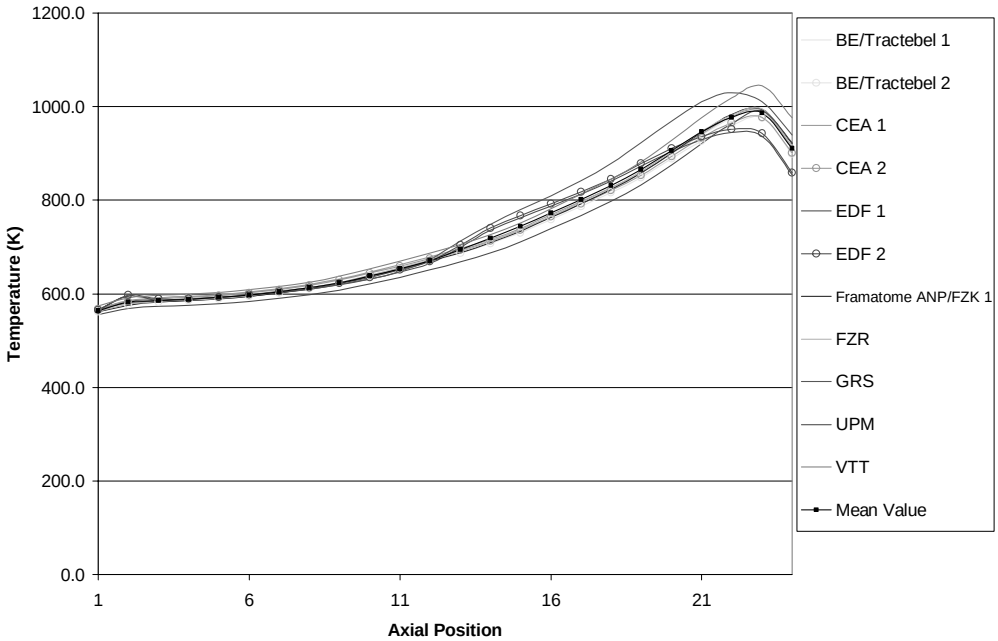

Figure 4.21. Axial coolant density distribution in stuck rod position, state 6 – 18 channels

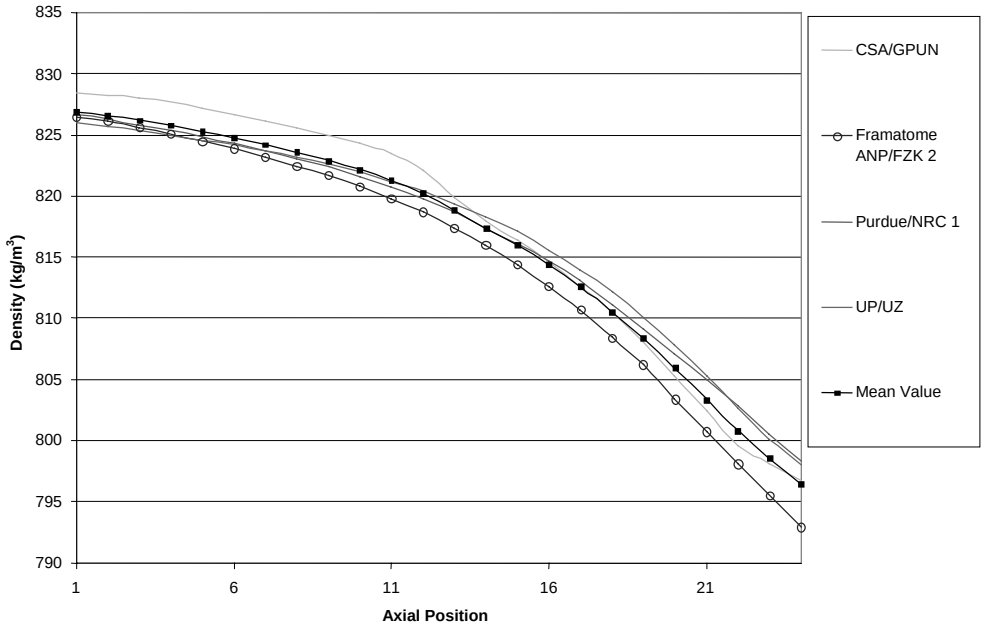

Figure 4.22. Axial coolant density distribution in stuck rod position, state 6 – 177 channels

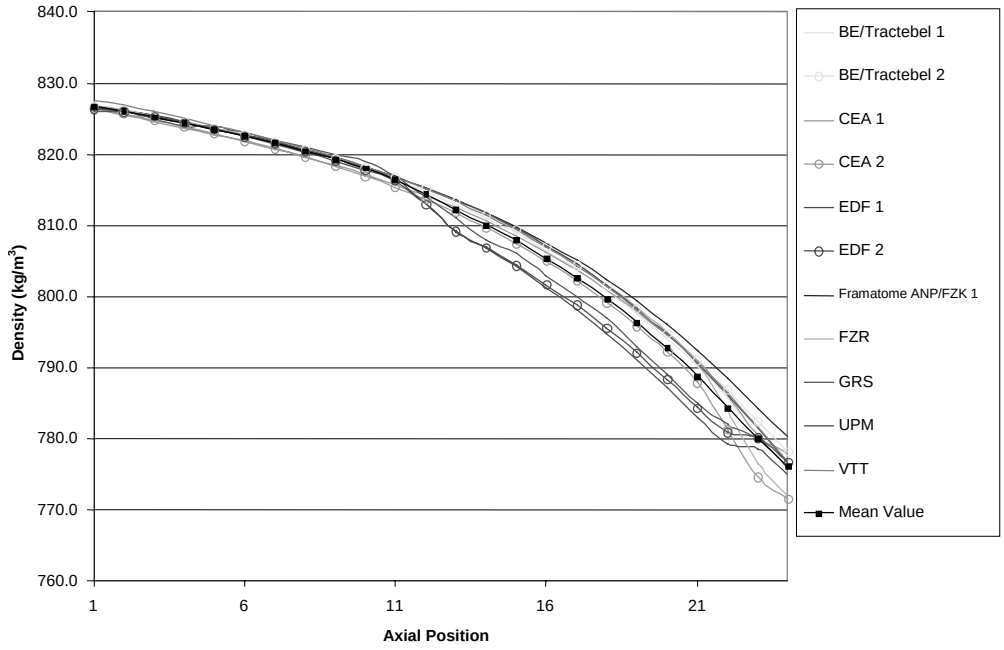

Figure 4.23. Relative axial power shape in stuck rod position, state 7 – 18 channels

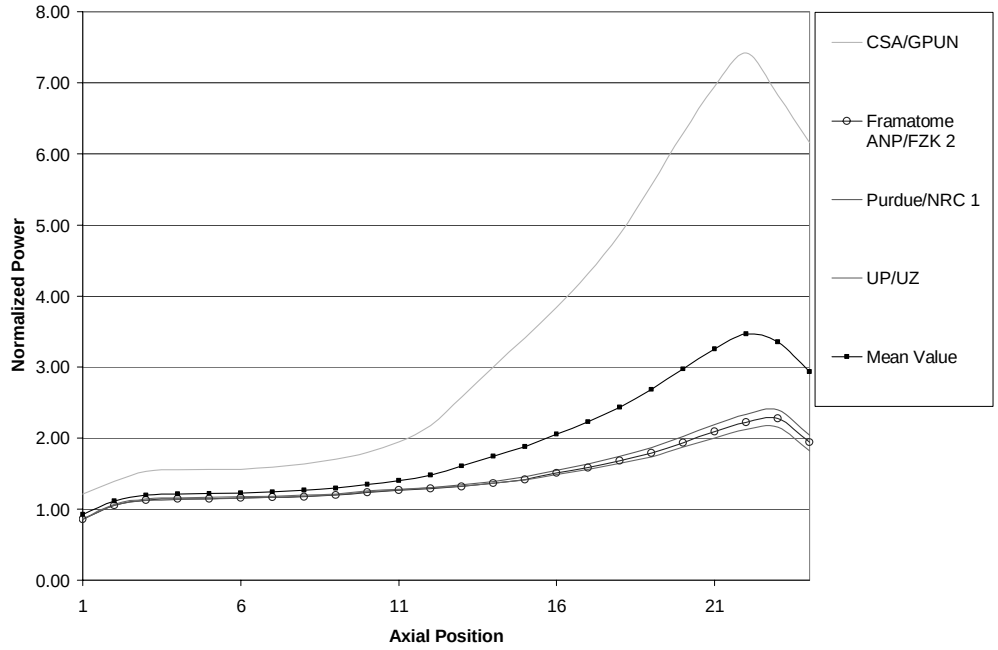

Figure 4.24. Relative axial power shape in stuck rod position, state 7 – 177 channels

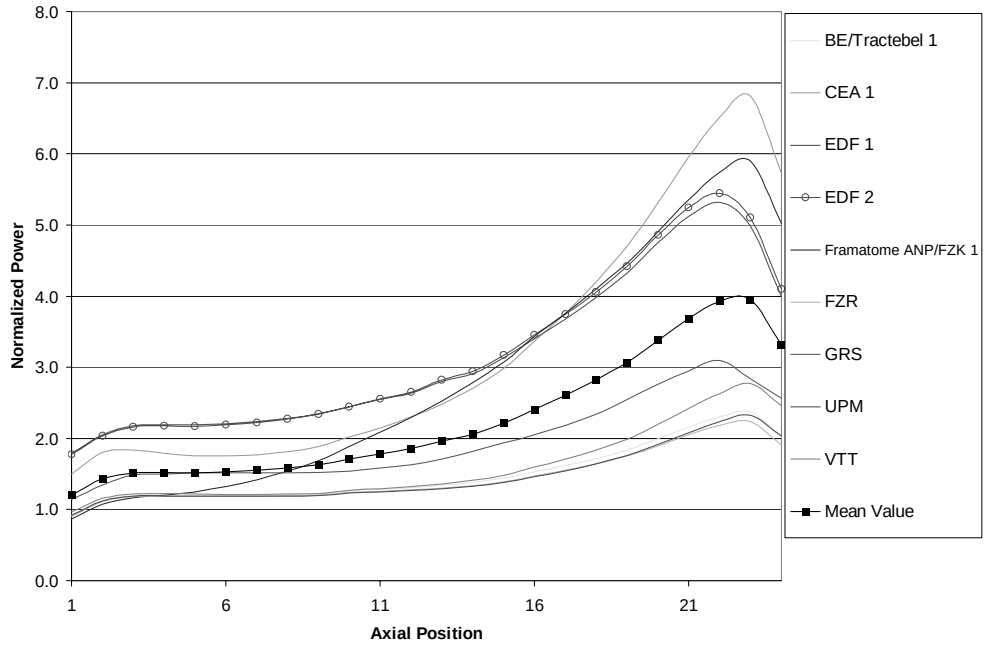

Figure 4.25. Relative axial power shape in stuck rod position, state8 – 18 channels

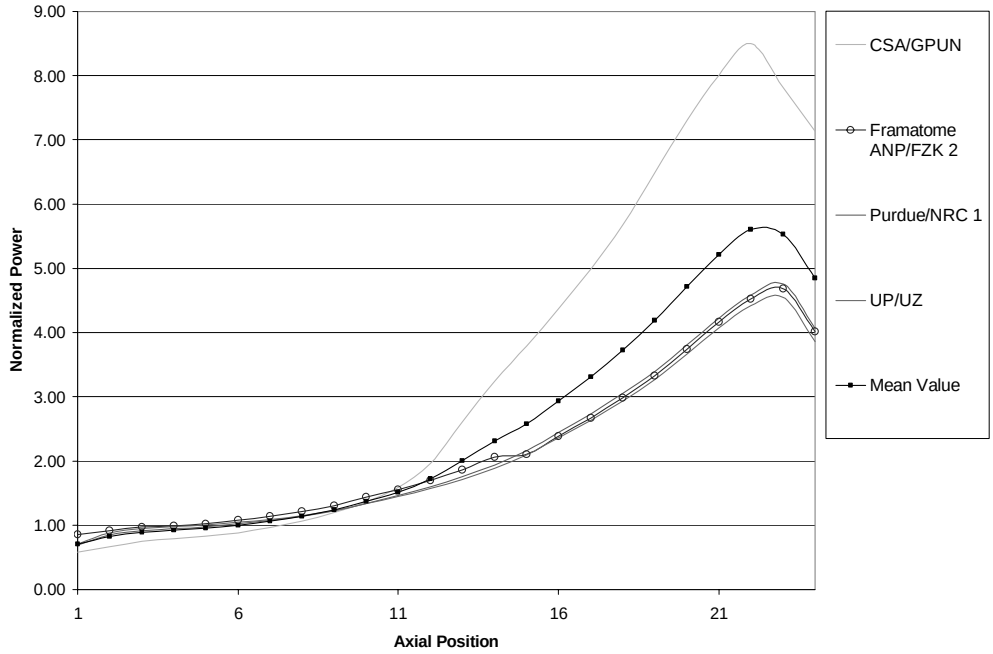

Figure 4.26. Relative axial power shape in stuck rod position, state 8 – 177 channels

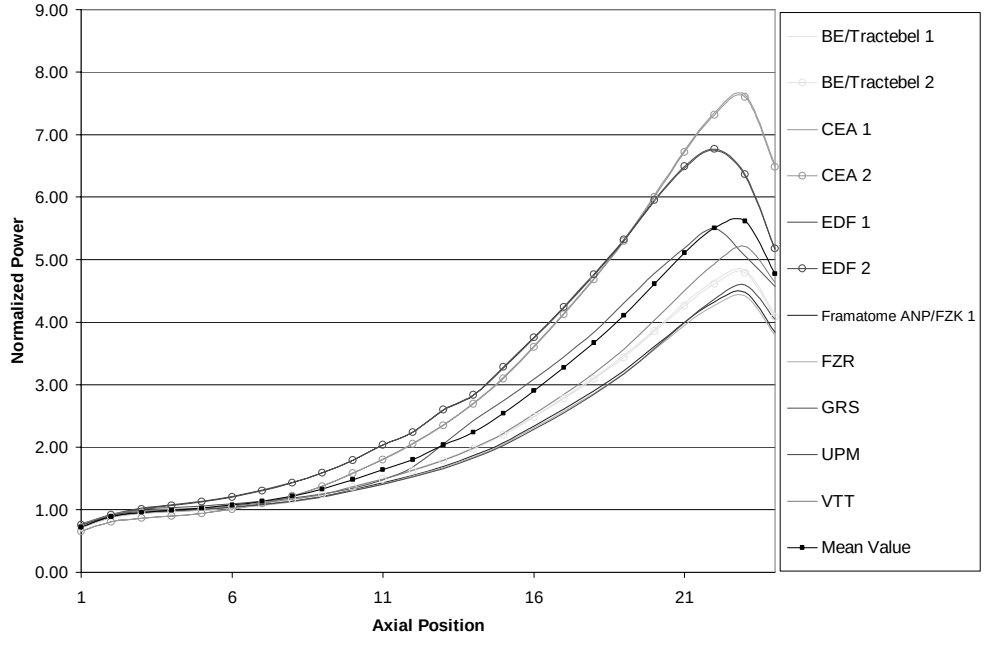

4.3 Time histories

Time histories (core volume averaged without the reflector region) are analysed and compared in the following order: total power, fission power; coolant density; and Doppler temperature. In addition, total reactivity and reactivity components and the maximum nodal Doppler temperature vs. time is compared also.

The mean curves for the time histories are provided in Appendix C (supplied on the CD-ROM). The standard deviations are represented as error bars at each time step. The participant deviations and figures of merit are presented in Appendix D (supplied also on the CD-ROM), and are listed in the same order as the reference solutions. In this section selected comparisons of the time histories for each of the two transient scenarios are presented and analysed.

The scenario 1 is the best estimate in which no return to power and criticality is observed in the second half of the transient. For this scenario the participants are in a good agreement and form a single cluster. As it can be seen from Figures 4.27 and 4.28 some small deviations in total and fission power as function of time can be seen only before the scram. Looking at the time histories of the core-averaged coolant density and Doppler temperature (which are the instantaneous feedback parameters for the benchmark calculations) – Figures 4.29 and 4.30 – one can attribute these small deviations to some differences in the feedback parameters at the beginning of transient. These differences are more pronounced in the Doppler feedback temperature values, and they are a result of the fact that not all of the participants are using the defined relation [1] for the Doppler feedback temperature. In case of the maximum nodal Doppler temperature this fact affects not only the values at the beginning of the transient but also during the transient. After the scram one can observe also deviations in the core-averaged coolant density deviations; however, their effect on the power histories cannot be seen since the reactor is sub-critical.

The scenario 2 is of special interest because of the observed return-to-power phenomenon, which represents a very good test case for coupled codes. The participants' results for total and fission power (Figures 4.32 and 4.33) form a cluster with larger local deviations observed after the scram and especially at the time of return-to-power (second peak) into the transient. These deviations can be explained with the differences in the participants' predictions of the total reactivity time behaviour and the core-averaged coolant density and Doppler temperature (Figures 4.34-4.36). The power response and the magnitude of the return to power during the transient as predicted by different codes are functions of the total reactivity time evolution.

The total reactivity has three components – negative tripped rod reactivity, and positive moderator (coolant) density and Doppler feedback reactivities. In difference of the point kinetics simulations [2], where the negative tripped rod reactivity inserted is specified *i.e.* it is the same for all the codes, in coupled calculations the actual inserted negative reactivity during the scram (with assumption for the maximum worth control rod stuck out) can be different. There are two reasons for this difference: first, there are differences in the calculated static tripped rod worth with different coupled codes (Table 4.9); second, in the coupled calculations there is a dynamic simulation of the scram, which accounts for real changes in the reactor core, connected with flux re-distribution and local feedback conditions change at each time step. As a result the actual value of inserted tripped rod (TR) reactivity is larger than the statically evaluated TR and this effect of the 3-D dynamic scram simulation is predicted differently by different coupled codes (as it can be seen in Figure 4.34 at the time of scram).

The moderator (coolant) reactivity component follows the moderator (coolant) density (Figure 4.35). Since the second exercise is a core boundary conditions calculations with boundary

conditions provided at the core inlet and outlet the discrepancies in coolant density predictions are mostly due to different density correlations and standards for water/steam property tables, incorporated into the codes.

The Doppler reactivity component follows the Doppler fuel temperature. The discrepancies in the core-averaged Doppler temperature time evolutions (Figure 4.36) are due to the used relation for calculation of Doppler fuel temperature, and correlations for fuel properties vs. temperature as well as to the radial and axial nodalization of the heat structure used (fuel rod). For example, in Figures 4.30 and 4.31 the ANL results are higher (approximately with 100 K) than the predictions of the rest of the participants at the beginning of the transient. This difference is due to the fact that ANL submitted core-averaged fuel temperature (which is based on pellet average temperature) instead the Doppler temperature, which is defined as weighted relation of pellet surface and centerline temperatures (Appendix B). Pellet average temperature is higher than the Doppler temperature since in the defined relation for the Doppler temperature in the specifications [1] the higher weight is given to the surface temperature. Apparently this difference did not affect the ANL power predictions since they have used the Doppler temperature for the feedback purposes in their MSLB simulations. For the maximum nodal Doppler temperature time evolution comparisons the deviations become more pronounced because in addition to above described sources of discrepancies the detail of thermal-hydraulic modelling (including the heat structure model) and coupling with the core neutronics model contributes to increasing the deviations among the participants' results around to the return-to-power time.

Figure 4.27. Core-averaged total power time history for scenario 1

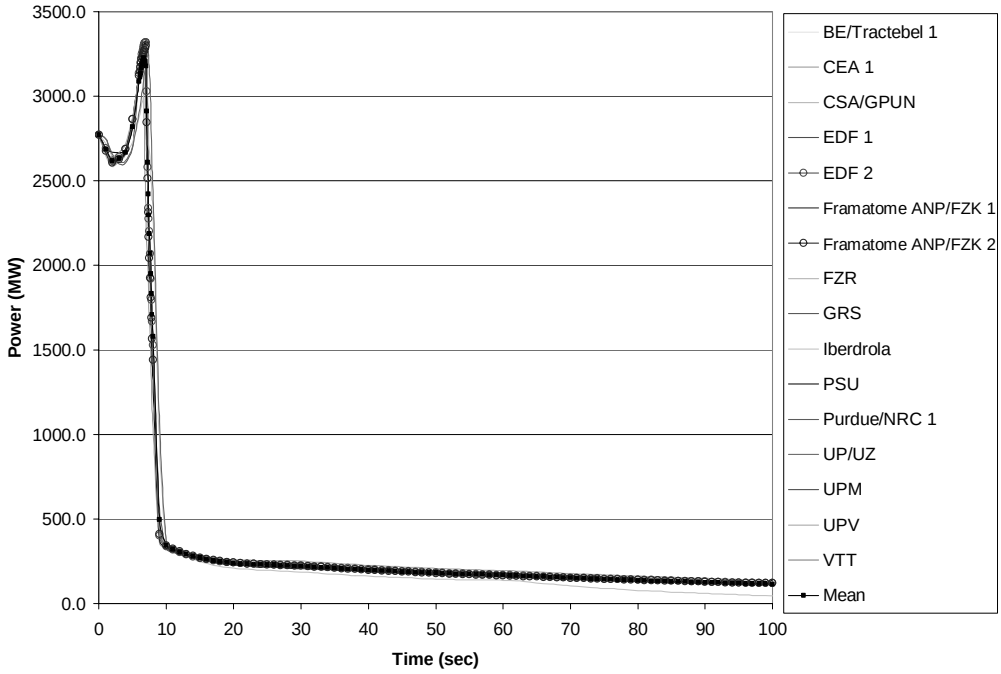

Figure 4.28. Core-averaged fission power time history for scenario 1

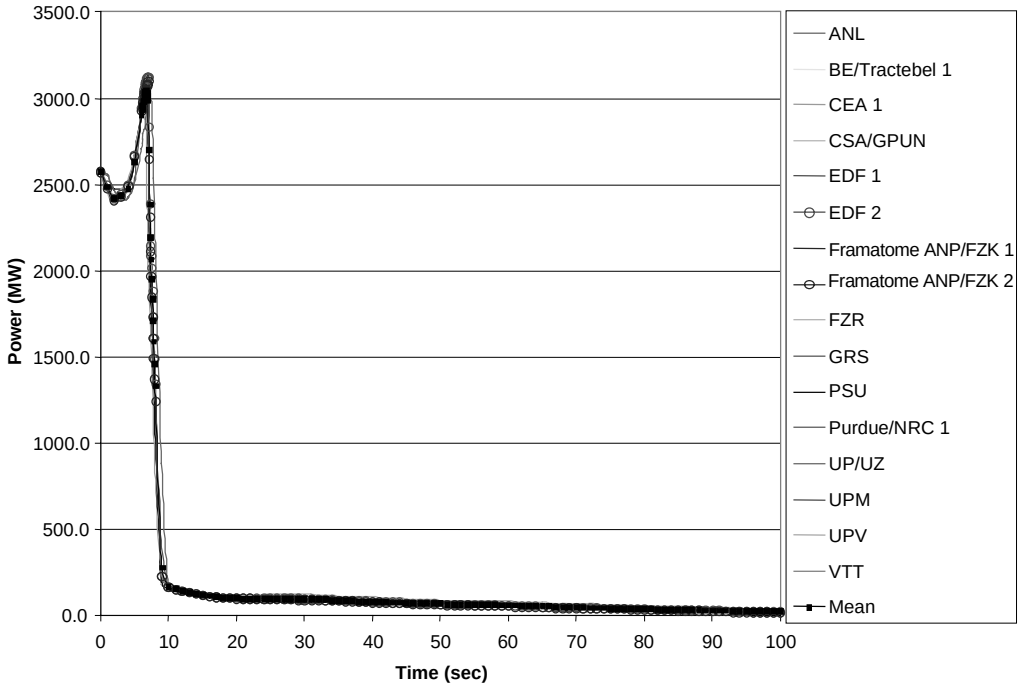

Figure 4.29. Core-averaged coolant density time history for scenario 1

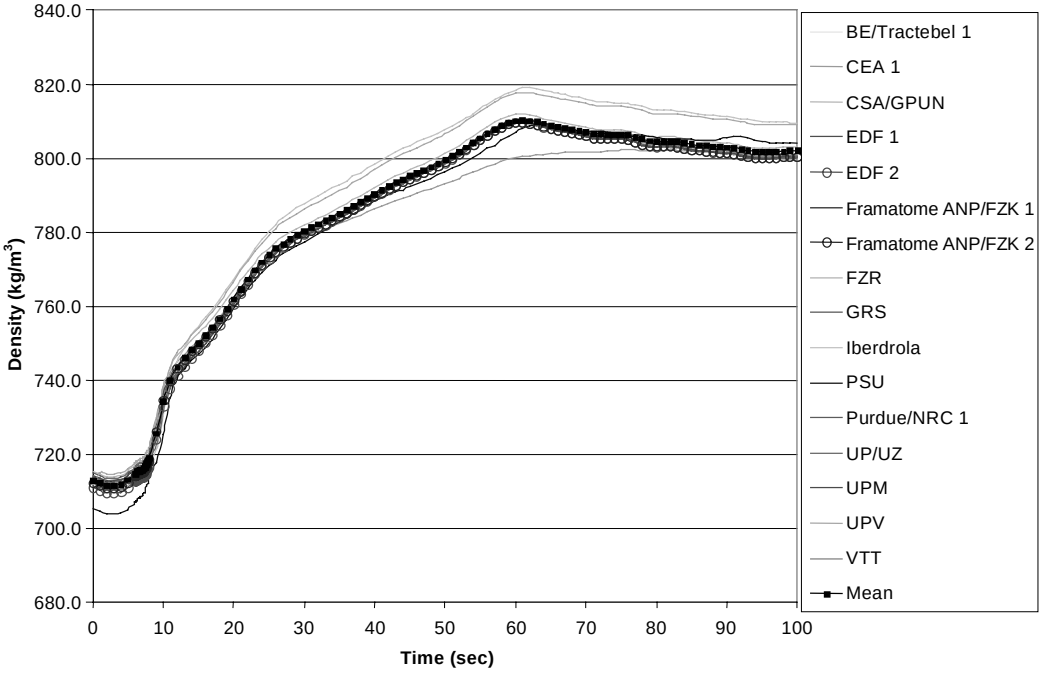

Figure 4.30. Core-averaged Doppler temperature time history for scenario 1

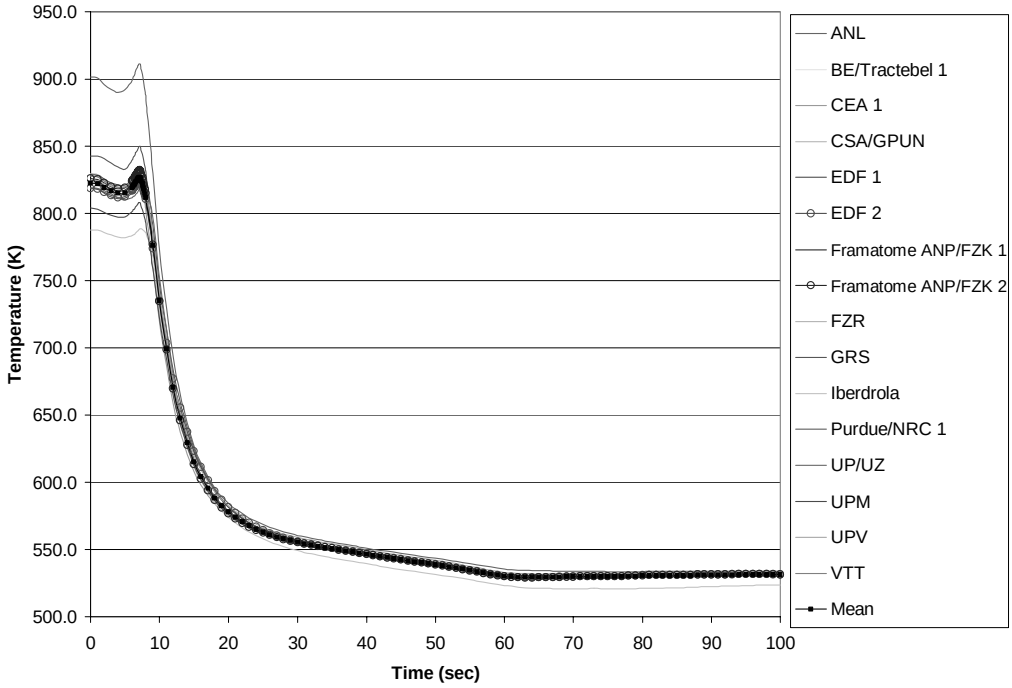

Figure 4.31. Maximum nodal Doppler temperature time history for scenario 1

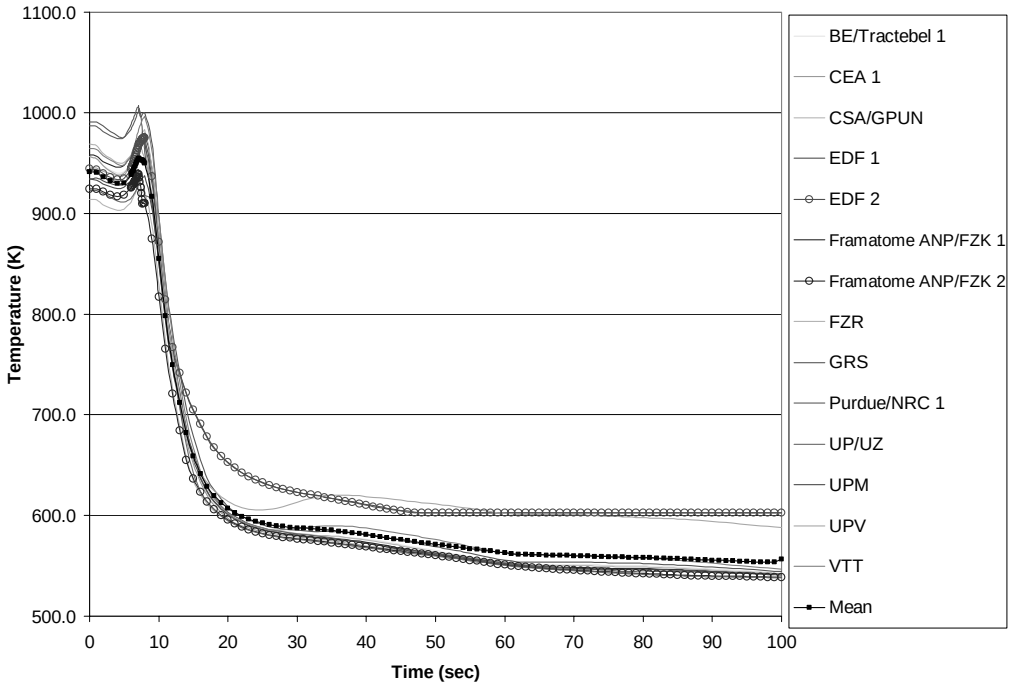

Figure 4.32. Core-averaged total power time history for scenario 2

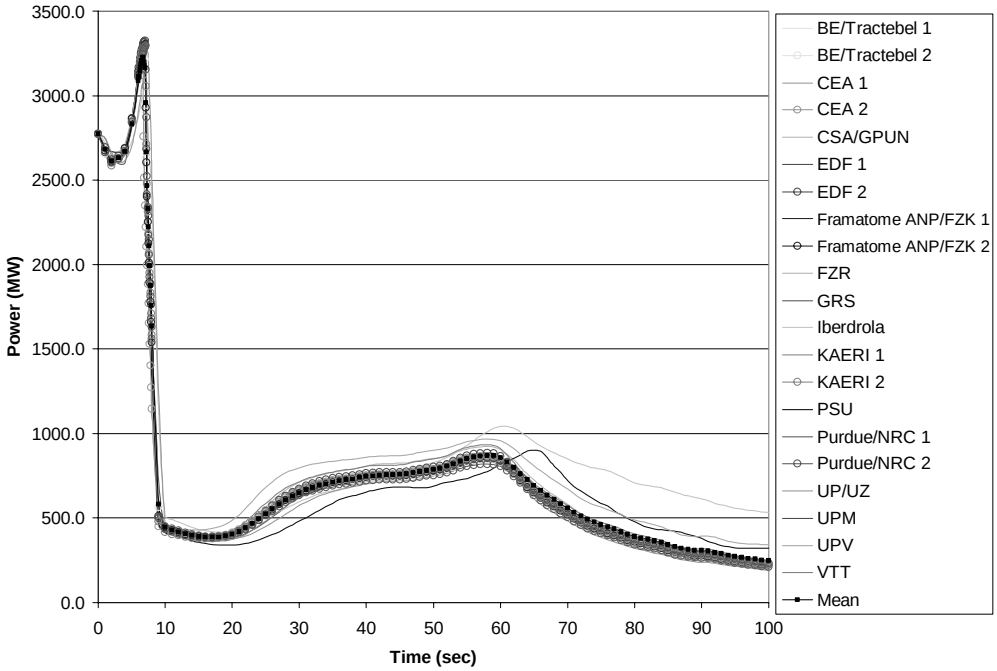

Figure 4.33. Core-averaged fission power time history for scenario 2

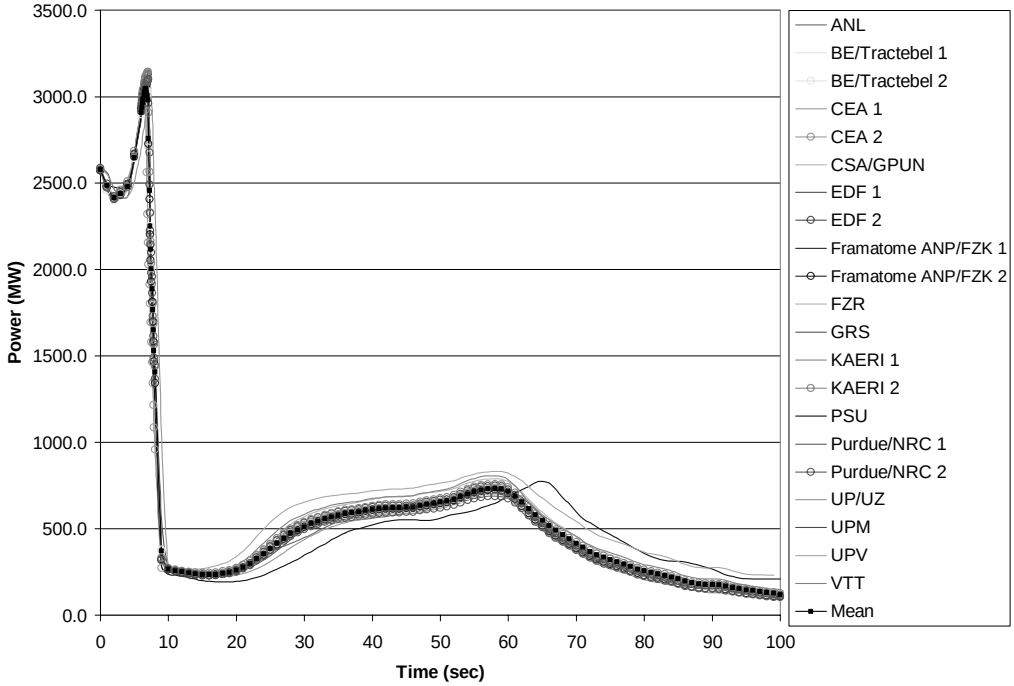

Figure 4.34. Core-averaged total reactivity time history for scenario 2

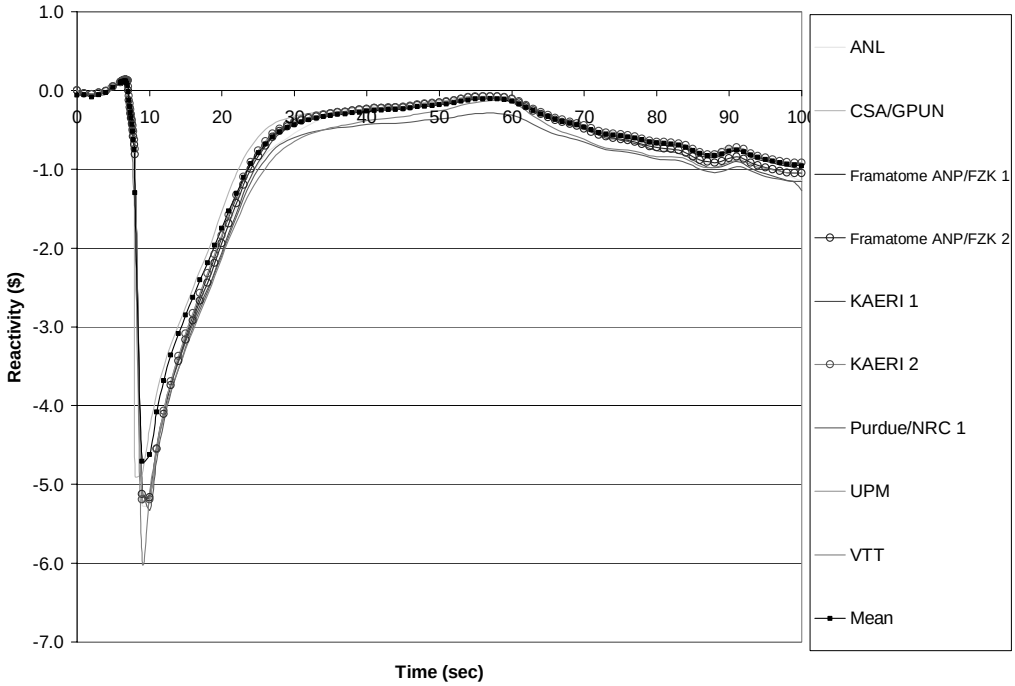

Figure 4.35. Core-averaged coolant density time history for scenario 2

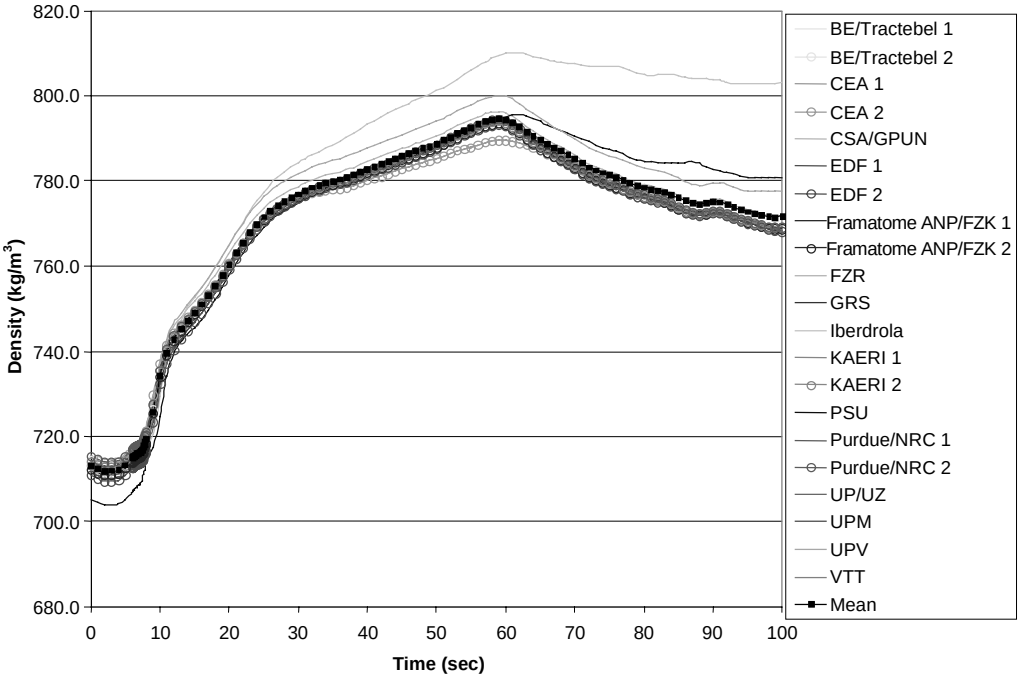

Figure 4.36. Core-averaged Doppler temperature time history for scenario 2

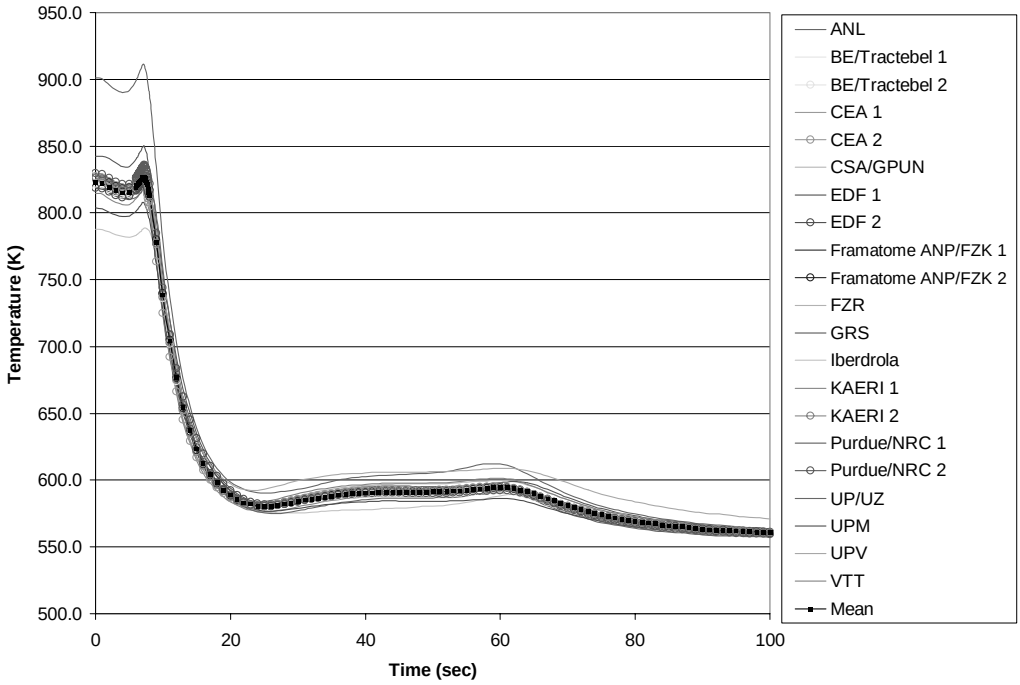

Figure 4.37. Maximum nodal Doppler temperature time history for scenario 2

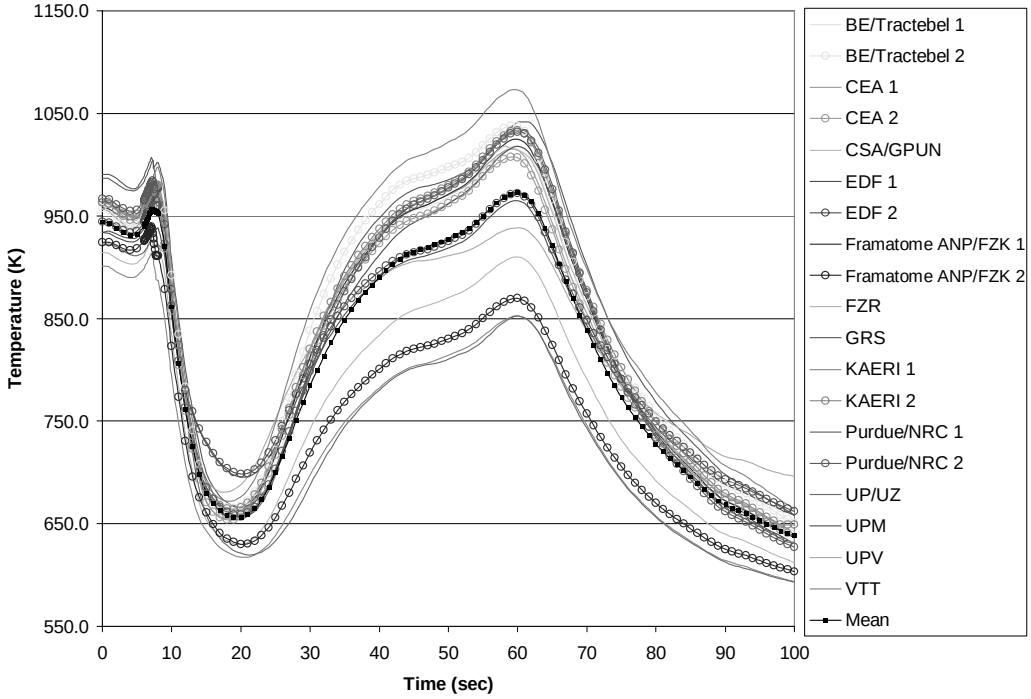

Chapter 5

CONCLUSIONS

In this volume, the second phase of the OECD/NRC PWR MSLB Benchmark was discussed in detail. The results of this benchmark problem are intended to assist in the understanding of the behaviour of the next generation of coupled computer codes. Overall, this benchmark has been well accepted internationally, with 16 participants representing 10 countries participating in the second phase, and a like number participating in the other two phases. The results submitted by the participants for the second phase are used to make code-to-code comparisons, and a subsequent statistical analysis. This information encompasses several types of data for both core thermal-hydraulic and neutronics parameters at the initial steady state conditions and throughout the MSLB transient: integral parameters, 1-D axial distributions, 2-D radial distributions, and time histories.

A detailed assessment of the differences between the calculated results submitted by the participants for the second exercise were presented in Chapter 4 of this volume. Overall, the participants' results for integral parameters, core-averaged axial distributions, and core-averaged time histories are in good agreement; however, one exception to this statement is the core-averaged axial power distributions for the transient snapshots (especially after the scram). This parameter shows more pronounced deviations amongst participant results, both in the value and behaviour throughout the transient. Any disagreement can be attributed to differences in the spatial decay heat modelling as explained in Chapter 4. These differences also affect the local (in the position of the stuck rod) relative axial power distributions for the transient snapshots.

The observed discrepancies in the core-averaged radial distributions, local axial distributions (in the position of the stuck rod), and maximum nodal Doppler temperature time history (especially for the return to power scenario) are mostly due to the detail of spatial coupling schemes: from very detailed spatial mesh overlays (one neutronics node per thermal-hydraulic cell/channel) to coarser mesh overlays. During the course of the MSLB transient, a power spike is seen at the position of the stuck rod. However, in the 18-channel model this assembly is averaged with several of the surrounding assemblies while mapping the neutronics model to the thermal-hydraulics model. This has the significant effect of underestimating the feedback in this part of the core. On the other hand, the 177-channel model is expected to more accurately predict the feedback (as a result of a better spatial feedback resolution), and therefore the relative power shape, near the stuck rod. This can be seen very clearly from the comparisons of participants' results for the snapshot taken at time of highest return to power for transient scenario 2. The observed deviations (up to 15%) in radial power distribution are due mostly to the different thermal-hydraulic (about 5%) and heat structure (about 10%) nodalisation and mapping schemes. This result is very important since from a safety point of view, the possibility of a return to power in the later half of a MSLB transient is of great importance [6].

Participants' kinetics models for the benchmark utilised mostly a one node per assembly (npa) scheme in the radial plane [7]. The benchmark team and some participants also developed a more detailed neutronic model using a 4-npa scheme in the radial plane and the subsequent mapping

schemes. Comparative studies were performed for the second MSLB benchmark scenario with expected return to power. The obtained results demonstrated that the refinement of the neutronic model in the radial plane does not impact the total power transient evolution. The neutronic scheme refinement impacts local radial power distributions but not to the extent of the impact of the T-H nodalisation.

These parametric studies indicated that the MSLB calculations are mostly sensitive to the detail of the thermal-hydraulic core modelling. The MSLB simulations are less sensitive to the radial refinements of neutronic model, especially when coarser nodalisation for the thermal-hydraulic core model is used. This reflects the feedback phenomena involved in the MSLB transient since the asymmetric cooling is the driving force of the transient.

Discussions that took place at the benchmark workshops made helped to clarify some benchmark modelling issues. Based on these discussions, the modifications summarised below were made to eliminate two of these issues.

In the original specification, the reflector region of the core was treated in the same manner as all the other core regions in terms of cross-section feedback modelling. After the third workshop, it was decided that PSU would provide a fuel average temperature for the radial reflector cross-section modelling since not all of the participants were able to model the radial reflector as specified. The coolant average density for the reflector is taken to be equal to the inlet coolant density. For the axial reflector regions, it was decided that fuel temperatures equal to the inlet (for bottom reflector) and outlet (for top reflector) channel coolant temperatures and subsequently channel inlet and outlet coolant densities will be used. The impact of using such a modified ("fixed") reflector feedback modelling on the initial HFP steady state can be estimated as follows – 2 pcm (per-cent-milli) difference in the eigenvalues prediction, maximum 0.05% deviations in normalised power distributions and practically no change in the core axial shape.

Exercise 2 is defined as an evaluation of the core response to imposed system T-H conditions. The Benchmark Specification provides a complete core description, cross-section library and initial and transient boundary conditions (BC) for 18 T-H cells. These BC include radial distribution of the mass flow rates, liquid temperatures at the core inlet and pressure at the core outlet. These BC are obtained from the best-estimate core-plant system calculations performed with the PSU version of TRAC-PF1/NEM. The radial distributions are provided for 18 T-H cells in radial plane following the nodalisation of the TMI-1 TRAC-PF1 model, which includes a 3-D vessel (including the core) model in cylindrical geometry. Difficulties have arisen in the interpretation of the mass flow BC, provided by the above-described TRAC-PF1 model, since the most of the participant's codes model the core thermal-hydraulically by parallel channels. In order to avoid this source of modelling uncertainties new BC have been generated, where mass flows are corrected for direct use as input data in the participants' codes. A geometrical interpolation method is used to process the TRAC-PF1/NEM BC in order to obtain inlet conditions per assembly.

Overall, it was determined that for the second phase of this benchmark, the key parameters were the thermal-hydraulic core modelling and spatial coupling schemes with the core neutronics model; the spatial decay heat modelling; and the Doppler temperatures and density correlations, used by the thermal-hydraulics codes. The other parameters were useful to analyse because they helped to determine what was causing the behaviour of the key parameters. As expected, the axial distributions after the scram were very sensitive to the spatial decay heat modelling. In addition, it was proven that the detail of the core thermal-hydraulic models a great effect on the radial power distribution throughout the transient. In particular, the differences can be up to 15% for the snapshot at the time of highest return to power affecting local safety parameters as maximum nodal fuel temperatures.

Different code formulations/correlations for Doppler temperature and moderator density, affected both core-averaged power and reactivity time histories and local distributions throughout the transient since these two parameters are the major feedback parameters for the cross-section modelling impacting in this way the neutronics predictions.

As it was with the case of the first exercise it was confirmed for the second exercise that this type of analysis requires considerable more output than was required by previous benchmarks; and this is especially true of the remaining phases. In addition to requesting more output, the process of determining which parameters to request from the participants must be completed well in advance. Throughout this process, a great deal of consideration should be given to the level of detail required for coupled 3-D neutronic/thermal-hydraulic problems in order to evaluate the results from both a neutronic and thermal-hydraulic perspective.

It should be noted that one issue has not been incorporated into the statistical comparison techniques. In the case of time history data and 1-D axial distributions, especially axial power shapes, the overall curve shape should be compared as well. Several methods exist to complete such analysis, the most promising being the fast Fourier transform technique developed by D'Auria [8]. Number of these methods are implemented in the ACAP automatic assessment tool [9].

For the purposes of this benchmark, such a comparison was judged to be unnecessary. Curve-fit comparison would become important when the shapes differ significantly among the sets of results. However, preliminary investigations showed that the results submitted by the participants were in quite good agreement regarding the general shapes, and the only significant differences lay in the values at certain levels or points in time. For this reason, full curve analysis is not included in the comparisons for this benchmark; however, in future problems such methods should be considered.

The results of the second phase will be combined with results from the first phase of the PWR MSLB benchmark to help verify coupled 3-D neutronics/thermal-hydraulic system codes results and to assist the users in gaining a more in-depth knowledge of these codes. While the purpose of this exercise is to initialise and test the primary and secondary system model responses the purpose of the second exercise was to initialise and test the coupled core thermal-hydraulic/3-D neutronics response. Both exercises prepare the foundation of conducting the exercise 3 in a consistent and systematic way. Exercise 3 is defined as a best-estimate coupled-core plant transient modelling. This phase provides the opportunity to study the impact of different neutronics and T-H models on code predictions, as well as the coupling between them. Developing a more in-depth knowledge of the coupled computer code systems is important because 3-D kinetic/thermal-hydraulic codes will play a critical role in the future of nuclear analysis.

REFERENCES

[1] Ivanov, K., T. Beam, A. Baratta, A. Irani, and N. Trikorous, "PWR MSLB Benchmark: Volume 1: Final Specifications", NEA/NSC/DOC(99)8, April 1999.

[2] Beam, T., K. Ivanov, B. Taylor, and A. Baratta,"PWR MSLB Benchmark: Volume 2: Results on Phase I on Point Kinetics", NEA/NSC/DOC(2000)21, December 2000.

[3] Taylor, B. and K. Ivanov, "Statistical Methods Used for Code-to-Code Comparisons in the OECD/NRC PWR MSLB Benchmark", *Annals of Nuclear Energy*, p. 27 (2000), 1589-1605.

[4] "Summary of the 2nd PWR MSLB Benchmark Workshop", Madrid, Spain, 25-26 June 1998, NEA/NSC/DOC(98)4.

[5] "Summary of the 3rd PWR MSLB Benchmark Workshop", Garching, Germany, 24-25 March 1999, NEA/NSC/DOC(99)6.

[6] "Summary of the 4th PWR MSLB Benchmark Workshop", Paris, France, 24-25 January 2000, NEA/NSC/DOC(2000)2.

[7] Ivanov, K., N. Todorova, E. Sartori , "Using the OECD/NRC PWR MSLB Benchmark to Study Current Numerical and Computational Issues of Coupled Calculations", TANSAO 84, p. 26-28, (2001).

[8] Ambrosini, W., R. Bovalini, F. D'Auria, and F. August, "Evaluation of Accuracy of Thermal-hydraulic Code Calculations", Energia Nucleare (2), (1990).

[9] Kunz, R. and J. Mahaffy, "A Review of Data Analysis techniques for Application in Automated Accuracy Assessments", Proc. of the International Meeting BE-2000, Washington, DC, November 2000 (Electronic Publication – CD-ROM).

Appendix A

DESCRIPTION OF COMPUTER CODES USED FOR ANALYSIS IN THE SECOND PHASE OF THE PWR MSLB BENCHMARK

SAS-DIF3DK (ANL, USA)

The DIF3D-K computer code is a follow on to the DIF3D static code developed by Argonne National Laboratory. It is used by ANL for the benchmark exercise. The code uses two different methods to solve the time dependence of the nodal multi-group diffusion equation, variable implicit or theta method and the factorization method. The factorisation options include the improved quasi static, the adiabatic option, and point kinetics. The Cartesian multi-dimensional solution involves the time-dependent polynomial approximations to the intranodal flux distribution.

The thermal hydraulic method is based on the SAS family of computer codes. The reactor core is represented by a large number of coolant channels, each of which is modeled hydraulically by an on-dimensional coolant path. The code uses a five-equation thermal-hydraulic two-phase homo-geneous non-equilibrium model to solve the two-phase problem. SAS does not model the balance of plant. RELAP5/MOD3.2 will be used for that purpose.

Cross-section modelling is done in DIF3D using MACOEF. The MACOEF represents changes in macroscopic cross-sections as mathematical functions of changes in material properties in the reactor. The spatially dependent material mass and temperature fields are computed in SAS and then mapped to DIF3D-K as specified in the model. The changes are then used to update the cross sections used in the solution of the multi-group diffusion equation.

CRONOS2/ISAS/FLICA4 (CEA, France)

CRONOS2 is the computer tool devoted to neutronic core computation in the SAPHYR system (SAPHYR also includes APOLLO2 for neutronic assembly calculation, and FLICA4 for TH core calculation). CRONOS2 has been designed to provide all the computational means needed for nuclear reactor core calculations, including design, fuel management, follow up and accidents. CRONOS2 allows steady state, kinetic, transient, perturbation and burn-up calculations. The power calculation takes into account the thermal-hydraulic feedback effects, either by a 1-D simplified model, or by the coupling with FLICA4. All of this can be done without any limitation on any parameter (angular discretisation, energy groups, spatial meshes). As part of SAPHYR, CRONOS2 has been written with the constant will of optimizing its performance and its portability. It is based on a modular structure that allows a great flexibility of use. A special user oriented language, named Gibiane, and a shared numerical toolbox are used to chain the various computation modules. The code solves either the diffusion equation or the even parity transport equation with anisotropic scattering and sources. Different geometries are available such as 1, 2 or 3-D Cartesian, 2 or 3-D hexagonal and cylindrical geometries. Four different solvers are available: PRIAM MINOS CDIF and VNM. The PRIAM solver uses the second order form of the transport equation and is based on SN angular discretization and a finite element approximation on the even flux (primal approximation); this solver is mainly devoted to accurate reference calculation for either Cartesian or hexagonal geometry. The MINOS nodal solver is based on mixed dual finite element for diffusion or simplified PN equations; this solver performs very fast kinetic and static calculations. The CDIF solver uses finite difference approximation for the diffusion equation, and is devoted to pin-by-pin rectangular calculation. The VNM solver based on the VARIANT method will be soon connected to CRONOS2; it is based on a mixed primal method and PN approximation and will be mainly devoted to computation of fast breeder reactors.

FLICA4 is the thermal-hydraulics code of the SAPHYR system, and like CRONOS. FLICA4 is a 3-D two-phase compressible flow code, specially devoted to reactor core analysis. The fluid is modeled by a set of four equations: mass, momentum, and energy conservation for the two-phase

mixture, and mass conservation for the vapour. The velocity disequilibria are taken into account by a drift flux correlation. A 1-D thermal module is used to solve the conduction in solids (fuel). Thanks to the modular design of the SAPHYR codes, numerous closure laws are available for wall friction, drift flux, heat transfer and Critical Heat Flux (CHF). A specific set has been qualified in FLICA3 for PWR applications. An extensive qualification program for FLICA4 is under way, based on recent experimental data, in order to cover a wider range of flow conditions. FLICA4 includes an object-oriented pre-processor to define the geometry and the boundary conditions. Radial unstructured meshes are available, without any limitation on the number of cells. Zooming on a specific radial zone can be performed by a second calculation using a finer mesh (for instance a sub-channel calculation on the hot assembly). The fully implicit numerical scheme is based on the finite volumes and a Roe solver. This kind of method is particularly accurate, with a low numerical diffusion.

ISAS is a general coupling tool, initially designed for the ITER project. It is based on the Parallel Virtual Machine (PVM) data exchange protocol, and provides a supervision language (Gibiane or Ocaml). Then each coupled code remains independent, and is run as an individual process within a master-slave relationship. Main advantages are fewer development needs and much reduced maintenance compared with code unification, and easy computation management (use of several machines, parallelism, etc.). As long as an ISAS interface exists in a code, this code can be coupled to any other code through ISAS without any more specific developments. This applies very conveniently to modular codes such as CATHARE2, CRONOS2, and FLICA4.

Since CRONOS2 and FLICA4 share the SAPHYR toolbox, which provides a PVM interface for ISAS, the coupling of CRONOS2 and FLICA4 is easily performed through the ISAS code supervisor. The SAPHYR toolbox also provides a common 3-D data structure, used to exchange the neutronic power from CRONOS2 to FLICA4, and the thermal-hydraulic feedback parameters (Doppler, moderator density, boron concentration, etc.) from FLICA4 to CRONOS2. Steady state calculations between FLICA4 and CRONOS2 are initialized by a power distribution obtained by CRONOS2 with its simplified feedback model; then an iterative procedure between CRONOS2 and FLICA4 is conducted until convergence. Transient coupling scheme is less standard, and is fully managed by ISAS. One can use a semi-implicit time scheme, where each code is run after the other, or an explicit time scheme allowing code parallelism.

RETRAN-3D (CSA Inc., USA and Iberdrola, Spain)

RETRAN-3D is a third generation system transient thermal-hydraulic code. It is a realistic, best-estimate code. Its predecessor, RETRAN-02, is used extensively by the US commercial nuclear industry for modelling a wide range of safety conditions and issues. It is the basis for many utility-specific licensing and safety analyses and for various industry generic safety analysis submittals to licensing authorities. Specifically, virtually all US utilities and about 20 international organisations have used RETRAN-02 as reflected in published papers and EPRI RETRAN User group membership.

Some of the new models incorporated in RETRAN-3D include:

- Multi-dimensional neutron kinetics.
- Non-equilibrium field equations.
- Non-condensable gas flow.
- Revised numerical solution methods.

RETRAN-3D has broad capabilities to simulate plant response at all power levels and over the full spectrum of design base accidents (DBA) and some beyond-DBA events, including complex core transients. These capabilities go beyond those of the approved RETRAN-02 code and most other codes. RETRAN-3D will be used to analyze all operational transients, *i.e.* all FSAR Chapter 15 events except LBLOCA, such as BWR Control Rod Drop, PWR Rod Ejection, and PWR Steam Line Break. It also will be used to address generic safety concerns such as boron dilution and full/partial ATWS events, and low power and shutdown cooling modes of operation in various outage configurations. RETRAN-3D contains a 3-D kinetics capability to meet the new criteria being proposed for high burnup fuel. The 3-D kinetics option allows RETRAN-3D to properly analyze the response of mixed oxide fuels to transients.

COCINELLE/THYC/CATHARE (EDF, France)

Scheme for coupling the computer codes COCCINELLE, THYC and CATHARE

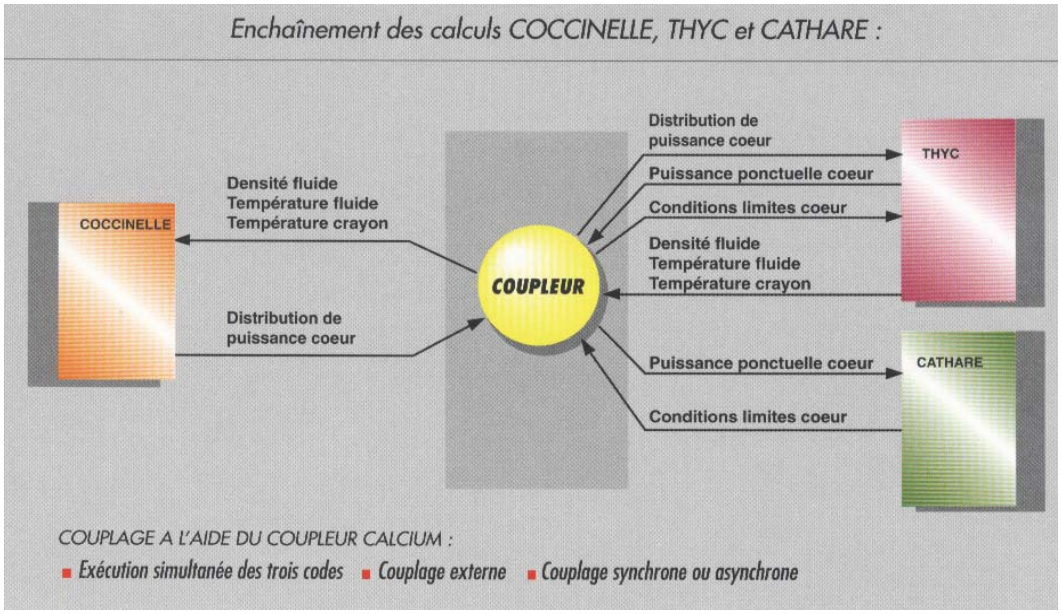

Fuel management is one of the major competitive elements in the nuclear power field. New management systems are based on safety demonstrations requiring an ever more sophisticated approach to physical phenomena, with a view to vindicating or even extending, operating margins. Use of the 3-D reference codes provides a basis for detailed models, indicating, in particular, fuel rod power fluctuations, the dynamic behavior of the core and, less specifically, of the reactor.

Coupling of the 3-D thermal hydraulic code (THYC), the 3-D neutronic code (COCCINELLE) and the normal, incident and accident 1-D code (CATHARE), using the overall code coupler CALCIUM. Coupling of the neutronic code (1-D COCCINELLE) with the thermo mechanical code (CYRANO 3). Coupling of the thermo mechanical code (CYRANO 3) with the fuel isotopic change code (STRAPONTIN).

Scope

- Calculation of postulated incident and accident scenarios.
- Parametric studies requiring coupling between different fields of physics.

Bibliography

DUVAL, Carole, “Code coupling development for nuclear safety studies”, ASME Summer Meeting, June 1996.

CARÉMOLI, Christian and Daniel BEAUCOURT, “A new tool for code coupling”, CRAY User Group Meeting, 1994.

MARGUET, Serge, “A new coupling of the 3-D thermo-hydraulic code THYC and a thermo-mechanical code CYRANO3 for PWR calculations”, NURETH 8, September 1997.

DYN-3D (FZR, Germany)

1. Neutron kinetic model

The 3-D neutron kinetic model is based on the solution of the 3-dimensional 2-group neutron diffusion equation by nodal expansion methods for the hexagonal and quadratic fuel assemblies. It is assumed that the macroscopic cross sections are spatially constant in a node being a part of the fuel assembly. Considering hexagonal-z geometry the 3-dimensional diffusion equation of each node is transformed by transverse integration in a two-dimensional equation in the hexagonal plane and a one-dimensional equation of axial direction. In the hexagonal plane the nodes can be coupled by the side averaged values or both the side averaged values and the corner point values of flux and current [1, 2]. Considering the cartesian geometry, the 3-dimensional diffusion equation of each node is transformed into 1-dimensional equations in each direction x, y, z by transversal integrations [3]. The equations are coupled by the transversal leakage term. The 1-dimensional or 2-dimensional equations are solved with the help of flux expansions in polynomials up to second order and exponential functions being the solutions of the homogeneous equation. The fission source in the fast group and the scattering source in the thermal group as well as the leakage terms are approximated by the polynomials. The outgoing partial currents are expressed by the incoming partial currents and the polynomial coefficients of the flux expansion.

Concerning the time integration over the neutronic time step an implicit difference scheme with exponential transformation is used. The exponents in each node are calculated from the previous time step or during the iteration process. In order to enable DYN3D users to independently calculate three-dimensional burn-up distributions for all possible states occurring during a reactor cycle, a burn-up version of the code has been developed.

2. The thermo-hydraulic model of DYN3D

The thermo-hydraulic model of the reactor core and the fuel rod model are implemented in the module FLOCAL [4] being a part of DYN3D. The reactor core is modelled by parallel cooling

channels, which can describe one or more fuel elements. Additionally, so-called hot channels can be considered connected to core channels with given power peaking factors. Thermo-hydraulic boundary conditions for the core like coolant inlet temperature, pressure, coolant mass flow rate or pressure drop must be given as input tables for DYN3D. This option was used for the calculations of the OECD Benchmark – Exercise 2. Applying the coupled DYN3D – ATHLET code the thermo-hydraulic boundary conditions are provided by the ATHLET code.

Mixing of coolant from different loops before entering the core can be modelled by applying mixing matrices. For VVER-440 type reactors, an analytical model for obtaining the time-dependent mixing matrices is available.

The module FLOCAL comprises:

- a one- or two-phase coolant flow model on the basis of four differential balance equations for mass, energy and momentum of the two-phase mixture and the mass balance for the vapour phase allowing the description of thermodynamic non-equilibrium between the phases;

- a heat transfer regime map from one-phase liquid up to post-critical heat transfer regimes and superheated steam;

- a fuel rod model for the calculation of fuel and cladding temperatures and the determination of some parameters for fuel rod failure estimation.

The two-phase flow model is closed by constitutive laws for heat mass and momentum transfer. Special emphasis is put on adopting the model to the conditions of RIA accidents where a combination of high heat fluxes with high degree of coolant sub-cooling is typical and thermodynamic non-equilibrium effects are important. Different packages of water and steam thermo-physical properties presentation can be used. For the estimation of fuel and cladding temperatures the heat conduction equation in one-dimensional radial geometry is solved. In the gas gap between fuel and cladding the heat transfer components due to conduction in the gas, radiation and fuel- cladding contact are considered. A thermo-mechanical model of the fuel and cladding behaviour is implemented into the code. The aim of this model is the estimation of gas gap conductance behaviour for a realistic temperature calculation. Additionally, following parameters for the diagnostic of possible fuel rod failure are provided:

- fuel enthalpy for each axial node of the rod;

- cladding oxide thickness;

- signalisation of possible cladding rupture, when the cladding stress is positive (inner pressure is larger than outer pressure) and exceeds the yield point.

3. Coupling neutron kinetics – thermal hydraulics

Different time steps are used for neutron kinetics and thermo-hydraulics. One or several time steps of neutron kinetics are performed within a thermo-hydraulic time step. The thermo-hydraulic time step is repeated to obtain convergence. The time steps are controlled automatically during the run of the code.

References

[1] Grundmann, U., F. Hollstein, "A Two-Dimensional Intranodal Flux Expansion Method for Hexagonal Geometry", *Nucl Sci Eng.*, 133, (1999), pp. 201-212.

[2] Grundmann, U., "HEXNEM – A Nodal Method for the Solution of the Neutron Diffusion Equation in Hexagonal Geometry", Proceedings of the M&C'99 – Conference on Mathematics and Computations in Nuclear Applications, pp. 1086-1095, Madrid, September, 27-30, 1999.

[3] Grundmann, U., "The Code DYN3DR for Steady-State and Transient Analyses of Light Water reactor Cores with Cartesian Geometry", Rep. FZR 114, Research Centre, Rossendorf, (1995).

[4] Rohde, U., "Modelling of Fuel Rod Behaviour and Heat Transfer in the Code FLOCAL for Reacrtivity Accident Analysis of Reactor Cores", 1st Baltic Heat Transfer Conference, Göteborg, (1991), published in: *Transport Processes in Engineering, 2*: Elsevier Publ., Amsterdam, (1992).

MARS/MASTER (KAERI, Korea)

MARS is a multi-dimensional system thermal-hydraulic code developed for best-estimate analyses of two-phase thermal-hydraulic transients in light water reactors. The backbones of the MARS code are the RELAP5/MOD3 and COBRA-TF codes developed by the USNRC and they provide the bases of the 1-D and 3-D modules of the MARS, respectively. The 3-D module is used for a realistic representation of the thermal-hydraulic field within the reactor vessel whereas the 1-D module is used for the rest of the system. The coupling of the 1-D and 3-D hydrodynamic models is resolved by solving an implicitly coupled system pressure matrix equation. Since MARS retains the unique features of the two base codes, it is as versatile and robust as RELAP5 while it allows multi-dimensional nodalization schemes as COBRA-TF. The real value of the MARS code is the enhanced solution accuracy attainable with realistic modeling. In addition, MARS has superb user-friendliness achieved by the Windows graphic feature.

MASTER is a two-group, three-dimensional neutron diffusion code capable of microscopic depletion, xenon dynamics, on-line DNB analysis, and kinetics calculation in both rectangular and hexagonal geometries. The primary neutronic solver of the MASTER code is the analytic function expansion nodal (AFEN) method formulated within the framework of coarse-mesh rebalancing technique. As optional solvers, it has also the conventional NEM as well as the nonlinear ANM solvers. The transient thermal-hydraulic solution in MASTER is achieved by the COBRA III-C/P module, which employs the homogeneous equilibrium model. The mapping between the neutronic and T-H nodes is basically one-to-one. The COBRA module provides MASTER with the features of cross flow modeling and subchannel analysis on the fly. The types of the transient calculation that can be analyzed by the MASTER code include control rod perturbation (ejection, withdrawal and drop), flow perturbation (steam line break), and boron dilution events.

MARS/MASTER is a coupled 3-D kinetics/system T-H code running on a personal computer. The two codes were coupled through the dynamic link library (DLL) feature available on Windows operating systems. The use of DLL allows maintaining the integrity of each code separately and the simpler coupled code structure. Only minor coding changes were needed for data communication and for incorporating feedback data, leaving the majority of the codes intact. In the couple mode, the core T-H conditions are determined at each time step by MARS and they are used to update group constants in MASTER. The power distribution newly obtained by MASTER is then sent back to

MARS for the next time step. The data communication is achieved by a common memory, which is shared by both codes.

PARCS -V1.00/TRAC-M (Purdue University/NRC, USA)

The Modernized Transient Reactor Analysis Code (TRAC-M) was developed to provide advanced best-estimate predictions of postulated accidents in light-water reactors. TRAC-M is a consolidated TRAC-P and TRAC-B program capable of modeling PWR, BWR and scaled thermal-hydraulic test facilities. It was developed by recoding the TRAC-P algorithms to take advantage of the advanced features available in the Fortran 90 programming language while conserving the computational models available in the original code.

The TRAC-M code features a one-, two- or three-dimensional treatment of the pressure vessel and its associated internals, a two-fluid non equilibrium hydrodynamics model with a non condensable gas field and solute tracking, flow-regime dependent constitutive equation treatment, optional re-flood tracking capability for bottom- and top-flood and falling-film quench fronts, and a consistent treatment of the entire set of accident sequences, including the generation of consistent initial conditions.

The stability-enhancing two-step (SETS) numerical algorithm is used in the solution of the 1-D, 2-D and 3-D hydrodynamics and permits violation of the material Courant condition. This technique permits large time steps, and thus, the running time for slow transients is reduced. A heat-structure component is included that allows the user to model heat transfer accurately for complicated geometries. An improved re-flood model that is based on mechanistic and defensible models has been added. TRAC-M also contains improved constitutive models and additions and refinements for several components.

PARCS is modularised FORTRAN77 code, which can be used to predict the transient behavior of light water nuclear reactors resulting from external perturbations. The code solves the time-dependent two-group neutron diffusion equation in three-dimensional Cartesian geometry to obtain the transient neutron flux distribution. During the course of solution, the thermal-hydraulic feedback effects are incorporated by performing heat transfer calculations. The code is capable of performing both steady-state eigenvalue calculations for initializing the transient calculation, and LWR transients such as control rod ejection/withdrawal/drop and boration/dilution events. When coupled via the NRC's General Interface (GI) to the two-fluid thermal-hydraulics codes RELAP5 and TRAC-M, the PARCS code is capable of analyzing boiling water reactor transients and PWR events involving a large change in coolant conditions such as steam line break accidents.

The numerical methods in PARCS to solve the transient fixed source problem include time integration using the theta method and analytic precursor integration technique, and spatial integration using a coarse mesh finite difference solver based on a Krylov subspace method and an analytic nodal kernel to solve the nodal coupling problems.

RELAP5/PANBOX (Framatome ANP/FZK, Germany)

The RELAP5/PANBOX code was developed by Framatome ANP, Germany and will be used for the benchmark. The coupled code uses the EUMOD interface code to combine RELAP5 and PANBOX enabling modeling of the entire reactor system.

PANBOX solves the three dimensional kinetics equations using the polynomial and the analytical nodal expansion method. Partial current formalism is used to couple the nodes. The code also can model the core using either one-dimensional or point kinetics equations.

Thermal hydraulics of PANBOX is solved in the core using the COBRA 3-CP module. This code models the core as one-dimensional channels with cross flow. A mapping procedure is used to map the kinetics to the thermal hydraulic channels. The balance of the system is modeled using RELAP5. Core inlet boundary conditions are passed from RELAP5 to PANBOX. This may be done on a core-averaged or an individual channel basis depending on the transient analysed. The power distribution is then calculated in PANBOX and collapsed back for use in RELAP5. Coupling of RELAP5 and PANBOX allows both the application of the external coupling (RELAP5/PANBOX-E) and the internal coupling (RELAP5/PANBOX-I) option. In the first one, the T-H results of COBRA 3-CP are used to update the neutronics cross-sections. In the second one, the RELAP5 core T-H results are directly used for the feedback to the neutronics.

SIMTRAN (University Polytechnic of Madrid, Spain)

SIMTRAN is a combination of the SIMULA three-dimensional kinetics code and COBRA IIIC. The COBRA code solves the thermal hydraulic transport in the core with cross flow. External coupling to RELAP5 allows the full system to be modeled.

TRAB-3D (VTT, Finland)

TRAB-3D is the latest member of the code system developed at VTT Energy for LWR reactor dynamics calculations. The neutron kinetics model of the new code is based on the three-dimensional VVER-dynamics code HEXTRAN, but the nodal equations are solved in rectangular, instead of hexagonal, fuel assembly geometry. Special features of the solution methods are construction of the two-group nodal fluxes from two spatial modes, the asymptotic or fundamental mode and the transient mode, and approximation of the former mode by polynomials and of the latter mode by exponential functions. Also, flux discontinuity factors can be specified on the transverse interfaces of nodes. The nodal flux model of TRAB-3D contains eight degrees of freedom per group in a transverse cross section and they are adjusted by continuity conditions for group fluxes and currents and for their first moments at nodal interfaces.

Thermal hydraulics models are taken from the one-dimensional dynamics code TRAB which includes descriptions of both the reactor core and the BWR-cooling circuit. Thus the dynamic behavior of the whole primary circuit of a reactor can be analyzed with TRAB-3D. For PWR dynamics the core model of TRAB-3D is coupled with the SMABRE PWR circuit model.

Comparison with fine-mesh finite difference calculations have shown that TRAB-3D solves the diffusion equations for homogeneous fuel assemblies of a two-dimensional reactor core with an accuracy of better than one percent in assembly powers. The validation history of TRAB-3D, so far, includes the calculation of OECD/NEACRP 3-D light water reactor benchmark problems and verification against measurements from real BWR plant transients. Much of the validations, however, have already been done by various calculations with HEXTRAN and TRAB since the same models for neutron kinetics and thermal hydraulics description are used in TRAB-3D.

RELAP5/QUABOX (Universities of Piza and Zagreb, Italy and Croatia)

The results are produced with RELAP5/QUABOX coupled code. RELAP5 is NRC sponsored code in version 3.2.2 gamma. QUABOX is GRS QUABOX/CUBBOX-HYCA code with some modifications. Direct explicit coupling is used. RELAP5 is performing all thermal-hydraulic calculation (it is responsible for controlling of time step) and QUABOX is solving 3-D coarse mesh neutron diffusion in two energy groups and for processing of interface arrays.

TRAC-PF1/NEM (The Pennsylvania State University, USA and University Polytechnic of Valencia, Spain)

The TRAC-PF1 code is a best estimate system transient analysis code, which has a 3-D thermal-hydraulic analysis capability. A modified version of TRAC-PF1/MOD2 version 5.4 is currently being used at The Pennsylvania State University (PSU). Version 5.4 incorporates a 1-D decay heat model that dynamically computes the decay heat axial shape during the transient. The code solves the general transient two-phase coolant conditions in one, two, or three dimensions using a realistic six-equation, two-fluid, finite-difference model. This six-equation model, in conjunction with specialized empirical models for a variety of PWR primary- and secondary-loop components and control systems, allows TRAC-PF1/MOD2 v.5.4 to accurately model both mild and severe thermal-hydraulic transients.

An accurate 3-D transient neutronics model based on the Nodal Expansion Method (NEM) was developed and integrated into the TRAC-PF1 Code by PSU. The NEM spatial model is based on the transverse integrated procedure. Two levels of approximation are used: fourth-degree transverse integrated flux representation and the quadratic leakage approximation. The nodal coupling relationships are expressed in a partial current formulation. The time dependence of the neutron flux is approximated by a first order, fully implicit, finite-difference scheme, whereas the time dependence of the neutron precursor distributions is modeled by a linear time-integrated approximation. The coarse-mesh rebalance and asymptotic extrapolation methods are used to accelerate convergence of the iterative solution process. Several benchmark problems were used to assess the NEM model in both steady state and transient conditions. Very good agreement was obtained among the reference results and those from NEM.

The coupling of the NEM neutronics to TRAC-PF1 has made use of the local thermal-hydraulic properties to simulate the core response during a transient. TRAC-PF1/NEM employs an improved semi-implicit neutronics/thermal-hydraulic coupling scheme. At the beginning of a time step, TRAC-PF1/MOD2 first performs its pre-pass stage, where fluid-state-dependent material properties and heat-transfer coefficients are calculated based on thermal-hydraulic conditions at the end of the previous time step. In the outer iteration stage, the multidimensional fluid-dynamic equations are solved using previous time-step fuel-rod heat fluxes. Then, the 3-D transient NEM neutronics model calculates the present time-step nodal power distribution using cross-section-dependent feedback parameters based on present time-step fluid conditions and previous time-step fuel-rod temperatures. Finally, in the postpass stage, the new nodal power distribution is used in the numerical solution of the heat-conduction equations. To ensure symmetry between the 3-D thermal-hydraulics vessel, the heat structure, and the neutronics core model, proper radial and axial noding and mapping schemes have to be developed for a given

A general control rod presence and movement algorithm was implemented in TRAC-PF1/NEM and integrated into the cross-section table’s procedure. Cross sections for nodes with control rods partially inserted are obtained by blending the rodded and unrodded cross sections, using a factor that is a function of the fractional amount of control-rod insertion in that cell. The control-rod algorithm is

capable of modeling initial steady-state conditions with the initial positions of the control-rod groups. Movement of single rods and control-rod groups, as well as dynamic scram can also be simulated. In addition to this flexibility, there is an option in the code that allows one to perform efficient evaluations of static control-rod reactivity and shutdown margins.

Appendix B

QUESTIONNAIRE FOR THE SECOND PHASE OF THE PWR MSLB BENCHMARK

QUESTIONNAIRE FOR THE SECOND EXERCISE

I. Thermal-hydraulic core model

1) *Core thermal-hydraulic (T-H) model and nodalization (1-D, 3-D, and number T-H channels or cells) – How are channels/T-H cells chosen?*

2) *Number of heat structures (fuel rods) modeled?*

3) *Which core thermal-hydraulic initial and transient boundary conditions are used and how?*

4) *Radial and axial heat structure (fuel rod) nodalization?*

5) *Relation used for Doppler temperature?*

6) *Used correlations for fuel properties vs. temperature?*

II. Core neutronics model

1) *Number of radial nodes per assembly?*

2) *Axial nodalization?*

3) *Radial and axial reflector modeling?*

4) *Spatial decay heat distribution modeling?*

5) *Cross-section interpolation procedure used?*

6) *Used method to get a critical reactor at the beginning of transient?*

III. Coupling schemes

1) *Hydraulics/heat structure spatial mesh overlays (mapping schemes in radial and axial plane)?*

2) *Hydraulics/neutronics spatial mesh overlays (mapping schemes in radial and axial plane)?*

3) *Heat structure/neutronics spatial mesh overlays (mapping schemes in radial and axial plane)?*

4) *Temporal coupling scheme?*

5) *Coupling numerics – explicit, semi-implicit or implicit?*

6) *Coupling method – external or internal?*

7) *Coupling design – serial integration or parallel processing?*

IV. General

1) *Deviations from the updated Final Specifications [April 1999 – NEA/NSC/DOC(99)8].*

2) *User assumptions?*

3) *Specific features of the used codes?*

4) *Number of solutions submitted per participant and how they differ?*

ANL
UNITED STATES OF AMERICA

I. Thermal-hydraulic core model

1) Core thermal-hydraulic (T-H) model and nodalization (1-D, 3-D, and number T-H channels or cells) – How are channels/T-H cells chosen?

SAS-DIF3DK uses 1-D T-H channels. 185 T-H channels were employed in the solution submitted – one channel for each fuel assembly and additional 8 channels for the reflector assemblies. Axially, 28 T-H nodes were used.

2) Number of heat structures (fuel rods) modeled?

One fuel rod per channel was employed. The code also used one heat structure per channel to represent the guide tube cells (using nearly zero power for these cells).

3) Which core thermal-hydraulic initial and transient boundary conditions are used and how?

Initial-state channel inlet flow rates; core outlet pressure vs. time (derived from given data); channel inlet temperature vs. time. The SAS-DIF3DK model derived a single curve of core normalised pump head versus time from the pressure drop and the inlet coolant density, under the assumption that all the active core channels have the same pressure drop.

4) Radial and axial heat structure (fuel rod) nodalization?

10 radial nodes were employed in the fuel pin and 3 in the cladding. 28 axial nodes were used.

5) Relation used for Doppler temperature?

Yes.

6) Used correlations for fuel properties vs. temperature?

II. Core neutronics model

1) Number of radial nodes per assembly?

One radial node per assembly was used in the solution submitted, because sensitivity studies indicated this was quite adequate. Largest differences between the 4 radial node and 1 radial node cases occurred in insignificant core locations/zones.

2) Axial nodalization?

28 axial neutronic nodes were employed.

3) Radial and axial reflector modeling?

Yes, these core zones were explicitly modeled.

4) Spatial decay heat distribution modeling?

No.

5) Cross-section interpolation procedure used?

Cross sections were fitted to polynomials. The polynomial forms were carefully selected, and sensitivity studies indicated that the accuracy of the fit is more than sufficient for this study.

6) Used method to get a critical reactor at the beginning of transient?

SAS-DIF3DK iterates between time-independent neutronic and T-H modules. Typically, 5 neutronic outer iterations were performed for each T-H re-calculation. A total of about 15-20 or so of these were required.

III. Coupling schemes

1) Hydraulics/heat structure spatial mesh overlays (mapping schemes in radial and axial plane)?

Each T-H channel was assigned its own heat structures.

2) Hydraulics/neutronics spatial mesh overlays (mapping schemes in radial and axial plane)?

One-to-one correspondence between T-H channels and fuel assemblies, so no grouping was required.

3) Heat structure/neutronics spatial mesh overlays (mapping schemes in radial and axial plane)?

One-to-one correspondence.

4) Temporal coupling scheme?

Explicit between modules.

5) Coupling numerics – explicit, semi-implicit or implicit?

Explicit between modules. Neutronic module uses an implicit scheme. Similarly for the T-H modules.

6) Coupling method – external or internal?

Not applicable, SAS-DIF3DK is a core dynamics code.

7) Coupling design – serial integration or parallel processing?

Serial.

IV. General

1) Deviations from the updated Final Specifications [April 1999 – NEA/NSC/DOC(99)8].

None.

2) User assumptions?

Note that for solution item D8, the core-averaged fuel temperature (not Doppler temperature) is submitted.

3) Specific features of the used codes?

N/A.

4) Number of solutions submitted per participant and how they differ?

One.

BE/TRACTEBEL
UNITED KINGDOM/BELGIUM

I. Thermal-hydraulic core model

1) Core thermal-hydraulic (T-H) model and nodalization (1-D, 3-D, and number T-H channels or cells) – How are channels/T-H cells chosen?

PANTHER PWR thermal-hydraulics module. Single isolated thermal-hydraulics channel. Independent calculation in each radial node (including reflector nodes), marching axially up the core. 241 radial nodes (core channels plus reflector channels), 26 axial nodes (24 core plus two axial reflector). Radial conduction within fuel pin, can and gap modeled, with homogeneous flow solution in the coolant, with slip and sub-cooled boiling corrections.

Reference calculation has 4 nodes per assembly, 964 radial nodes in all, double number of nodes axially (50 in total).

2) Number of heat structures (fuel rods) modeled?

One fuel rod in each assembly, with average linear rating for that assembly, surrounded by a representative quantity of coolant.

Reference calculation has one representative fuel rod in each quarter assembly.

3) Which core thermal-hydraulic initial and transient boundary conditions are used and how?

Each channel allocated to the 18 flow zones as given in specification, and inlet temperature and flow set from the data files supplied. For nodes along the horizontal centerline, where two data values for flow and inlet temperature are supplied, an average of the two is applied. A single global system pressure is defined based on the average of the supplied pressure values over all the zones. The supplied data files are used to set up tabulation as a function of time. Data is linearly interpolated to the time-points visited in the transient.

4) Radial and axial heat structure (fuel rod) nodalization?

26 axial nodes, as above. For radial conduction solution, 10 radial nodes within the fuel pin, two of near-zero width at center and edge (8 real nodes). One node each for clad and gap.

Reference calculation has 18 radial nodes within fuel pin (16 real nodes), one node each for clad and gap.

5) Relation used for Doppler temperature?

$T_{Doppler}=0.3*T_{centre}+0.7*T_{edge}$, center and edge temperatures from near zero-width nodes in fuel.

6) Used correlations for fuel properties vs. temperature?

Tabulation based on specified relations in specifications.

II. Core neutronics model

1) Number of radial nodes per assembly?

One node per assembly.

Reference calculation has four nodes per assembly.

2) Axial nodalization?

As for thermal nodalization, 26 axial nodes per assembly.

Reference calculation has 50 axial nodes.

3) Radial and axial reflector modeling?

Using supplied cross sections. Fuel temperature set to a constant 600 K. Coolant density set to inlet density (radial reflector, bottom reflector), outlet density (top reflector).

4) Spatial decay heat distribution modeling?

Node-by-node transient evolution of decay heat. Exponential source terms and time constants from ANS/79 as in specifications. Steady-state initialisation based on infinite operation at the steady-state power distribution. Burnup modelled via fission fractions at approximate 50 GWd/te of ^{235}U=0.539, ^{239}Pu=0.384, ^{238}U=0.077. Model predicts total decay heat of approximately 6.7%. Therefore source fractions scaled to give specified decay heat of 7.1%.

In each node during the transient, the transient evolution of the decay heat sources is modelled, based on time step (decay) and current fission power (production) in that node. Total decay heat level is then the sum of the individual node decay heat powers. Therefore decay heat is essentially spatially distributed according to the steady-state power distribution.

5) Cross-section interpolation procedure used?

Linear interpolation between tabulation cross-section points in data files. Results submitted both allowing extrapolation beyond the tabulation points (on 7th November 1999) and restricting extrapolation beyond the defined boundaries (on 29th February 2000).

6) Used method to get a critical reactor at the beginning of transient?

K_{eff} search.

III. Coupling schemes

1) Hydraulics/heat structure spatial mesh overlays (mapping schemes in radial and axial plane)?

One-to-one. No mapping necessary. Coupled solution of coolant and fuel pin conditions.

2) Hydraulics/neutronics spatial mesh overlays (mapping schemes in radial and axial plane)?

One-to-one. No mapping necessary.

3) Heat structure/neutronics spatial mesh overlays (mapping schemes in radial and axial plane)?

One-to-one. No mapping necessary.

4) Temporal coupling scheme?

Steady-state solution at t=0. Inlet conditions updated to time t=0.1, transient thermal solution from t=0 to t=0.1. Cross-sections updated using new temperatures. Neutronics transient solution using new cross-sections from t=0 to t=0.1. Then procedure repeats.

Time-steps:

- 0.10 secs until 7 secs.
- 0.05 secs until 10 secs.
- 0.25 secs until 12 secs.
- 0.50 secs until 15 secs.
- 1.00 secs until 100 secs.

Reference solution divides all the time-steps by 2.

5) Coupling numerics – explicit, semi-implicit or implicit?

Explicit thermal-hydraulics. Implicit neutronics.

6) Coupling method – external or internal?

Internal. Fully integrated.

7) Coupling design – serial integration or parallel processing?

Serial integration.

IV. General

1) Deviations from the updated Final Specifications [April 1999 – NEA/NSC/DOC(99)8].

Decay heat modeling; model is as described above.

2) User assumptions?

Energy deposition in the coolant = 1.9%.

Zero flux boundary conditions outside radial and axial reflectors.

3) Specific features of the used codes?

N/A.

4) Number of solutions submitted per participant and how they differ?

Standard and reference solutions, which differ as specified above.

CEA
FRANCE

I. Thermal-hydraulic core model [1]

1) Core thermal-hydraulic (T-H) model and nodalization (1-D, 3-D, and number T-H channels or cells) – How are channels/T-H cells chosen?

Radial mesh: 1 node per assembly, *i.e.* 177 radial nodes.

Axial mesh: 4 nodes of 10.9 cm for the reflector, and 24 nodes of 14.88 cm for the fuel, *i.e.* 28 nodes.

Global mesh: 4 956 nodes for the core (177x28).

Thermal-Hydraulics: fully 3-D (first set of results) or 1-D (second set of results).

2) Number of heat structures (fuel rods) modeled?

1 heat structure per assembly, *i.e.* 177 heat structures.

3) Which core thermal-hydraulic initial and transient boundary conditions are used and how?

Inlet boundary conditions: liquid mass flow rate, vapor mass flow rate, enthalpy (calculated from temperature and pressure at core inlet).

Outlet boundary conditions: pressure.

Each value for one assembly is obtained from the value of the corresponding TRAC radial zone (1 to 18, defined in the MASS_FLOWS.BC, TEMP.BC, Press_Outlet.BC, and Press_Inlet.BC files). Initial boundary conditions are defined as the first value of the transient (*i.e.* time = 0).

4) Radial and axial heat structure (fuel rod) nodalization?

Axial mesh: 4 nodes of 10.9 cm for the reflector, and 24 nodes of 14.88 cm for the fuel, *i.e.* 28 nodes (*cf.* thermal-hydraulics).

Radial mesh: 10 nodes for the pellet, and 6 nodes for the clad.

1. All cited pages are relative to Ivanov, K., T. Beam, A. Baratta, A. Irani, and N. Trikorous, "PWR MSLB Benchmark: Volume 1: Final Specifications", NEA/NSC/DOC(99)8, April 1999.

5) Relation used for Doppler temperature?

Specified relation: $0.3*T_{center}+0.7*T_{surface.}$

6) Used correlations for fuel properties vs. temperature?

Specified correlations (page 30 of the Final Specifications report)[1].

II. Core neutronics model

1) Number of radial nodes per assembly?

Radial mesh: 1 node per assembly, *i.e.* 177 radial nodes.

2) Axial nodalization?

Axial mesh: 53 nodes.

3) Radial and axial reflector modeling?

Radial mesh: 1 node per assembly, *i.e.*112 radial nodes (17x17 – 177).

Axial mesh: 53 nodes (*cf.* fuel assemblies).

4) Spatial decay heat distribution modeling?

Fission power distribution at steady state (time = 0 of transient), as defined in Garching.

5) Cross-section interpolation procedure used?

Bi-linear interpolation for fuel temperature and moderator density (regular module of CRONOS2). No extrapolation outside of the cross-section library was necessary.

6) Used method to get a critical reactor at the beginning of transient?

Fission cross-section matrix divided by the steady-state eigenvalue ($\nu\Sigma_f/k_{eff}$).

III. Coupling schemes

1) Hydraulics/heat structure spatial mesh overlays (mapping schemes in radial and axial plane)?

No specific procedure, as the axial mesh are the same, and there is one heat structure per radial node.

2) Hydraulics/neutronics spatial mesh overlays (mapping schemes in radial and axial plane)?

Radial mesh: same nodalization for neutronics and thermal-hydraulics.

Axial mesh: linear projection between the two nodalizations (regular module of FLICA4 and CRONOS2).

3) Heat structure/neutronics spatial mesh overlays (mapping schemes in radial and axial plane)?

Cf. III.2.

4) Temporal coupling scheme?

Same time-step for thermal-hydraulic, fuel structures, and neutronics.

5) Coupling numerics – explicit, semi-implicit or implicit?

Explicit coupling between thermal-hydraulics and neutronics.

6) Coupling method – external or internal?

External coupling trough ISAS coupling software.

7) Coupling design – serial integration or parallel processing?

Parallel processing on 3 CPU (CRONOS2, FLICA4, ISAS), or serial processing on a single CPU, depending on the calculation.

IV. General

1) Deviations from the updated Final Specifications [April 1999 – NEA/NSC/DOC(99)8].

No deviation.

2) User assumptions?

One assumption: no singular pressure drop (for grids), which results in tuning the friction coefficient to match the specified core pressure drop.

3) Specific features of the used codes?

Full 3-D thermal-hydraulic model in FLICA4.

4) Number of solutions submitted per participant and how they differ?

Two sets of solutions: reference solution (for scenario 1 and 2) based on 3-D thermal-hydraulics, and simplified solution (for scenario 1 only) based on 1-D thermal-hydraulics.

CSA
UNITED STATES OF AMERICA

I. Thermal-hydraulic core model

1) Core thermal-hydraulic (T-H) model and nodalization (1-D, 3-D, and number T-H channels or cells) – How are channels/T-H cells chosen?

For exercises II and III, eighteen parallel core channels were used (as defined in the specification). Each core channel had 24 axial T-H nodes.

2) Number of heat structures (fuel rods) modeled?

See # 4 below.

3) Which core thermal-hydraulic initial and transient boundary conditions are used and how?

As defined in the specification.

4) Radial and axial heat structure (fuel rod) nodalization?

24 axial heat structures in each of the eighteen parallel core channels.

5) Relation used for Doppler temperature?

As defined in the specification.

6) Used correlations for fuel properties vs. temperature?

As defined in the specification.

II. Core neutronics model

1) Number of radial nodes per assembly?

One.

2) Axial nodalization?

Spacing and number as defined in the specification (24).

3) Radial and axial reflector modeling?

As defined in the specification.

4) Spatial decay heat distribution modeling?

As defined in the specification, proportional to initial power distribution.

5) Cross-section interpolation procedure used?

Used FORTRAN interpolation subroutine provided by PSU.

6) Used method to get a critical reactor at the beginning of transient?

Iterative coupling between the RETRAN-3D steady-state thermal hydraulic module and the kinetics.

III. Coupling schemes

1) Hydraulics/heat structure spatial mesh overlays (mapping schemes in radial and axial plane)?

One heat structure for each hydraulic node.

2) Hydraulics/neutronics spatial mesh overlays (mapping schemes in radial and axial plane)?

One hydraulic node was used for each axial neutronic spatial mesh. In the radial direction, 18 channels mapped over 177 fuel assemblies per the specification.

3) Heat structure/neutronics spatial mesh overlays (mapping schemes in radial and axial plane)?

One heat structure for each neutronic spatial mesh.

4) Temporal coupling scheme?

3-D kinetics solution advanced with each hydraulic solution time step.

5) Coupling numerics – explicit, semi-implicit or implicit?

Explicit.

6) Coupling method – external or internal?

Internal.

7) Coupling design – serial integration or parallel processing?

Serial.

IV. General

1) Deviations from the updated Final Specifications [April 1999 – NEA/NSC/DOC(99)8].

For exercise II and III, RETRAN-3D requires a one to one axial correspondence between T-H, fuel and neutronic nodes. The specification had only 6 axial T-H/fuel nodes per channel. Also, the specification split several assemblies between hydraulic channels. RETRAN-3D requires whole assemblies in a channel. Consequently, the specification could not be duplicated, but we approximated the specified core mapping as closely as we could.

1979 ANS decay heat model used to get the total decay heat magnitude rather than the decay heat versus timetable in the specification.

2) User assumptions?

None.

3) Specific features of the used codes?

Used standard code features.

4) Number of solutions submitted per participant and how they differ?

Only one submitted for each the return-to-power and one for the no return-to-power per specification requirements.

EDF
FRANCE

I. Thermal-hydraulic core model

1) Core thermal-hydraulic (T-H) model and nodalization (1-D, 3-D, and number T-H channels or cells) – How are channels/T-H cells chosen?

1-D (without cross-flow) and 3-D, 192 T-H channels with 4x4 cells.

2) Number of heat structures (fuel rods) modeled?

One average heat structure by cell.

3) Which core thermal-hydraulic initial and transient boundary conditions are used and how?

Specifications.

4) Radial and axial heat structure (fuel rod) nodalization?

5+2 nodes for the radial description.

25 nodes for the axial description.

5) Relation used for Doppler temperature?

Specifications.

6) Used correlations for fuel properties vs. temperature?

Specifications.

II. Core neutronics model

1) Number of radial nodes per assembly?

4x4.

2) Axial nodalization?

25 nodes for the active area.

3) Radial and axial reflector modeling?

4 nodes for the axial reflectors.

4x4 for the radial reflectors.

4) Spatial decay heat distribution modeling?

No, use the time-history given.

5) Cross-section interpolation procedure used?

Specifications.

6) Used method to get a critical reactor at the beginning of transient?

Division of the fission cross-sections by the reactivity of the critical calculation just before the transient.

III. Coupling schemes

1) Hydraulics/heat structure spatial mesh overlays (mapping schemes in radial and axial plane)?

None.

2) Hydraulics/neutronics spatial mesh overlays (mapping schemes in radial and axial plane)?

None.

3) Heat structure/neutronics spatial mesh overlays (mapping schemes in radial and axial plane)?

None.

4) Temporal coupling scheme?

Implicit for the neutronic power and explicit for the T-H.

5) Coupling numerics – explicit, semi-implicit or implicit?

Implicit for the neutronic power and explicit for the T-H.

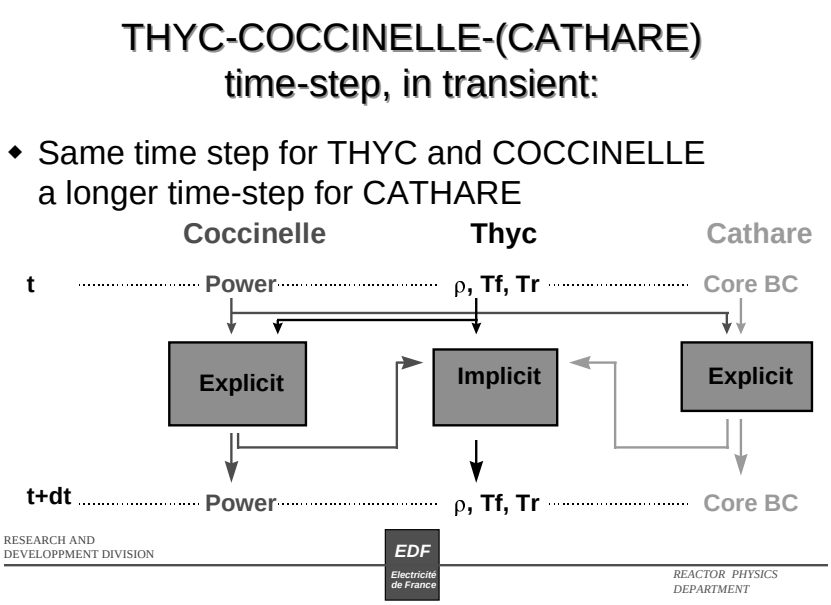

6) Coupling method – external or internal?

External.

7) Coupling design – serial integration or parallel processing?

Serial.

IV. General

1) Deviations from the updated Final Specifications [April 1999 – NEA/NSC/DOC(99)8].

None.

2) User assumptions?

None.

3) Specific features of the used codes?

Cf. PowerPoint files.

4) Number of solutions submitted per participant and how they differ?

Two solutions: 1-D and 3-D T-H.

FZR
GERMANY

I. Thermal-hydraulic core model [1].

1) Core thermal-hydraulic (T-H) model and nodalization (1-D, 3-D, and number T-H channels or cells) – How are channels/T-H cells chosen?

Radial T-H nodalization: 1 averaged T-H channel/assembly (177 core channels + 64 reflector channels).

Axial T-H Nodalization: 28 layers:

21.811 cm (bottom reflector), 14.88 cm, 4.7 cm, 10.17 cm, 20x14.88 cm, 12.266 cm, 2.614 cm, 14.88 cm, 21.811 cm (top reflector).

2) Number of heat structures (fuel rods) modeled?

One average fuel pin/T-H channel.

Axial Nodalization: 28 layers as described in I.1.

3) Which core thermal-hydraulic initial and transient boundary conditions are used and how?

Inlet conditions of NEM/TRAC used (Figure 1): Channels with numbers 1-18 use NEM/TRAC boundary conditions (mass flow rates, inlet moderator temperatures) of the 18 NEM/TRAC channels (page 57) [1]. Reflector channels with numbers 19-24 use inlet conditions of adjacent core channels. Channels of horizontal row with numbers 25-33 use averaged values of adjacent upper and lower channel (for example: channel with number 25 use average value of channel with number 21 and 22, channels with number 26 use average value of channels with numbers 15 and 16).

1. All cited pages are relative to Ivanov, K., T. Beam, A. Baratta, A. Irani, and N. Trikorous, "PWR MSLB Benchmark: Volume 1: Final Specifications", NEA/NSC/DOC(99)8, April 1999.

Figure 1. DYN3D mapping scheme for T-H boundary conditions

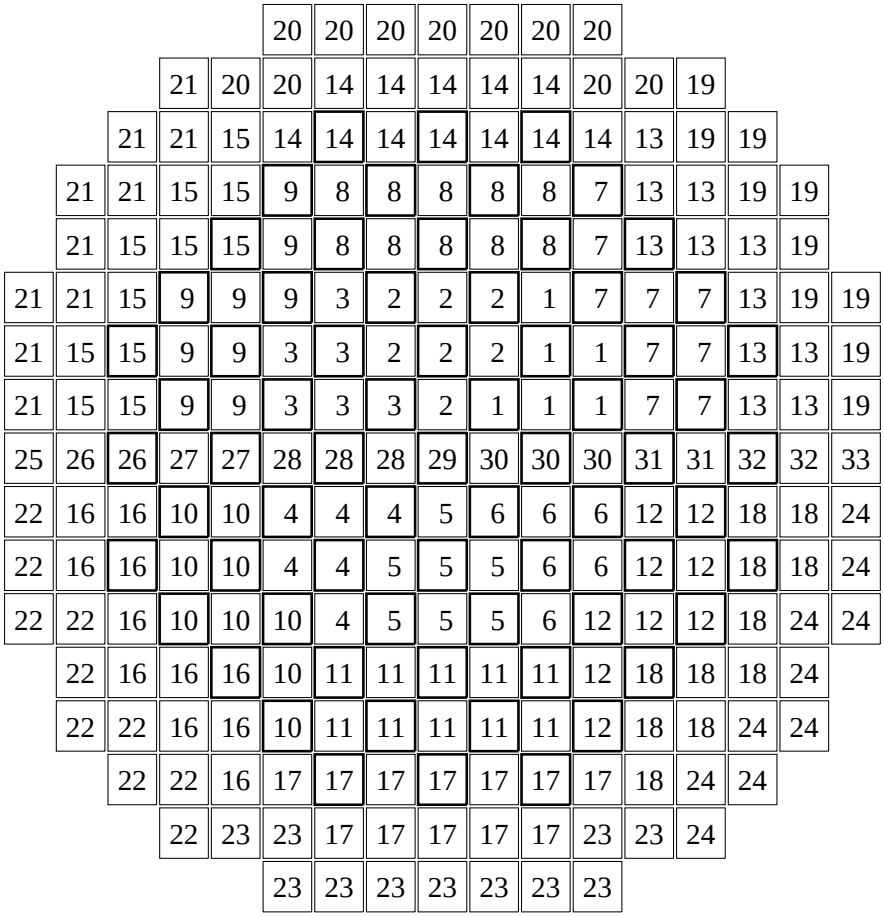

4) Radial and axial heat structure (fuel rod) nodalization?

Each fuel pin in an axial layer was divided in 10 radial zones of equal area.

5) Relation used for Doppler temperature?

Equation on page 29 of Final Specifications was used. The Doppler temperature of the reflectors follows the specifications on page 15 of Final Specifications.

6) Used correlations for fuel properties vs. temperature?

Correlations of page 30 of Final Specifications were used.

II. Core neutronics model

1) Number of radial nodes per assembly?

One node per assembly.

2) Axial nodalization?

28 axial layers of I.1.

3) Radial and axial reflector modeling?

One node per reflector assembly.

28 axial layers of I.1.

4) Spatial decay heat distribution modeling?

Normalized decay heat distribution equal normalized power distribution of initial state. PSU timetables used.

5) Cross-section interpolation procedure used?

Linear cross-section interpolation without extrapolation was used.

6) Used method to get a critical reactor at the beginning of transient?

Node values of $\nu\Sigma_{f,1}, \nu\Sigma_{f,2}$ divided by initial k_{eff}.

III. Coupling schemes

1) Hydraulics/heat structure spatial mesh overlays (mapping schemes in radial and axial plane)?

1 heat structure (fuel pin) node equal to 1 T-H node.

2) Hydraulics/neutronics spatial mesh overlays (mapping schemes in radial and axial plane)?

1 T-H node equal to 1 neutronic node.

3) Heat structure/neutronics spatial mesh overlays (mapping schemes in radial and axial plane)?

1 heat structure node equal to 1 neutronic node.

4) Temporal coupling scheme?

Different time-steps for neutronic and thermal-hydraulics with heat structure equations. Neutronics time-steps smaller or equal to thermal-hydraulic time-steps.

5) Coupling numerics – explicit, semi-implicit or implicit?

Iteration between neutronics and thermal-hydraulics (implicit scheme).

6) Coupling method – external or internal?

Coupling in the stand-alone version of DYN3D comparable with internal coupling.

7) Coupling design – serial integration or parallel processing?

Serial integration.

IV. General

1) Deviations from the updated Final Specifications [April 1999 – NEA/NSC/DOC(99)8].

Described in I.

2) User assumptions?

Time variation of NEM/TRAC core outlet pressure was used.

3) Specific features of the used codes?

Fuel rod model adjusted to specifications. Specific fuel rod model of DYN3D not used.

4) Number of solutions submitted per participant and how they differ?

One solution.

GRS
GERMANY

I. Thermal-hydraulic core model

1) Core thermal-hydraulic (T-H) model and nodalization (1-D, 3-D, and number T-H channels or cells) – How are channels/T-H cells chosen?

ATHLET parallel channel T-H model is applied (1-D). To each fuel assembly is assigned a separate T-H channel. T-H channel axial nodalization corresponds to the specified axial node dimensions for the neutron kinetics calculations, *i.e.* the core nodalization scheme is the same for the T-H and the neutron kinetics calculations. The total number of T-H channels is 178 (177 fuel assemblies + 1 reflector channel).

2) Number of heat structures (fuel rods) modeled?

Each T-H channel corresponds to a fuel rod. The total number of heat structures is 177.

3) Which core thermal-hydraulic initial and transient boundary conditions are used and how?

The specified 18 T-H channel initial and boundary conditions are used. On the basis of the given T-H channel mass flow, mass flow density is calculated for each assembly according to the assembly location in the core. If the assembly is positioned at the border of two or of three from the specified 18 T-H channels, then the assembly mass flow is calculated as area-weighted sum of the mass flows of the attached T-H channels.

4) Radial and axial heat structure (fuel rod) nodalization?

The axial heat structure nodalization is the same as the specified axial neutron kinetics nodalization, which also corresponds to the axial T-H channel nodalization. The radial nodalization of the fuel rod consists of 4 zones (nodes) with equal volumes.

5) Relation used for Doppler temperature?

The specified Doppler temperature relation is used.

6) Used correlations for fuel properties vs. temperature?

The ATHLET specific fuel property correlations are used, which are very near to the specified one.

II. Core neutronics model

1) Number of radial nodes per assembly?

Each assembly corresponds to one radial node.

2) Axial nodalization?

The applied axial nodalization is the same as specified – 24 active core nodes + 2 reflector nodes.

3) Radial and axial reflector modeling?

Radial and axial reflectors are modeled by adding at core boundaries one node with dimensions that correspond in radial direction to the assembly size and at the top and at the bottom of the core they have axial height of 21.811 cm.

4) Spatial decay heat distribution modeling?

We applied in our calculations the time dependent decay heat model specified by PSU team.

5) Cross-section interpolation procedure used?

We used for the interpolation in the cross section libraries the proposed interpolation procedure integrated in the subroutine lint4d.f.

6) Used method to get a critical reactor at the beginning of transient?

Applied is the usual procedure of dividing the neutron balance value with the eigenvalue determined in the steady state calculations.

III. Coupling schemes

1) Hydraulics/heat structure spatial mesh overlays (mapping schemes in radial and axial plane)?

Almost any combination of spatial meshing is possible between the T-H structures and the heat structures. It is a standard built-in procedure in ATHLET, which is controlled by input.

2) Hydraulics/neutronics spatial mesh overlays (mapping schemes in radial and axial plane)?

Free choice by axial and radial meshing overlays are possible between hydraulics and neutronics. There is only one limitation by radial overlays: it is not possible to assign a smaller than assembly size T-H channel to a neutronics node which has the assembly size, *i.e.* if the kinetics calculations are done for one node per assembly, it is not possible to have two T-H channels assigned to this assembly, only one.

3) Heat structure/neutronics spatial mesh overlays (mapping schemes in radial and axial plane)?

The same is valid as already mentioned in the above point #2 for heat structure/neutronics spatial mesh overlays.

4) Temporal coupling scheme?

Our coupling is a standard interface procedure and cannot be changed. There is no possibility to use any kind of other temporal coupling scheme.

5) Coupling numerics – explicit, semi-implicit or implicit?

By steady state calculations a simplified coupling implicit method is used to get better convergence between hydraulics and neutronics solutions and by transient one explicit numerics is applied.

6) Coupling method – external or internal?

ATHLET and QUABOX/CUBBOX are coupled internally.

7) Coupling design – serial integration or parallel processing?

Serial coupling is applied. The T-H code ATHLET makes the first calculation step and when it is finished the core model QUABOX/CUBBOX calculates the same step for the neutronics on the same computer. A special time synchronization algorithm is built-in.

IV. General

1) Deviations from the updated Final Specifications [April 1999 – NEA/NSC/DOC(99)8].

No deviations are made.

2) User assumptions?

No additional assumptions are applied.

3) Specific features of the used codes?

ATHLET code – 1-D T-H code, two phases, 6 equation model.

QUABOX/CUBBOX – 2 group, 3-D kinetics core model, nodal expansion method.

4) Number of solutions submitted per participant and how they differ?

We submitted two solutions for the base case and one for the return to power case. The difference between the first and second calculations was that the first solution of the base case was done with the decay heat tables for the return to power case which was our mistake coming from misunderstanding of the downloaded decay heat file names

IBERDROLA
SPAIN

I. Thermal-hydraulic core model

1) Core thermal-hydraulic (T-H) model and nodalization (1-D, 3-D, and number T-H channels or cells) – How are channels/T-H cells chosen?

The cells have been chosen following the Final Specifications:

Radial nodalization (19 channels): Specifications

- 18 active channels (channel number 1-18).
- 1 reflector channel (channel number 19).

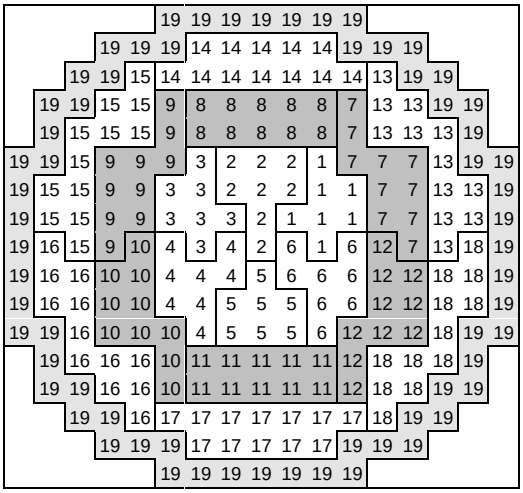

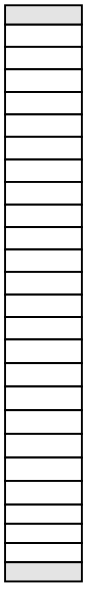

Axial nodalization (26 levels):

- 24 active core levels (number 2-25).
- 2 reflector levels:
  - Number 1: lower reflector.
  - Number 26: upper reflector.

2) Number of heat structures (fuel rods) modeled?

432 HEAT STRUCTURES (18 radial heat structures and 24 axial heat structures)

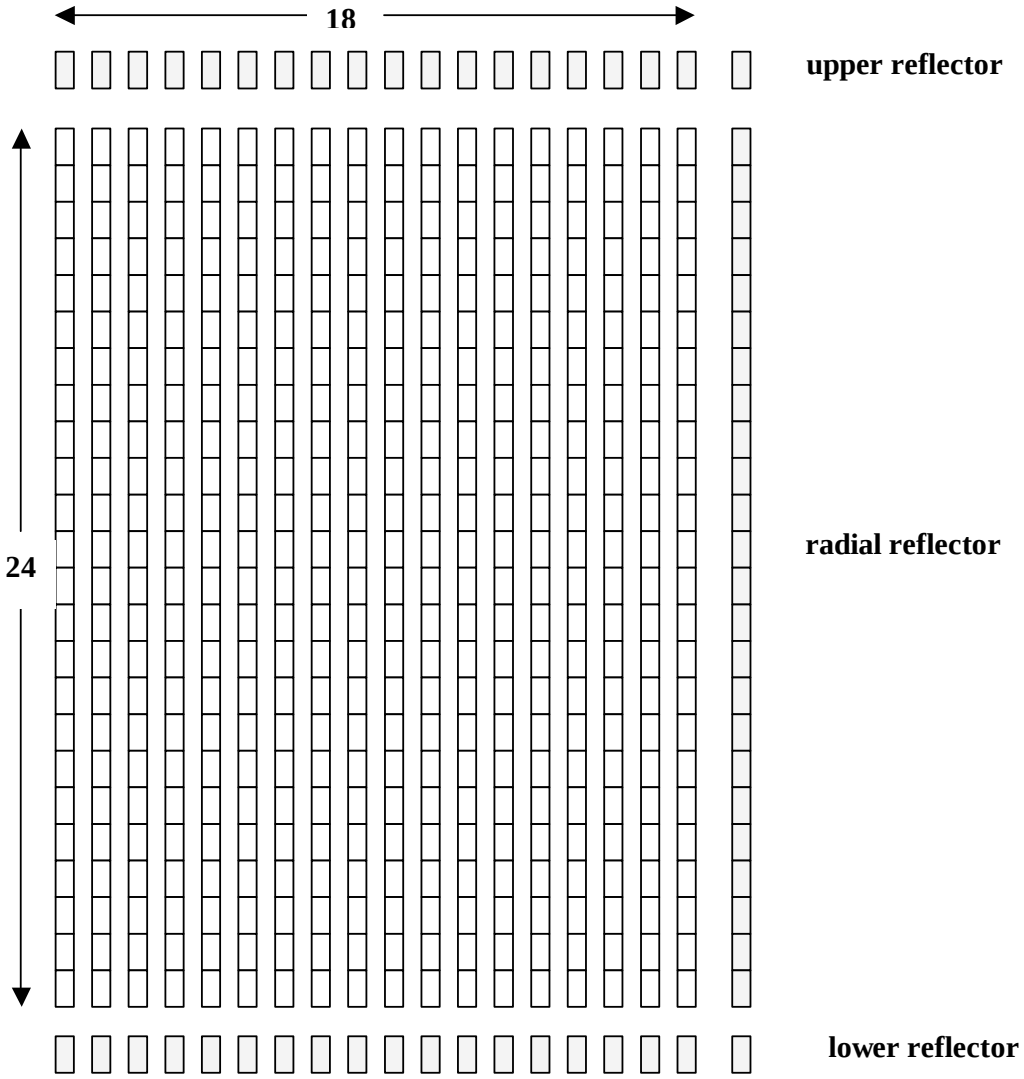

3) Which core thermal-hydraulic initial and transient boundary conditions are used and how?

Specifications: TEMP.BC, MASS_FLOWS.BC, Press_Inlet.BC, Press_Outlet.BC.

The boundary conditions have been used as follows:

- INLET condition at the vessel bottom, by the definition of a FILL.
- OUTLET condition at the vessel top, by the definition of a TDV (Time Dependent Volume).

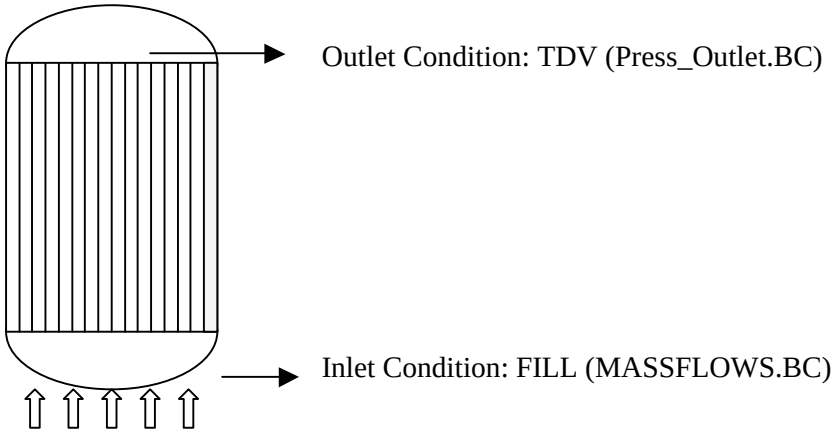

4) Radial and axial heat structure (fuel rod) nodalization?

The nodalization has been made assigning 1 heat conductor for each volume of the core model. The heat conductor is divided in three parts:

1. Fuel Pellet.
2. Gap.
3. Clad.

5) Relation used for Doppler temperature?

Doppler temperature has been modeled using an AVERAGED fuel temperature, as does RETRAN. The relation $T_f = 0.3*T_{f,c} + 0.7*T_{f,s}$ cannot be applied by RETRAN-3D/MOD002.

6) Used correlations for fuel properties vs. temperature?

FUEL PELLET

Thermal conductivities

Temp(F)	*500.0*	*650.0*	*800.0*	*950.0*	*1100.0*
Vol.Heat.(Btu/F ft h.)	*3.341*	*2.971*	*2.677*	*2.439*	*2.242*
Temp(F)	*1250.0*	*1400.0*	*1550.0*	*1700.0*	*1850.0*
Vol.Heat.(Btu/F ft h.)	*2.078*	*1.940*	*1.823*	*1.724*	*1.639*
Temp(F)	*2000.0*	*2150.0*	*2300.0*	*2450.0*	*2600.0*
Vol.Heat.(Btu/F ft h.)	*1.568*	*1.507*	*1.457*	*1.415*	*1.382*
Temp(F)	*3100.0*	*3600.0*	*4100.0*	*4600.0*	*5100.0*
Vol.Heat.(Btu/F ft h.)	*1.323*	*1.333*	*1.406*	*1.538*	*1.730*

Volumetric heat capacity

Temp(F)	*32.0*	*122.0*	*212.0*	*392.0*	*752.0*
Vol.Heat.(Btu/F ft^3)	*34.45*	*38.35*	*40.95*	*43.55*	*46.80*
Temp(F)	*2012.0*	*2732.0*	*3092.0*	*3452.0*	*3812.0*
Vol.Heat.(Btu/F ft^3)	*51.35*	*52.65*	*56.55*	*63.05*	*72.80*
Temp(F)	*4352.0*	*4532.0*	*4712.0*	*4892.0*	*5144.0*
Vol.Heat.(Btu/F ft^3)	*89.70*	*94.25*	*98.15*	*100.10*	*101.40*
Temp(F)	*8000.0*				
Vol.Heat.(Btu/F ft^3)	*101.40*				

Linear expansion coefficient

Temp(F)	*440.0*	*890.0*	*1340.0*	*1790.0*	
Coef (F^{-1})	*$3.4\cdot10^{-6}$*	*$4.27\cdot10^{-6}$*	*$4.77\cdot10^{-6}$*	*$5.19\cdot10^{-6}$*	

CLAD

Thermal conductivities

Temp(F)	*32.0*	*212.0*	*392.0*	*572.0*	*752.0*
Vol.Heat.(Btu/F ft h.)	*7.812*	*7.992*	*8.208*	*8.512*	*8.956*
Temp(F)	*2192.0*	*2372.0*	*2552.0*	*2732.0*	*3292.0*
Vol.Heat.(Btu/F ft h)	*17.784*	*19.656*	*21.780*	*24.048*	*28.908*
Temp(F)	*3360.0*				
Vol.Heat.(Btu/F ft h)	*33.120*				

Volumetric heat capacity

Temp(F)	*32.0*	*932.0*	*1112.0*	*1184.0*	*1490.0*
Vol.Heat.(Btu/F ft^3)	*28.75*	*32.56*	*34.40*	*35.22*	*35.22*
Temp(F)	*1508.0*	*1544.0*	*1580.0*	*1616.0*	*1652.0*
Vol.Heat.(Btu/F ft^3)	*49.14*	*57.74*	*60.20*	*70.43*	*79.85*
Temp(F)	*1688.0*	*1724.0*	*1760.0*	*1787.0*	*3300.0*
Vol.Heat.(Btu/F ft^3)	*75.35*	*59.34*	*45.86*	*34.81*	*34.81*

Linear expansion coefficient

Temp(F)	*80.6*	*260.6*	*440.6*	*620.6*	
Coef (F^{-1})	*0.0*	*$2.69\cdot10^{-6}$*	*$2.72\cdot10^{-6}$*	*$3.22\cdot10^{-6}$*	

FUEL GAP

Heat conductivities

Temp(F)	*700.0*				
Vol.Heat.(Btu/F ft h)	*0.625*				

Volumetric heat capacity

Temp(F)	*700.0*				
Vol.Heat.(Btu/F ft^3)	*0.00593*				

Linear expansion coefficient

Temp(F)	*0.0*	*2000.0*			
Coef (F^{-1})	*0.0*	*$9.0 \cdot 10^{-6}$*			

II. Core neutronics model

1) Number of radial nodes per assembly?

There is one neutronic node per assembly, and 30 types of fuel assemblies (1-30).

	1	2	3	4	5	6	7	8	9	10	11	12	13	14	15	16	17
1	30	30	30	30	30	30	30	30	30	30	30	30	30	30	30	30	30
2	30	30	30	30	30	30	21	15	8	15	21	30	30	30	30	30	30
3	30	30	30	30	28	25	20	14	7	14	20	25	28	30	30	30	30
4	30	30	30	29	27	24	19	13	6	13	19	24	27	29	30	30	30
5	30	30	28	27	26	23	18	12	5	12	18	23	26	27	28	30	30
6	30	30	25	24	23	22	17	11	4	11	17	22	23	24	25	30	30
7	30	21	20	19	18	17	16	10	3	10	16	17	18	19	20	21	30
8	30	15	14	13	12	11	10	9	2	9	10	11	12	13	14	15	30
9	30	8	7	6	5	4	3	2	1	2	3	4	5	6	7	8	30
10	30	15	14	13	12	11	10	9	2	9	10	11	12	13	14	15	30
11	30	21	20	19	18	17	16	10	3	10	16	17	18	19	20	21	30
12	30	30	25	24	23	22	17	11	4	11	17	22	23	24	25	30	30
13	30	30	28	27	26	23	18	12	5	12	18	23	26	27	28	30	30
14	30	30	30	29	27	24	19	13	6	13	19	24	27	29	30	30	30
15	30	30	30	30	28	25	20	14	7	14	20	25	28	30	30	30	30
16	30	30	30	30	30	30	21	15	8	15	21	30	30	30	30	30	30
17	30	30	30	30	30	30	30	30	30	30	30	30	30	30	30	30	30

SYMMETRY 1/8

2) Axial nodalization?

11 axial nodes:

- 9 core nodes (number 2-10).
- 2 reflector nodes (number 1, 11).

RETRAN-3D/MOD002 only works with a limited number of compositions (298). Due to the number of compositions given in the specifications is 438, a procedure of reduction has been made to obtain the desired number. The final number of compositions used is 264 (261 compositions + 3 reflector comp.). The reduction for each fuel assembly is made as follows: The different compositions of an assembly are reduced to get 9 compositions per fuel assembly, obtaining a number of compositions < 298. For this exercise, the final number of compositions used was 264.

[(29 FA * 9 comp. = 261) + 3 reflector = 264 compositions]

Composition number: [1 2 3 4 5 6 7 8 9]
[AA BB CC DDDD EEEE FFFF GG HH II]
[2 2 2 4 4 4 2 2 2]

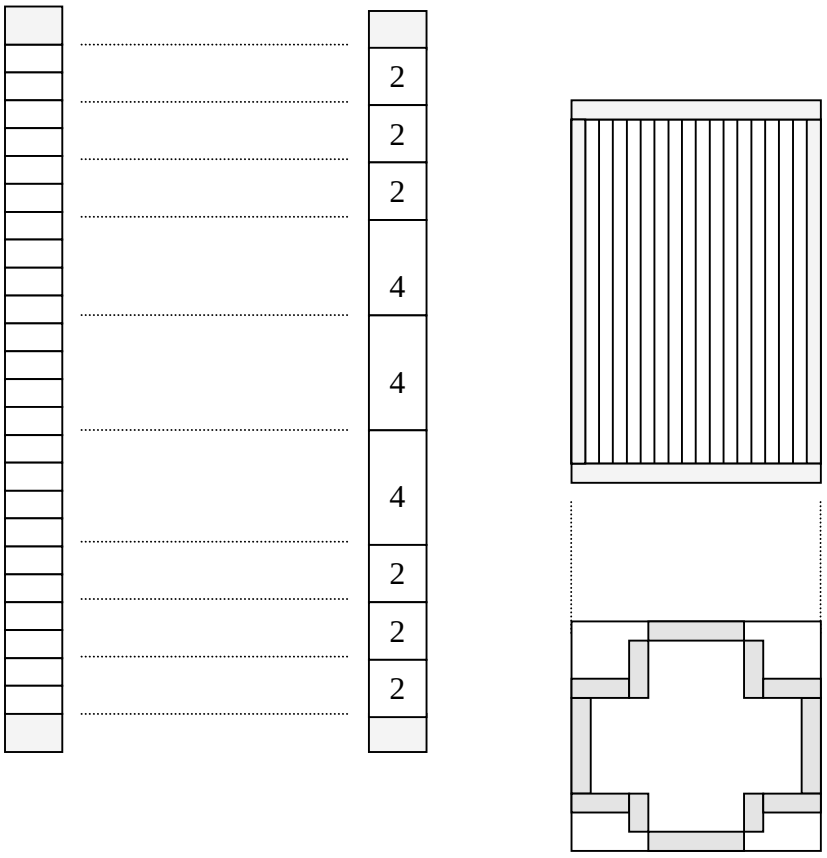

3) Radial and axial reflector modeling?

The reflector modeling used by RETRAN-3D/MOD002 has been applied defining a radial reflector (ASEMBLY TYPE 30, composition 25) and two axial reflector (**lower reflector =** composition number 24) (**upper reflector** = composition number 26).

4) Spatial decay heat distribution modeling?

In this version of RETRAN (RETRAN-3D/MOD002), the decay heat model option for multidimensional kynetic is not available.

5) Cross-section interpolation procedure used?

Not used.

6) Used method to get a critical reactor at the beginning of transient?

RETRAN-3D/MOD002 applies its own internal code to get the critical reactor.

III. Coupling schemes

1) Hydraulics/heat structure spatial mesh overlays (mapping schemes in radial and axial plane)?

Mapping schemes have been chosen from the specifications, modeling 18 T-H cells. One heat structure is associated for each T-H cell.

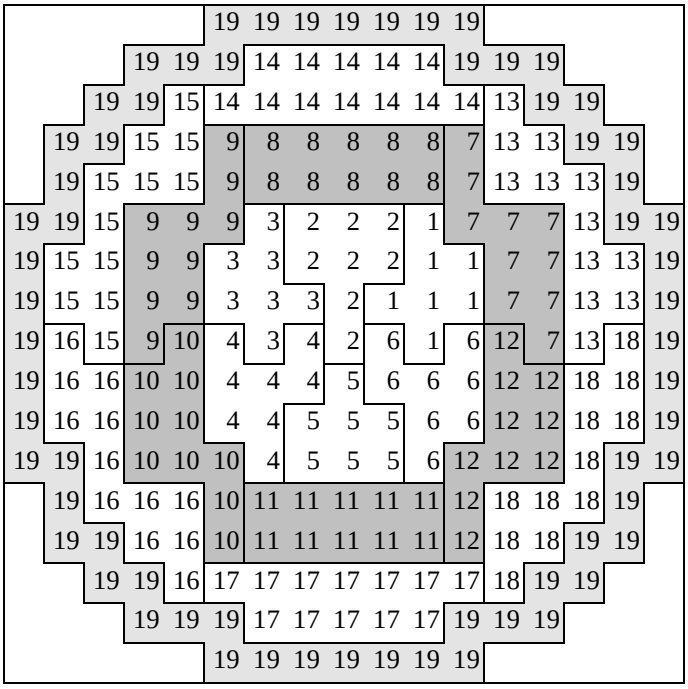

2) Hydraulics/neutronics spatial mesh overlays (mapping schemes in radial and axial plane)?

Mapping schemes following specifications, based on TRAC-PF1/NEM

					30	30	30	30	30	30	30					
			30	30	30	21	15	8	15	21	30	30	30			
		30	30	28	25	20	14	7	14	20	25	28	30	30		
	30	30	29	27	24	19	13	6	13	19	24	27	29	30	30	
	30	28	27	26	23	18	12	5	12	18	23	26	27	28	30	
30	30	25	24	23	22	17	11	4	11	17	22	23	24	25	30	30
30	21	20	19	18	17	16	10	3	10	16	17	18	19	20	21	30
30	15	14	13	12	11	10	9	2	9	10	11	12	13	14	15	30
30	8	7	6	5	4	3	2	1	2	3	4	5	6	7	8	30
30	15	14	13	12	11	10	9	2	9	10	11	12	13	14	15	30
30	21	20	19	18	17	16	10	3	10	16	17	18	19	20	21	30
30	30	25	24	23	22	17	11	4	11	17	22	23	24	25	30	30
	30	28	27	26	23	18	12	5	12	18	23	26	27	28	30	
	30	30	29	27	24	19	13	6	13	19	24	27	29	30	30	
		30	30	28	25	20	14	7	14	20	25	28	30	30		
			30	30	30	21	15	8	15	21	30	30	30			
					30	30	30	30	30	30	30					

|||

					19	19	19	19	19	19	19					
			19	19	19	14	14	14	14	14	19	19	19			
		19	19	15	14	14	14	14	14	14	14	13	19	19		
	19	19	15	15	9	8	8	8	8	8	7	13	13	19	19	
	19	15	15	15	9	8	8	8	8	8	7	13	13	13	19	
19	19	15	9	9	9	3	2	2	2	1	7	7	7	13	19	19
19	15	15	9	9	3	3	2	2	2	1	1	7	7	13	13	19
19	15	15	9	9	3	3	3	2	1	1	1	7	7	13	13	19
19	16	15	9	10	4	3	4	2	6	1	6	12	7	13	18	19
19	16	16	10	10	4	4	4	5	6	6	6	12	12	18	18	19
19	16	16	10	10	4	4	5	5	5	6	6	12	12	18	18	19
19	19	16	10	10	10	4	5	5	5	6	12	12	12	18	19	19
	19	16	16	16	10	11	11	11	11	11	12	18	18	18	19	
	19	19	16	16	10	11	11	11	11	11	12	18	18	19	19	
		19	19	16	17	17	17	17	17	17	17	18	19	19		
			19	19	19	17	17	17	17	17	19	19	19			
					19	19	19	19	19	19	19					

3) Heat structure/neutronics spatial mesh overlays (mapping schemes in radial and axial plane)?

RETRAN-3D/MOD002 internal code applies the overlay. Same as hydraulics/neutronics spacial mesh overlay.

4) Temporal coupling scheme?

Explicit.

5) Coupling numerics – explicit, semi-implicit or implicit?

Semi-implicit.

6) Coupling method – external or internal?

Internal.

7) Coupling design – serial integration or parallel processing?

Serial integration.

IV. General

1) Deviations from the updated Final Specifications [April 1999 – NEA/NSC/DOC(99)8].

None.

2) User assumptions?

None.

3) Specific features of the used codes?

The used version of RETRAN-3D MOD002 has some lacks and restrictions (described in the results report).

4) Number of solutions submitted per participant and how they differ?

One.

KAERI – 1
KOREA

I. Thermal-hydraulic core model

1) Core thermal-hydraulic (T-H) model and nodalization (1-D, 3-D, and number T-H channels or cells) – How are channels/T-H cells chosen?

18 channels and 6 axial nodes (only for the active core region).

2) Number of heat structures (fuel rods) modeled?

18.

3) Which core thermal-hydraulic initial and transient boundary conditions are used and how?

For each of the 18 channels specified in the Final Specifications:

a) Core outlet pressure vs. time.

b) Core inlet mass flow rate vs. time.

c) Core inlet temperature vs. time.

4) Radial and axial heat structure (fuel rod) nodalization?

6 radial rings in the Pellet, 6 uniformly spaced axial meshes.

5) Relation used for Doppler temperature?

0.3 * centerline temp + 0.7 * Pellet surface temp.

6) Used correlations for fuel properties vs. temperature?

What is given by the NEACRP PWR Rod Ejection Benchmark Specifications.

II. Core neutronics model

1) Number of radial nodes per assembly?

One node/FA.

2) Axial nodalization?

26 axial nodes.

3) Radial and axial reflector modeling?

Modeled as is, no heat removal by reflector.

4) Spatial decay heat distribution modeling?

Flux dependent.

5) Cross-section interpolation procedure used?

Identical to lint4d.f in terms of accuracy.

6) Used method to get a critical reactor at the beginning of transient?

Divide $\nu\Sigma_f$ by k_{eff} (1.00711).

III. Coupling schemes

1) Hydraulics/heat structure spatial mesh overlays (mapping schemes in radial and axial plane)?

One-to-one.

2) Hydraulics/neutronics spatial mesh overlays (mapping schemes in radial and axial plane)?

Radially one-to-multi (about 10 neutronic nodes to 1 T-H node), axially averaging.

3) Heat structure/neutronics spatial mesh overlays (mapping schemes in radial and axial plane)?

Radially one-to-multi (about 10 neutronic nodes to 1 T-H node), axially averaging.

4) Temporal coupling scheme?

T-H leading neutronics every time step. No iteration in a time step.

5) Coupling numerics – explicit, semi-implicit or implicit?

Explicit.

6) Coupling method – external or internal?

Internal.

7) Coupling design – serial integration or parallel processing?

Serial.

IV. General

1) Deviations from the updated Final Specifications [April 1999 – NEA/NSC/DOC(99)8].

Independent decay heat data (consistent with ISO 10645, 1992).

2) User assumptions?

None.

3) Specific features of the used codes?

3-D T-H modeling possible within the core region.

4) Number of solutions submitted per participant and how they differ?

Two. Separate answer sheet is prepared for the other case (MASTER standalone case).

KAERI – 2
KOREA

I. Thermal-hydraulic core model

1) Core thermal-hydraulic (T-H) model and nodalization (1-D, 3-D, and number T-H channels or cells) – How are channels/T-H cells chosen?

177 channels and 24 axial nodes (only for the active core region).

2) Number of heat structures (fuel rods) modeled?

177.

3) Which core thermal-hydraulic initial and transient boundary conditions are used and how?

For each of the 18 channels specified in the Final Specifications:

a) Core outlet pressure vs. time.

b) Core inlet mass flow rate vs. time.

c) Core inlet temperature vs. time.

The fuel assemblies belonging to the same channel use the same boundary condition. The fuel assemblies located on the horizontal axis belong to two channels and averaging of the two channel properties were performed for these fuel assemblies.

4) Radial and axial heat structure (fuel rod) nodalization?

6 radial rings in the Pellet, 24 uniformly spaced axial meshes.

5) Relation Used for Doppler Temperature?

0.3 * centerline temp + 0.7 * Pellet surface temp.

6) Used correlations for fuel properties vs. temperature?

What is given by the NEACRP PWR Rod Ejection Benchmark Specifications.

II. Core neutronics model

1) Number of radial nodes per assembly?

One node/FA.

2) Axial nodalization?

26 axial nodes.

3) Radial and axial reflector modeling?

Modeled as is, no heat removal by reflector.

4) Spatial decay heat distribution modeling?

Flux dependent.

5) Cross-section interpolation procedure used?

Identical to lint4d.f in terms of accuracy.

6) Used method to get a critical reactor at the beginning of transient?

Divide $\nu\Sigma_f$ by k_{eff} (1.00509).

III. Coupling schemes

1) Hydraulics/heat structure spatial mesh overlays (mapping schemes in radial and axial plane)?

One-to-one.

2) Hydraulics/neutronics spatial mesh overlays (mapping schemes in radial and axial plane)?

Radially one-to-one, axially linear interpolation.

3) Heat structure/neutronics spatial mesh overlays (mapping schemes in radial and axial plane)?

One-to-one, axially averaging.

4) Temporal coupling scheme?

T-H leading neutronics every time step. No iteration in a time step.

5) Coupling numerics – explicit, semi-implicit or implicit?

Explicit.

6) Coupling method – external or internal?

Internal.

7) Coupling design – serial integration or parallel processing?

Serial.

IV. General

1) Deviations from the updated Final Specifications [April 1999 – NEA/NSC/DOC(99)8].

Independent decay heat data (consistent with ISO 10645, 1992).

2) User assumptions?

None.

3) Specific features of the used codes?

Able to perform on-line DNB calculations and to incorporate cross flow.

4) Number of solutions submitted per participant and how they differ?

Two. Separate answer sheet is prepared for the other case (MARS/MASTER case).

PSU
UNITED STATES OF AMERICA

I. Thermal-hydraulic core model [1]

1) Core thermal-hydraulic (T-H) model and nodalization (1-D, 3-D, and number T-H channels or cells) – How are channels/T-H cells chosen?

The TRAC-PF1 3-D vessel modeling capability in cylindrical geometry is used. The 3-D TRAC-PF1 pressure vessel is subdivided into 14 axial layers, 5 radial rings, and 6 azimuthal sectors for a total of 420 hydrodynamic cells as shown in Figures 2.4, 2.5 and 2.6 of Chapter 2 of this volume. The core region is contained within the inner three rings and between axial layers four through nine. In the TRAC-PF1 model the four inner T-H rings have the following radius: R_1 = 0.945 m, R_2 = 1.3365 m, R_3 = 1.637 m, and R_4 = 1.9115 m. The flow areas of T-H cells in the core region are: for cells number 1-6 -1.515 m^2; for cells number 7-12 -1.515 m^2; and for cells number 13-18 -1.530 m^2.

2) Number of heat structures (fuel rods) modeled?

Eighteen heat-structures (rods) in radial plane and six in axial plane.

3) Which core thermal-hydraulic initial and transient boundary conditions are used and how?

Original.

4) Radial and axial heat structure (fuel rod) nodalization?

Eight radial and hundred axial nodes are used.

5) Relation used for Doppler temperature?

As specified.

6) Used correlations for fuel properties vs. temperature?

The fuel and clad properties as a function of temperature were given by the equations on page 30 of the Final Specifications. Furthermore, the gap conductance used in the TRAC-PF1 input was the value provided on page 30 of the Final Specifications.

1. All cited pages are relative to Ivanov, K., T. Beam, A. Baratta, A. Irani, and N. Trikorous, "PWR MSLB Benchmark: Volume 1: Final Specifications", NEA/NSC/DOC(99)8, April 1999.

II. Core neutronics model

1) Number of radial nodes per assembly?

Each node in the radial plane represents one fuel assembly with the exception of the center row of nodes, which is subdivided into two nodes. Each axial level is divided into 258 nodes, 192 fuel nodes and 66 water reflector nodes.

2) Axial nodalization?

Twenty-four axial nodes in the framework of the active core as specified in Chapter 2 of the Final Specifications plus bottom (one axial node) and top (one axial node) reflectors resulting in total of twenty-six axial neutronics nodes.

3) Radial and axial reflector modeling?

As described in the specifications.

4) Spatial decay heat distribution modeling?

Following the fission power distribution at the initial steady state.

5) Cross-section interpolation procedure used?

The original version without linear extrapolation.

6) Used method to get a critical reactor at the beginning of transient?

As specified.

III. Coupling schemes

1) Hydraulics/heat structure spatial mesh overlays (mapping schemes in radial and axial plane)?

Each heat structure is mapped to a thermal-hydraulic cell in radial and axial planes in the framework of the active core.

2) Hydraulics/neutronics spatial mesh overlays (mapping schemes in radial and axial plane)?

The neutronic nodes are mapped to the T-H rings and azimuthal sectors as shown in Figures 1 and 2. Table 1 summarizes completely the radial spatial overlays for the TRAC-PF1/NEM coupling.

Figure 1. Description of radial mapping of the T-H rings to the neutronic nodes

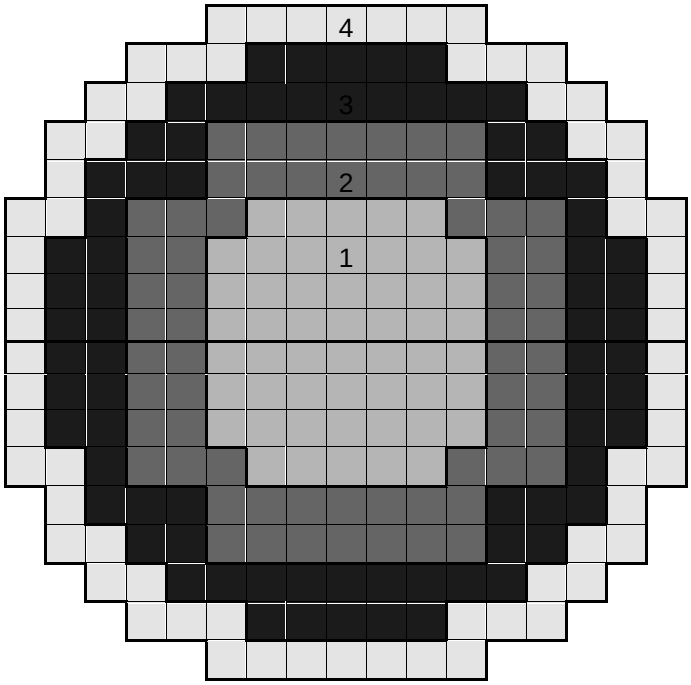

Figure 2. Description of radial mapping of the T-H sectors to the neutron nodes

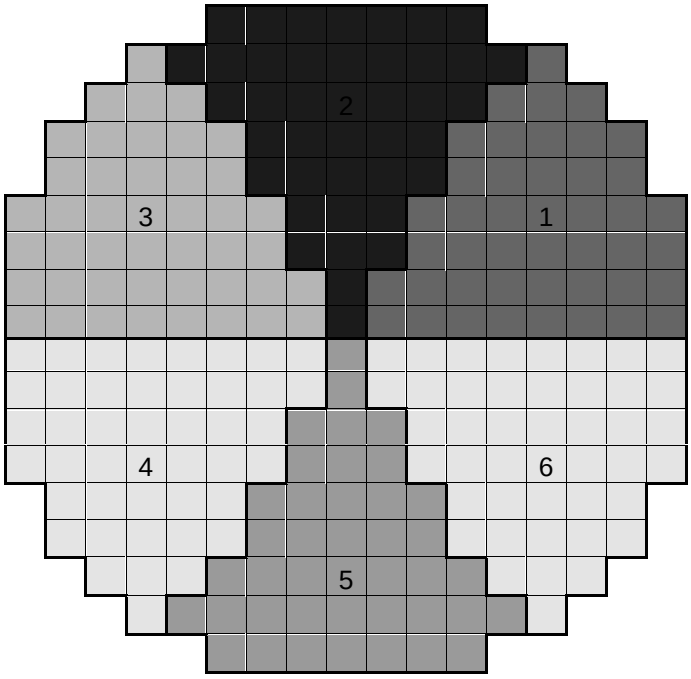

Table 1. Radial coupling summary

Thermal hydraulic (T-H) mapping

1st (T-H) radial ring	– *45 neutronic assemblies*
2nd (T-H) radial ring	– *60 neutronic assemblies*
3rd (T-H) radial ring	– *72 neutronic assemblies*
4th (T-H) radial ring	– *64 reflector water assemblies*
Each theta zone	– *29.5 neutronic assemblies*

Axially, the 24 core neutronics nodes are mapped to the 6 T-H nodes representing the TRAC-PF1 core. The bottom and top reflector are mapped thermal-hydraulically to VESSEL layers 3 and 10 respectively.

3) Heat structure/neutronics spatial mesh overlays (mapping schemes in radial and axial plane)?

The radial spatial mesh overlays between the core neutronics model and heat structure component is shown in Figure 3, which is consistent with the original TRAC-PF1/NEM radial mapping scheme, provided in the Chapter 2 of this Volume. For the purpose of neutronics/heat structure coupling axial reflector regions are mapped to layers 4 and 9.

Figure 3. Description of the radial mapping of heat structures to the neutronics nodes

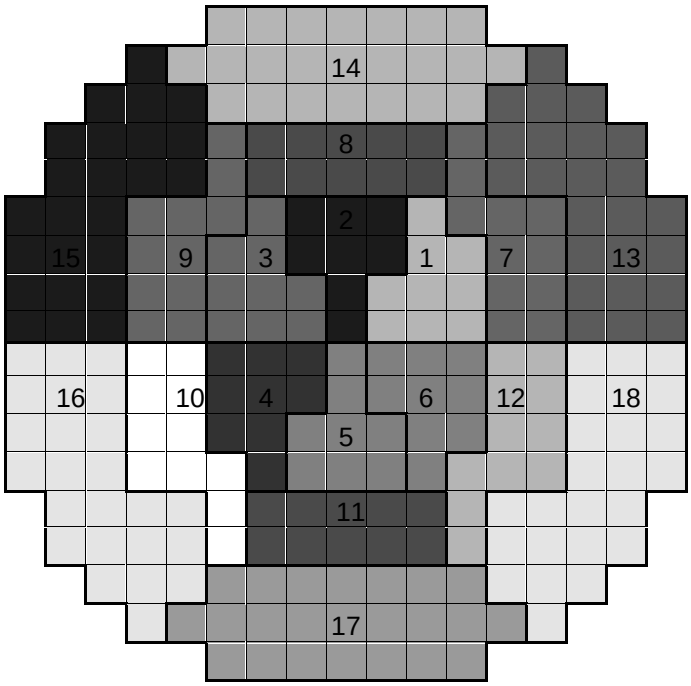

Table 2. Heat structure mapping

Inner ring heat structures	– *7.5 neutronic assemblies*
Mid ring heat structures	– *10 neutronic assemblies*
Outer ring heat structures	– *12 neutronic assemblies*

4) Temporal coupling scheme?

One neutronics time step per one T-H step.

5) Coupling numerics – explicit, semi-implicit or implicit?

Semi-implicit.

6) Coupling method – external or internal?

Internal.

7) Coupling design – serial integration or parallel processing?

Serial integration.

IV. General

1) Deviations from the updated Final Specifications [April 1999 – NEA/NSC/DOC(99)8].

2) User assumptions?

3) Specific features of the used codes?

4) Number of solutions submitted per participant and how they differ?

PURDUE UNIVERSITY/NRC – 1
UNITED STATES OF AMERICA

I. Thermal-hydraulic core model [1]

1) Core thermal-hydraulic (T-H) model and nodalization (1-D, 3-D, and number T-H channels or cells) – How are channels/T-H cells chosen?

The flow paths through the core were represented by 19 1-D pipe components: 18 for the channels specified by Figure 3.2.3 of the Final Specifications, and an additional pipe representing flow through the radial reflector (core periphery) region. Each pipe contained 8 cells of 59.52 cm height, which includes the top and bottom (axial) reflectors. Thus, the total active core height is maintained at 357.12 cm. The axial reflector heights were increased from 21.811 cm to 59.52 cm each in order to increase the Courant limit of the model. This has no effect on the final results since the reflector regions are tall enough to be considered "infinite reflectors".

2) Number of heat structures (fuel rods) modeled?

A single heat structure component was used for each neutronic node in the active region of the core. This would ordinarily be 177 heat structures, except that an axis of symmetry exists in the mapping as defined by Figure 3.2.3 in the Final Specifications. Those fuel assemblies along this axis of symmetry were divided into two half-assemblies, bringing the number of heat structure components to 192. Finally, a single heat structure component was used to model the entire radial reflector region. Thus, the total number of heat structure components used in the model is 193.

3) Which core thermal-hydraulic initial and transient boundary conditions are used and how?

The inlet mass flow rates for each channel as provided by the benchmark specifications were converted to liquid velocities per channel using the inlet fluid temperature and pressure. A water property table written by the former National Bureau of Standards (NBS) was used to compute the fluid density, making this conversion possible. The inlet velocities, temperatures, and pressures were used as input conditions for each channel, and the per-channel outlet pressures were used as boundary conditions at the top of the core. Since there were only 18 channels of thermal-hydraulic data provided by the benchmark specifications, the reflector channel (channel 19) used the data assigned to channel 18.

1. All cited pages are relative to Ivanov, K., T. Beam, A. Baratta, A. Irani, and N. Trikorous, "PWR MSLB Benchmark: Volume 1: Final Specifications", NEA/NSC/DOC(99)8, April 1999.

4) Radial and axial heat structure (fuel rod) nodalization?

Throughout most of the core, each assembly is represented by an individual heat structure component. The exceptions, as mentioned above, are those fuel assemblies along the axis of symmetry and the radial reflector region. Each heat structure component contained 9 radial conduction nodes, at 0.0000, 0.9391, 1.8782, 2.8173, 3.7564, 4.6955, 4.7910, 5.1275, and 5.4640 mm from the centerline of the fuel pin. The gas gap was modeled between nodes 6 and 7 (4.6955 and 4.7910 mm from the fuel centerline). Each heat structure was divided into 6 axial intervals, making 7 total axial conduction nodes (in TRAC-M, conduction nodes are defined at boundaries rather than at the center of regions). Each axial interval was 59.52 cm in height. The height of the heat structures corresponds to the exact active core height of the core, and does not account of the axial reflectors. In order to simplify the TRAC-M input, the bottom reflector heat structure axial interval was lumped into the bottom-most interval in the active core. In the same manner, the top axial reflector was lumped into the top-most interval in the active core. It was decided that this would not have a noticeable effect on the results, as the effect of "fuel" temperature on the reflector is small compared to the much larger feedback drivers in this transient.

5) Relation used for Doppler temperature?

The common 70/30 split between fuel surface and centerline as specified on page 29 in the Final Specifications was used for computing Doppler temperature.

6) Used correlations for fuel properties vs. temperature?

The fuel and clad properties as a function of temperature were given by the equations on page 30 of the Final Specifications. Furthermore, the gap conductance used in the TRAC-M input was the value provided on page 30 of the Final Specifications.

II. Core neutronics model

1) Number of radial nodes per assembly?

A single neutronics node was used per assembly, regardless of whether the assembly represents fuel or reflector.

2) Axial nodalization?

The core model was divided into a total of 28 axial levels. Of these, 2 levels are modeling the axial reflectors, while the remaining 26 levels are used to model the active core region. The nodalization outlined in the Final Specifications was not used. Instead, the axial nodalization was (from the bottom): 21.811, 14.88, 4.71, 10.17, 20*14.88, 12.266, 2.614, 14.88, and 21.811 cm. Note the axial reflector nodes are of the height as suggested in the Final Specifications, despite the fact that the axial thermal-hydraulic nodalization does not match exactly. This mismatch of heights in the reflector region has a negligible effect on the final results. Also note that no axial levels in the active core region have a height greater than 14.88 cm. This does not follow the suggested nodalization in the Final Specifications in order to match the thermal-hydraulic axial nodalization in a more consistent manner.

3) Radial and axial reflector modeling?

The radial reflector was modeled in the neutronics model by a single neutronic node per reflector assembly on each axial level of the core. The axial reflector was modeled using an axial level consisting of reflector assemblies only on the top and bottom of the core.

4) Spatial decay heat distribution modeling?

PARCS uses a 6-group per neutronic node decay heat model based on the past 3-D power shapes calculated by the code. The model operates under the assumption of saturation of the decay heat precursors, sometimes called “infinite operation time”.

5) Cross-section interpolation procedure used?

The method used for interpolating the cross-sections was given in the Final Specifications. This is a 4-point interpolation scheme designed to interpolate the tabular format of the cross-section sets.

6) Used method to get a critical reactor at the beginning of transient?

PARCS adjusts the fission source before beginning a transient calculation by dividing by k_{eff}.

III. Coupling schemes

1) Hydraulics/heat structure spatial mesh overlays (mapping schemes in radial and axial plane)?

Since each assembly in the active core region is represented by a heat structure, the mapping shown in Figure 3.2.3 describes the hydraulics to heat structure mapping. Each block in this figure represents a heat structure component (with the exception of the all-black reflector, modeled by a single heat structure component), and the number in each block is the channel number coupled with that particular heat structure component. The radial reflector (channel 19) is coupled with heat structure 193. Again, there are 8 axial cells in the hydraulic components and 6 axial intervals in the heat structure components (all are of the same height: 59.52 cm). The heat structures are coupled to the hydraulic cells in the middle of the pipe (cells 2-7, inclusive, numbering from the bottom). This is due to the lumping of the axial reflector into the bottom- and top-most regions of the active core.

2) Hydraulics/neutronics spatial mesh overlays (mapping schemes in radial and axial plane)?

Since each neutronic assembly in the active core is represented by a heat structure component in TRAC-M, the description above also demonstrates the hydraulic-to-neutronics mapping. All 64 radial reflector assemblies are mapped to channel 19 in the hydraulics model.

3) Heat structure/neutronics spatial mesh overlays (mapping schemes in radial and axial plane)?

The mapping of neutronic assemblies in the active core is one-to-one to heat structure nodalization. All 64 radial reflector assemblies in the neutronics model are mapped to heat structure 193.

4) Temporal coupling scheme?

Both TRAC-M and PARCS are locked into the same time step, and the time step size is determined by TRAC-M. TRAC-M updates its hydraulics solution first, followed by the conduction solution. These new data are passed to PARCS so the neutronics solution can be updated. The updated neutronics solution (in the form of a heat source) is passed back to TRAC-M and is used to update the hydraulics and conduction solution for the subsequent time step.

5) Coupling numerics – explicit, semi-implicit or implicit?

TRAC-M/PARCS operates in an explicit manner.

6) Coupling method – external or internal?

TRAC-M/PARCS uses an internal coupling scheme.

7) Coupling design – serial integration or parallel processing?

Although the PVM (Parallel Virtual Machine) message-passing package is used to pass the data between TRAC-M and PARCS, the coupled code actually operates in a serial mode, with PVM providing only an interface for passing data between the two processes.

IV. General

1) Deviations from the updated Final Specifications [April 1999 – NEA/NSC/DOC(99)8].

The axial nodalization of the neutronics model was finer than given in the Final Specifications. There are no axial levels in the core with a height of 29.76 cm. The heat structure portion of the axial reflectors are not modeled explicitly in TRAC-M, but are instead lumped into the bottom- and top-most axial intervals in the heat structures representing the core.

2) User assumptions?

The wall roughness of the channels was 0.05% of the hydraulic diameter. This value was chosen in order to more closely match the pressure drops across the core calculated by TRAC-M and provided by the benchmark specifications.

3) Specific features of the used codes?

PARCS has a transient pin power capability, using form functions from the lattice physics code. The use of this feature makes best-estimate analysis and, specifically, DNB analysis easier throughout the important transient state points.

4) Number of solutions submitted per participant and how they differ?

There were a total of 3 solutions from TRAC-M/PARCS. The first was delivered before the 2nd meeting. At this meeting, specifications were corrected, and another solution was generated. It was discovered that the second solution (submitted in summer of 1999) did not use the correct boundary conditions for the two scenarios. The final solution, given late in the summer of 1999 is the final TRAC-M/PARCS solution, matching specifications as closely as possible.

PURDUE UNIVERSITY/NRC – 2
UNITED STATES OF AMERICA

I. Thermal-hydraulic core model [1]

1) Core thermal-hydraulic (T-H) model and nodalization (1-D, 3-D, and number T-H channels or cells) – How are channels/T-H cells chosen?

The flow paths through the core were represented by 19 1-D pipe components: 18 for the channels specified by Figure 3.2.3 of the Final Specifications, and an additional pipe representing flow through the radial reflector (core periphery) region. Each pipe contained 8 cells of 59.52 cm height, which includes the top and bottom (axial) reflectors. Thus, the total active core height is maintained at 357.12 cm. The axial reflector heights were increased from 21.811 cm to 59.52 cm each in order to increase the Courant limit of the model. This has no effect on the final results since the reflector regions are tall enough to be considered "infinite reflectors".

2) Number of heat structures (fuel rods) modeled?

A single heat structure component was used for each neutronic node in the active region of the core. This would ordinarily be 177 heat structures, except that an axis of symmetry exists in the mapping as defined by Figure 3.2.3 in the Final Specifications. Those fuel assemblies along this axis of symmetry were divided into two half-assemblies, bringing the number of heat structure components to 192. Finally, a single heat structure component was used to model the entire radial reflector region. Thus, the total number of heat structure components used in the model is 193.

3) Which core thermal-hydraulic initial and transient boundary conditions are used and how?

The inlet mass flow rates, fluid temperatures, and pressures for each channel as provided by the benchmark specifications were used for inlet conditions. The per-channel outlet pressures were used as boundary conditions at the top of the core. Since there were only 18 channels of thermal-hydraulic data provided by the benchmark specifications, the reflector channel (channel 19) used the data assigned to channel 18.

4) Radial and axial heat structure (fuel rod) nodalization?

Throughout most of the core, each assembly is represented by an individual heat structure component. The exceptions, as mentioned above, are those fuel assemblies along the axis of symmetry and the radial reflector region. Each heat structure component contained 9 radial

1. All cited pages are relative to Ivanov, K., T. Beam, A. Baratta, A. Irani, and N. Trikorous, "PWR MSLB Benchmark: Volume 1: Final Specifications", NEA/NSC/DOC(99)8, April 1999.

conduction nodes, at 0.0000, 0.9391, 1.8782, 2.8173, 3.7564, 4.6955, 4.7910, 5.1275, and 5.4640 mm from the centerline of the fuel pin. The gas gap was modeled between nodes 6 and 7 (4.6955 and 4.7910 mm from the fuel centerline. Each heat structure was divided into 8 axial intervals 59.52 cm in height. The height of the heat structures corresponds to the core height of the core, including the axial reflectors.

5) Relation used for Doppler temperature?

The common 70/30 split between fuel surface and centerline as specified on page 29 in the Final Specifications was used for computing Doppler temperature.

6) Used correlations for fuel properties vs. temperature?

The fuel and clad properties as a function of temperature were given by the equations on page 30 of the Final Specifications. Furthermore, the gap conductance used in the RELAP input was the value provided on page 30 of the Final Specifications.

II. Core neutronics model

1) Number of radial nodes per assembly?

A single neutronics node was used per assembly, regardless of whether the assembly represents fuel or reflector.

2) Axial nodalization?

The core model was divided into a total of 28 axial levels. Of these, 2 levels are modeling the axial reflectors, while the remaining 26 levels are used to model the active core region. The nodalization outlined in the Final Specifications was not used. Instead, the axial nodalization was (from the bottom): 21.811, 14.88, 4.71, 10.17, 20*14.88, 12.266, 2.614, 14.88, and 21.811 cm. Note the axial reflector nodes are of the height as suggested in the Final Specifications, despite the fact that the axial thermal-hydraulic nodalization does not match exactly. This mismatch of heights in the reflector region has a negligible effect on the final results. Also note that no axial levels in the active core region have a height greater than 14.88 cm. This does not follow the suggested nodalization in the Final Specifications in order to match the thermal-hydraulic axial nodalization in a more consistent manner.

3) Radial and axial reflector modeling?

The radial reflector was modeled in the neutronics model by a single neutronic node per reflector assembly on each axial level of the core. The axial reflector was modeled using an axial level consisting of reflector assemblies only on the top and bottom of the core.

4) Spatial decay heat distribution modeling?

PARCS uses a 6-group per neutronic node decay heat model based on the past 3-D power shapes calculated by the code. The model operates under the assumption of saturation of the decay heat precursors, sometimes called “infinite operation time”.

5) Cross-section interpolation procedure used?

The method used for interpolating the cross-sections was given in the Final Specifications. This is a 4-point interpolation scheme designed to interpolate the tabular format of the cross-section sets.

6) Used method to get a critical reactor at the beginning of transient?

PARCS adjusts the fission source before beginning a transient calculation by dividing by k_{eff}.

III. Coupling schemes

1) Hydraulics/heat structure spatial mesh overlays (mapping schemes in radial and axial plane)?

Since each assembly in the active core region is represented by a heat structure, the mapping shown in Figure 3.2.3 describes the hydraulics to heat structure mapping. Each block in this figure represents a heat structure component (with the exception of the all-black reflector, modeled by a single heat structure component), and the number in each block is the channel number coupled with that particular heat structure component. The radial reflector (channel 19) is coupled with heat structure 193. Again, there are 8 axial cells in the hydraulic components and 6 axial intervals in the heat structure components (all are of the same height: 59.52 cm). The heat structures are coupled to the hydraulic cells in the middle of the pipe (cells 2-7, inclusive, numbering from the bottom). This is due to the lumping of the axial reflector into the bottom- and top-most regions of the active core.

2) Hydraulics/neutronics spatial mesh overlays (mapping schemes in radial and axial plane)?

Since each neutronic assembly in the active core is represented by a heat structure component in RELAP, the description above also demonstrates the hydraulic-to-neutronics mapping. All 64 radial reflector assemblies are mapped to channel 19 in the hydraulics model.

3) Heat structure/neutronics spatial mesh overlays (mapping schemes in radial and axial plane)?

The mapping of neutronic assemblies in the active core is one-to-one to heat structure nodalization. All 64 radial reflector assemblies in the neutronics model are mapped to heat structure 193.

4) Temporal coupling scheme?

Both RELAP and PARCS are locked into the same time step, and the time step size is determined by RELAP. RELAP updates its conduction solution first, followed by the hydraulics solution. These new data are passed to PARCS so the neutronics solution can be updated. The updated neutronics solution (in the form of a heat source) is passed back to RELAP and is used to update the hydraulics and conduction solution for the subsequent time step.

5) Coupling numerics – explicit, semi-implicit or implicit?

RELAP/PARCS operates in an explicit manner.

6) Coupling method – external or internal?

RELAP/PARCS uses an internal coupling scheme.

7) Coupling design – serial integration or parallel processing?

Although the PVM (Parallel Virtual Machine) message passing package is used to pass the data between RELAP and PARCS, the coupled code actually operates in a serial mode, with PVM providing only an interface for passing data between the two processes.

IV. General

1) Deviations from the updated Final Specifications [April 1999 – NEA/NSC/DOC(99)8].

The axial nodalization of the neutronics model was finer than given in the Final Specifications. There are no axial levels in the core with a height of 29.76 cm.

2) User assumptions?

The wall roughness of the channels was 0.05% of the hydraulic diameter. This value was chosen in order to more closely match the pressure drops across the core calculated by RELAP and provided by the benchmark specifications.

3) Specific features of the used codes?

PARCS has a transient pin power capability, using form functions from the lattice physics code. The use of this feature makes best-estimate analysis and, specifically, DNB analysis easier throughout the important transient state-points.

4) Number of solutions submitted per participant and how they differ?

There were a total of 2 solutions from RELAP/PARCS. The first was delivered before the 2nd meeting. At this meeting, specifications were corrected, and another solution was generated. The final solution, given late in the summer of 1999 is the final RELAP/PARCS solution, matching specifications as closely as possible.

FRAMATOME-ANP/FZK
GERMANY

I. Thermal-hydraulic core model

1) Core thermal-hydraulic (T-H) model and nodalization (1-D, 3-D, and number T-H channels or cells) – How are channels/T-H cells chosen?

External coupling:

- T-H module = COBRA 3-CP.
- 177 channels = 1 channel per FA.
- 24 equidistant layers.

Internal Coupling:

- T-H module = RELAP5.
- 19 channels according to TRAC-PF1 with exception of FAs lying on x-axis; these are lumped together into one additional channel.
- 11 equidistant layers.

2) Number of heat structures (fuel rods) modeled?

- 177 fuel rods = 1 rod per channel for **external coupling.**
- 19 fuel rods = 1 rod per channel for **internal coupling.**

3) Which core thermal-hydraulic initial and transient boundary conditions are used and how?

Boundary conditions according to the specification. All channels on the x-axis get the average of the corresponding TRAC-PF1 channels.

4) Radial and axial heat structure (fuel rod) nodalization?

External coupling:

- 24 equidistant layers.
- 16 rings in fuel, 1 in gap, 2 in cladding.

Internal Coupling:

- 11 equidistant layers.
- 6 rings in fuel, 1 in gap, 2 in cladding.

5) Relation used for Doppler temperature?

According to specification.

6) Used correlations for fuel properties vs. temperature?

According to specification.

II. Core neutronics model

1) Number of radial nodes per assembly?

1 node per FA.

2) Axial nodalization?

28 layers, 26 in core and 2 for upper and lower reflector.

3) Radial and axial reflector modeling?

According to specified neutronics cross-sections.

4) Spatial decay heat distribution modeling?

3-D distribution according to the nodal fission rates.

Time dependence according to specified table vs. time.

5) Cross-section interpolation procedure used?

Routine lint4d.f provided by PSU.

6) Used method to get a critical reactor at the beginning of transient?

Eigenvalue calculation.

III. Coupling schemes

1) Hydraulics/heat structure spatial mesh overlays (mapping schemes in radial and axial plane)?

None.

2) Hydraulics/neutronics spatial mesh overlays (mapping schemes in radial and axial plane)?

See I/1.

3) Heat structure/neutronics spatial mesh overlays (mapping schemes in radial and axial plane)?

See I/2.

4) Temporal coupling scheme?

Explicit.

5) Coupling numerics – explicit, semi-implicit or implicit?

Explicit.

6) Coupling method – external or internal?

External.

7) Coupling design – serial integration or parallel processing?

Serial.

IV. General

1) Deviations from the updated Final Specifications [April 1999 – NEA/NSC/DOC(99)8].

None.

2) User assumptions?

None.

3) Specific features of the used codes?

N/A.

4) Number of solutions submitted per participant and how they differ?

2 solutions: external and internal coupling solution.

UNIVERSITY OF PIZA (UP), ITALY
UNIVERSITY OF ZAGREB (UZ), CROATIA

I. Thermal-hydraulic core model

1) Core thermal-hydraulic (T-H) model and nodalization (1-D, 3-D, and number T-H channels or cells) – How are channels/T-H cells chosen?

The core T-H model with 19 closed 1-D T-H channels was used. 18 channels correspond to 18 flow regions on Figure 3.2.3 (Final Specifications) and one is used for core bypass. There are 26 axial layers in each channel. First and last are for bottom and top reflector (0.21811 m) and 24 equidistant layers (0.14880 m) are used for core region.

2) Number of heat structures (fuel rods) modeled?

18 heat structures were used to model fuel rods belonging to core channel (*e.g.* core structure attached to channel one represents 7.5 fuel elements with 1 560 fuel rods).

3) Which core thermal-hydraulic initial and transient boundary conditions are used and how?

For each of 18 core channels one RELAP5 time dependent volume component was used to define inlet pressure and temperature. The pressures and temperatures provided in specification for 18 flow regions were used (to define energy content of incoming fluid). One time dependent volume per channel was used to define outlet pressure (RELAP5 uses downstream pressure as reference pressure in calculation). RELAP5 time-dependent junction component (one per channel) was used to prescribe inlet flow for each channel (per FA flows from specification were multiplied by number of FAs in the channel). RELAP5 single junction component (one per channel) was used to connect outlet of the channel to corresponding outlet time dependent volume). All boundary condition data provided in benchmark specification were filtered, using appropriate error criteria, to limit number of time points to 99 (RELAP5 limitation on number of entries for time dependent volumes and junctions).

4) Radial and axial heat structure (fuel rod) nodalization?

The heat structure is based on real radial dimensions of fuel rod, height of axial layer and number of fuel rods belonging to the structure (*e.g.* for HS 01 7.5 fuel elements with 1560 fuel rods). There are 10 radial mesh points in the structure (5 mesh intervals in the fuel, two in gap and two in cladding). 24 equidistant axial subdivisions were used (0.14880 m).

5) Relation used for Doppler temperature?

The relation as requested in the specification with weighting factor 0.7 was used.

6) Used correlations for fuel properties vs. temperature?

Fuel and cladding properties are taken from the specification and used to produce table dependencies required in RELAP5. Gap conductance is converted to corresponding conductivity (small value for volumetric heat capacity was used for gap region).

II. Core neutronics model

1) Number of radial nodes per assembly?

One node per fuel assembly was used in radial direction.

2) Axial nodalization?

26 axial nodes were used for core region. The nodalization is as requested in the specification but two central regions were additionally divided in two equal parts.

3) Radial and axial reflector modeling?

The radial and axial reflectors are explicitly modeled. The thickness of the axial reflectors is 0.21881 m. For radial reflector modeling cells of the same size as fuel elements were used and with the same axial subdivisions. Fuel temperature used in feedback calculation for radial reflector composition is 551 K for HZP and 600 K for HFP. Fuel temperatures used for top and bottom reflector compositions are equal to corresponding fluid temperature.

4) Spatial decay heat distribution modeling?

The decay heat is calculated internally in the code using ANS-79 decay heat model with 23 groups for ^{235}U only. 2σ uncertainty was used. Steady state decay heat fraction is 0.071. In revised calculation the spatial distribution of decay heat is frozen at initial HFP conditions and total decay heat is calculated for each time step.

5) Cross-section interpolation procedure used?

New version of subroutines (with extrapolation) and provided files were directly used in final calculation.

6) Used method to get a critical reactor at the beginning of transient?

Fast and thermal fission cross sections are corrected using factor calculated during steady state to get critical reactor.

III. Coupling schemes

1) Hydraulics/heat structure spatial mesh overlays (mapping schemes in radial and axial plane)?

There are 18 core channels and corresponding 18 heat structures. The axial subdivision of the channel and the heat structure is the same.

2) Hydraulics/neutronics spatial mesh overlays (mapping schemes in radial and axial plane)?

The fuel elements/neutronic cells are connected to core channels according to Figure 3.2.3 from the specification. For central row of fuel elements coolant densities used for T-H feedback calculation are based on neighboring channel properties with weight 0.5. In axial direction one to one mapping was used except for T-H core layers 2 and 23. In that case two neutronic nodes correspond to one T-H node and both neutronic nodes have the same T-H conditions.

3) Heat structure/neutronics spatial mesh overlays (mapping schemes in radial and axial plane)?

The fuel elements/neutronic cells are connected to core structures according to Figure 3.2.3 from the specification. For central row of fuel elements fuel temperatures used for T-H feedback calculation are based on neighboring channel properties with weight 0.5. In axial direction one to one mapping was used except for T-H core layers 2 and 23. In that case two neutronic nodes correspond to one T-H node and both neutronic nodes have the same T-H conditions. The power delivered to heat structure is sum of powers from neutronic nodes.

4) Temporal coupling scheme?

Thermal-hydraulic part of the coupled code uses semi-implicit numerics. The time step is influenced by both hydraulics and heat transfer and it is the same. RELAP5 is leading part of the coupled code and QUABOX uses the same time step. The neutronics part can influence time step size only indirectly by influence on heat transfer calculation (power of heat structure).

5) Coupling numerics – explicit, semi-implicit or implicit?

Explicit coupling of T-H and neutronic calculation.

6) Coupling method – external or internal?

Internal coupling.

7) Coupling design – serial integration or parallel processing?

Serial integration.

IV. General

1) Deviations from the updated Final Specifications [April 1999 – NEA/NSC/DOC(99)8].

The trip is on 114% high neutron flux and it is calculated by the code. The boundary conditions were reduced to 99 time points using reasonable error criteria.

2) User assumptions?

Input and output values for bypass channel were calculated by volume averaging of corresponding data for 18 core channels and mass flow is constant and equal to core bypass flow for nominal conditions (Final Specifications).

3) Specific features of the used codes?

None.

4) Number of solutions submitted per participant and how they differ?

One solution using coupled RELAP5 mod 3.2 gamma and QUABOX.

UNIVERSITY POLYTECHNIC OF MADRID
SPAIN

I. Thermal-hydraulic core model

1) Core thermal-hydraulic (T-H) model and nodalization (1-D, 3-D, and number T-H channels or cells) – How are channels/T-H cells chosen?

COBRA-IIC-MIT2 with many extensions. 3-D T-H core model with 177 parallel channels with cross-flows (implicit) in 32 axial nodes.

2) Number of heat structures (fuel rods) modeled?

177 heat-structures or fuel rods (one per fuel assembly) in 32 axial nodes (same as T-H).

3) Which core thermal-hydraulic initial and transient boundary conditions are used and how?

From benchmark specifications of BC. The core-averaged pressure is interpolated from lower and upper plenum pressures at each time-step. The core-inlet channel flows; temperatures and densities are taken from the values of the corresponding T-H zone (18 in-core) of the specifications.

4) Radial and axial heat structure (fuel rod) nodalization?

Radial: 5 zones inside fuel rod and 1 for clad, in 32 axial nodes.

5) Relation used for Doppler temperature?

Weighted surface-centerline fuel temperatures: $T_{Doppler}=0.7*T_{surface}+0.3*T_{centre}$.

6) Used correlations for fuel properties vs. temperature?

From benchmark specifications.

II. Core neutronics model

1) Number of radial nodes per assembly?

4 radial nodes per fuel assembly.

2) Axial nodalization?

32 axial nodes (same as T-H and heat), where the specified 24 axial XS zones are divided in: 3,1,2,2, 16*1,2,2,1,3 equal axial nodes.

3) Radial and axial reflector modeling?

Radial reflector: 2-group albedos synthetically pre-calculated from fine-mesh (pin-by-pin) 2-D diffusion calculations of the 15 axial XS compositions. Axial reflector: explicitly modeled in fine-mesh 2-group embedded 1-D calculations.

4) Spatial decay heat distribution modeling?

From the tabulated specifications.

5) Cross-section interpolation procedure used?

2-D linear-linear, without extrapolation outside tabulated range.

6) Used method to get a critical reactor at the beginning of transient?

K_{eff} eigenvalue of the initial steady state divides $\nu\Sigma_f$ (prompt and delayed) during the whole transient. Inverse PK to yield the 3-D power evolution calculates total core reactivity.

III. Coupling schemes

1) Hydraulics/heat structure spatial mesh overlays (mapping schemes in radial and axial plane)?

Same mesh for hydraulics and heat structures (177 channels and rods, one per fuel assembly, in 32 axial nodes).

2) Hydraulics/neutronics spatial mesh overlays (mapping schemes in radial and axial plane)?

4 neutronic nodes per T-H channel or rod, with equal T-H properties in the nodes of the same fuel assembly, in the same 32 axial zones.

3) Heat structure/neutronics spatial mesh overlays (mapping schemes in radial and axial plane)?

As before.

4) Temporal coupling scheme?

Staggered time mesh where NK advances one-half time-step ahead of the T-H solution and this then one-half time-step ahead of the NK.

5) Coupling numerics – explicit, semi-implicit or implicit?

Semi-implicit: the T-H variables are linearly extrapolated over one-half time-step up to the NK time for every node. Since the neutronic power is centered at the T-H time-step, energy is conserved up to high order, with exponential frequency corrections at each 3-D node.

6) Coupling method – external or internal?

Internal, via commons in an integrated code (SIMTRAN=SIMULA+COBRA).

7) Coupling design – serial integration or parallel processing?

Serial integration.

IV. General

1) Deviations from the updated Final Specifications [April 1999 – NEA/NSC/DOC(99)8].

The radial reflector coolant density is kept constant, at the initial nominal conditions.

2) User assumptions?

Linear interpolation in time of core BC and T-H channels or rods of the fuel assemblies at core centerline.

3) Specific features of the used codes?

Linear discontinuous finite-difference scheme with synthetic 2-group generalized discontinuity factors.

4) Number of solutions submitted per participant and how they differ?

1 solution (updated in April 2000).

UNIVERSIDAD POLITECNICA DE VALENCIA (UPV)
SPAIN

I. Thermal-hydraulic core model

1) Core thermal-hydraulic (T-H) model and nodalization (1-D, 3-D, and number T-H channels or cells) – How are channels/T-H cells chosen?

Cores were created both using 6-equation thermal hydraulic model. The core was divided into 18 thermal-hydraulic 1-dimensional flow channels. Each channel, was divided into 24 levels of equal length.

2) Number of heat structures (fuel rods) modeled?

3 744 heat structures.

3) Which core thermal-hydraulic initial and transient boundary conditions are used and how?

In the second exercise used the BC proposed for the organization, and for the third exercise, the BC calculated by the code.

4) Radial and axial heat structure (fuel rod) nodalization?

Fuel Rod was divided in radial direction into 7 nodes, whereof 4 in fuel, 1 at outer ring of fuel, 1 at cladding inner ring and 1 at cladding outer ring. Fuel rod was divided in axial direction into 24 levels.

5) Relation used for Doppler temperature?

The following Doppler temperature was used: $T_f=0.3*T_{f,c}+0.7*T_{f,s}$

6) Used correlations for fuel properties vs. temperature?

The frame as the proposed by the benchmark.

II. Core neutronics model

1) Number of radial nodes per assembly?

One.

2) Axial nodalization?

It used 24 axial nodes of equal length.

3) Radial and axial reflector modeling?

Flux equal zero at the end of the reflector.

4) Spatial decay heat distribution modeling?

It used the ANSI-79 decay-heat standard.

5) Cross-section interpolation procedure used?

Linear interpolation.

6) Used method to get a critical reactor at the beginning of transient?

Tuning with multiplication of fission cross-section with a constant factor.

III. Coupling schemes

1) Hydraulics/heat structure spatial mesh overlays (mapping schemes in radial and axial plane)?

Hydraulics-heat structure mapped one-to-one automatically, since heat-structure in the code part of the thermal hydraulic channel.

2) Hydraulics/neutronics spatial mesh overlays (mapping schemes in radial and axial plane)?

Neutronics-hydraulics mapping with 24 axial nodes in neutronics each directly connected with the corresponding axial node (24 of equal length) of the thermal hydraulic channel.

3) Heat structure/neutronics spatial mesh overlays (mapping schemes in radial and axial plane)?

4) Temporal coupling scheme?

Implicit.

5) Coupling numerics – explicit, semi-implicit or implicit?

Implicit for neutronic and semi-implicit for thermal-hydraulics.

6) Coupling method – external or internal?

Internal.

7) Coupling design – serial integration or parallel processing?

Serial integration.

IV. General

1) Deviations from the updated Final Specifications [April 1999 – NEA/NSC/DOC(99)8].

None.

2) User assumptions?

None.

3) Specific features of the used codes?

Nodal collocation method in neutronics.

4) Number of solutions submitted per participant and how they differ?

We have submitted two solutions: one for the TRACB and the other for the TRACP. The solutions are different because the thermal-hydraulics models are different.

TECHNICAL RESEARCH CENTER (VTT)
FINLAND

I. Thermal-hydraulic core model [1]

1) Core thermal-hydraulic (T-H) model and nodalization (1-D, 3-D, and number T-H channels or cells) – How are channels/T-H cells chosen?

Cores were created both using five- and six-equation thermal hydraulic model. In each the core was divided radially into 177 thermal hydraulic one-dimensional flow channels. Each channel was divided axially into 24 sections of equal length.

2) Number of heat structures (fuel rods) modeled?

4 248 heat structures.

3) Which core thermal-hydraulic initial and transient boundary conditions are used and how?

All four initial and transient thermal hydraulic boundary conditions were used with the help of APROS boundary-condition module. For the five-equation thermal hydraulic model the temperatures had to be modified into enthalpies.

4) Radial and axial heat structure (fuel rod) nodalization?

Fuel rod was divided in radial direction into 10 nodes, whereof 7 in fuel, 1 at outer rim of fuel 1 at cladding inner rim and 1 at cladding outer rim.

5) Relation used for Doppler temperature?

Definition at page 29 was used: $T_f=(1-a)T_{f,c}+aT_{f,s}$.

6) Used correlations for fuel properties vs. temperature?

Correlations given at page 30 of the Final Specifications were used.

II. Core neutronics model

1) Number of radial nodes per assembly?

One.

1. All cited pages are relative to Ivanov, K., T. Beam, A. Baratta, A. Irani, and N. Trikorous, "PWR MSLB Benchmark: Volume 1: Final Specifications", NEA/NSC/DOC(99)8, April 1999.

2) Axial nodalization?

24 axial nodes of equal length.

3) Radial and axial reflector modeling?

With extrapolation lengths.

4) Spatial decay heat distribution modeling?

ANSI-curve (included as standard into the code).

5) Cross-section interpolation procedure used?

Special new section had to be written/programmed to handle the cross-section interpolation.

6) Used method to get a critical reactor at the beginning of transient?

Tuning with multiplication of fission cross-sections with a constant factor.

III. Coupling schemes

1) Hydraulics/heat structure spatial mesh overlays (mapping schemes in radial and axial plane)?

Hydraulics/heat structure mapped one-to one automatically, since heat structure in the code part of thermal hydraulics.

2) Hydraulics/neutronics spatial mesh overlays (mapping schemes in radial and axial plane)?

Neutronics/hydraulics mapping with 24 axial nodes in neutronics each directly connected with the corresponding axial node (24 of equal length) of the thermal hydraulic channel.

3) Heat structure/neutronics spatial mesh overlays (mapping schemes in radial and axial plane)?

See above.

4) Temporal coupling scheme?

None.

5) Coupling numerics – explicit, semi-implicit or implicit?

Explicit.

6) Coupling method – external or internal?

Direct coupling.

7) Coupling design – serial integration or parallel processing?

Direct coupling.

IV. General

1) Deviations from the updated Final Specifications [April 1999 – NEA/NSC/DOC(99)8].

In thermal hydraulics and in neutronics, division into sections of equal length was used. For neutronics the cross-sections adapted for the TRAB-3D code for equal length of neutronics nodes were used instead of those delivered originally.

2) User assumptions?

None.

3) Specific features of the used codes?

Finite difference solution in neutronics.

4) Number of solutions submitted per participant and how they differ?

No solution delivered, since the results obtained both with the five- and six-equation thermal hydraulics produce too high re-criticality in comparison with other codes. The reason must be either misinterpretation of some part of the definition or programming error in the parts that had to be programmed for this benchmark. The reason will be clarified and reported later on. Task 2 was supposed to be a simple check of the neutronics. Yet, there is also a difference between the results obtained with the five- and six-equation thermal hydraulics. In other types of applications with standard types of cross section definition the code behavior agrees with experiments and behavior of other well-known codes. Thus, the problem encountered is specific to the benchmark.

ALSO AVAILABLE

NEA Publications of General Interest

2001 Annual Report (2002) *Free: paper or Web.*

NEA News
ISSN 1605-9581 Yearly subscription: € 40 US$ 45 GBP 26 ¥ 4 800

Nuclear Science

Physics of plutonium Recycling (2002)
Volume VI: Multiple plutonium Recycling in Advanced PWRs
ISBN 92-64-19957-8 Price: € 45 US$ 45 GBP 28 ¥ 5250

Advanced Reactors with Innovative Fuels (2002)
ISBN 92-64-19847-4 Price: € 130 US$ 113 GBP 79 ¥ 15 000

Basic Studies in the Field of High-temperature Engineering (2002)
ISBN 92-64-19796-6 Price: € 75 US$ 66 GBP 46 ¥ 8 600

Utilisation and Reliability of High Power Proton Accelerators (2002)
ISBN 92-64-18749-9 Price: € 130 US$ 116 GBP 80 ¥ 13 100

Fission Gas Behaviour in Water Reactor Fuels (2002)
ISBN 92-64-19715-X Price: € 120 US$ 107 GBP 74 ¥ 12 100

Shielding Aspects of Accelerators, Targets and Irradiation Facilities – SATIF 5 (2001)
ISBN 92-64-18691-3 Price: € 84 US$ 75 GBP 52 ¥ 8 450

Nuclear Production of Hydrogen (2001)
ISBN 92-64-18696-4 Price: € 55 US$ 49 GBP 34 ¥ 5 550

Pyrochemical Separations (2001)
ISBN 92-64-18443-0 Price: € 77 US$ 66 GBP 46 ¥ 7 230

Evaluation of Speciation Technology (2001)
ISBN 92-64-18667-0 Price: € 80 US$ 70 GBP 49 ¥ 7 600

Speciation, Techniques and Facilities for Radioactive Materials at Synchrotron Light Sources (2002)
ISBN 92-64-18485-6 *Free: paper or web.*

A VVER-1000 LEU and MOX assembly Computational Benchmark (2002)
ISBN 92-64-18491-0 *Free: paper or web.*

Comparison Calculations for an Accelerator-driven Minor Actinide Burner (2002)
ISBN 92-64-18478-3 *Free: paper or web.*

Forsmark 1 & 2 Boiling Water Reactor Stability Benchmark (2001)
ISBN 92-64-18669-4 *Free: paper or web.*

Pressurised Water Reactor Main Steam Line Break (MSLB) Benchmark (Volume II) (2000)
ISBN 92-64-18280-2 *Free: paper or web.*

Order form on reverse side.

ORDER FORM

OECD Nuclear Energy Agency, 12 boulevard des Iles, F-92130 Issy-les-Moulineaux, France
Tel. 33 (0)1 45 24 10 15, Fax 33 (0)1 45 24 11 10, E-mail: nea@nea.fr**, Internet: www.nea.fr**

Qty	Title	ISBN	Price	Amount
			Total*	

* Prices include postage fees.

❑ Payment enclosed (cheque payable to OECD Publications).

Charge my credit card ❑ VISA ❑ Mastercard ❑ Eurocard ❑ American Express

Card No.	Expiration date	Signature
Name		
Address	Country	
Telephone	Fax	
E-mail		

OECD PUBLICATIONS, 2 rue André-Pascal, 75775 PARIS CEDEX 16
Printed in France.